Alma Mater Studiorum – Università di Bologna

DOTTORATO DI RICERCA IN:

Scienze Farmacologiche e Tossicologiche dello Sviluppo e del Movimento Umano

Ciclo **XXVIII**

Settore Concorsuale di afferenza: 05/G1

Settore Scientifico disciplinare: BIO/14

"Chronic Obstructive Pulmonary Disease: genetic polymorphisms and intermediary metabolism alterations"

Presentata da: NICOLA CONSOLINI

Coordinatore Dottorato

Prof.ssa PATRIZIA HRELIA

Relatore

Prof.ssa PATRIZIA HRELIA

Co-relatore

Prof.ssa SABRINA ANGELINI

Esame finale anno 2016

TABLE OF CONTENTS

PAGE

ABSTRACT

“Chronic Obstructive Pulmonary Disease: genetic polymorphisms and intermediary metabolism alterations”

Chronic obstructive pulmonary disease (COPD) is a multifactorial disease characterized by airflow obstruction that is usually progressive and associated with an abnormal inflammatory response of the lungs to noxious particles and gases. Cigarette smoke (CS) is the main risk factor, but only a small proportion of smokers (15-20%) develop symptomatic disease, this suggests that there are individual susceptibility factors involved in disease onset and progression. Considering the impact of environmental and genetic risk factors in COPD, this dissertation sought to uncover genetic susceptibility biomarkers in a population affected by COPD and explore tissue metabolic alterations induced by chronic CS exposure in a mouse model.

A case-control study was carried on in a COPD population, aiming to investigate whether polymorphisms of microsomal epoxide hydrolase (EPHX1) gene, and related phenotypes, had any bearing on individual susceptibility to COPD onset and severity. DNA of COPD patients and controls was genotyped for functional polymorphisms of EPHX1 gene (exon 3 Tyr113His, exon 4 His139Arg), and haplotype analysis was performed using PCR-RFLP and PCR-RT techniques. The statistical analysis did not show any significant result about the potential relationship between analyzed SNPs, related phenotypes, and COPD risk and severity.

Stable isotope-resolved metabolomics approach was used to study glycolytic pathway alterations induced by chronic CS exposure in lung and liver tissue of an emphysema mouse model. C57BL/6J mice, after CS exposure, were injected via IP injection with glucose tracer containing carbon stable isotope - $^{13}C_6$-glucose – then, tissues were collected and the incorporation of ^{13}C into metabolites was monitored by mass spectrometry and nuclear magnetic resonance spettroscopy. Lung tissue analyses did not reveal any significant alteration in lung tissue glycolysis of mice exposed to CS. On the other hand, CS may contribute to dysregulated glycolysis, PPP, glycogen synthesis and utilization, in emphysema mouse model liver tissue.

PREFACE

“EVERY BREATH WE TAKE: epidemiological overview of chronic respiratory diseases”

The human lung is subject to airborne pollutants and irritants with each breath. Tobacco smoke, including passive smoke exposures, is a leading cause of the respiratory disease burden, along with air pollution and workplace exposure to unsafe air. Contact with smoke from fires used in heating and cooking causes acute and chronic respiratory illness.

With an aging global population, chronic respiratory diseases (CRDs) are becoming a more prominent cause of death and disability. Over two billion people are regularly exposed to the toxic effects of indoor and outdoor air pollution, which is responsible for 3.5 million premature deaths each year [1]. Much of the morbidity and mortality associated with exposure to poor indoor air quality occurs in women and children, especially in low-income families [2-4].

Respiratory diseases are among the leading causes of death worldwide (**Table 1**). Lung infections (mostly pneumonia and tuberculosis), lung cancer and chronic obstructive pulmonary disease (COPD) together accounted for one sixth of all deaths worldwide (~10 milion). The World Health Organization (WHO) estimates that the same four diseases accounted for one-tenth of the disability-adjusted life years (DALYs) lost worldwide in 2008 (~150 milion) (**Table 2**) [5].

Deaths attributed to	Worldwide	WHO European Region
Ischaemic heart disease	7.3 million (12.8%)	2.40 million (24.7%)
Cerebrovascular disease	6.2 million (10.8%)	1.40 million (14.0%)
Lower respiratory infections	**3.5 million (6.1%)**	**0.23 million (2.3%)**
COPD	**3.3 million (5.8%)**	**0.25 million (2.5%)**
Diarrhoeal diseases	2.5 million (4.3%)	0.03 million (0.3%)
HIV/AIDS	1.8 million (3.1%)	0.08 million (0.8%)
Trachea/bronchus/lung cancer	**1.4 million (2.4%)**	**0.38 million (3.9%)**
Tuberculosis	**1.3 million (2.4%)**	**0.08 million (0.8%)**
Diabetes mellitus	1.3 million (2.2%)	0.17 million (1.7%)
Road traffic accidents	1.2 million (2.1%)	0.12 million (1.2%)

Table 1. The 10 most common causes of death in 2008. Source: World Health Organization (WHO) World Health Statistics 2011.

DALYs lost to	Worldwide	WHO European Region
Lower respiratory infections	**79 million (5.4%)**	**2.2 million (1.5%)**
HIV/AIDS	65 million (4.4%)	2.6 million (1.8%)
Ischaemic heart disease	64 million (4.4%)	16.0 million (11.3%)
Diarrhoeal diseases	56 million (3.8%)	1.1 million (0.7%)
Cerebrovascular disease	48 million (3.3%)	9.3 million (6.4%)
Road traffic accidents	45 million (3.1%)	3.4 million (2.4%)
COPD	**33 million (2.3%)**	**2.9 million (2.0%)**
Tuberculosis	**29 million (2.0%)**	**1.7 million (1.2%)**
Diabetes mellitus	22 million (1.5%)	2.6 million (1.8%)
Trachea/bronchus/lung cancer	**13 million (0.9%)**	**3.2 million (2.2%)**

Table 2. The 10 most common causes of disability-adjusted life-years (DALYs) lost worldwide in 2008.Source: World Health Organization World Health Statistics 2011.

CRDs are diseases of the airways and other structures of the lung, including asthma and respiratory allergies, COPD, occupational lung diseases, sleep apnea syndrome and pulmonary hypertension.

COPD and lung cancer are leading causes of death worldwide, and their numbers are rising. Lung cancer is the most common malignancy worldwide, and is largely preventable by smoking prevention and cessation.

CRDs are often under-recognized, under-diagnosed, under-treated and insufficiently prevented. Many are preventable, but are not curable, however, various forms of treatment, that help to dilate major air passages and improve shortness of breath, can help control symptoms and increase the quality of life for people with the disease.

CRDs adversely impact the quality of life of affected individuals and can lead to premature deaths and disabilities. The prevalence of these diseases is increasing everywhere, particularly among children and elderly people [4].

By 2030, the WHO estimates that the four major potentially fatal respiratory diseases (pneumonia, tuberculosis, lung cancer and COPD) will account for about one in five deaths worldwide, compared to one sixth of all deaths globally in 2008.

In the *WHO European Region* respiratory disease causes about 1 million deaths annually, of which two-thirds (~660.000 people) occur in the 28 countries of the European Union (EU), with at least 6 million hospital admissions, accounting for over 43 million in-patient bed-days (Figure 1).

The main respiratory diseases among the ten leading causes of death are: pneumonia, COPD, lung cancer and tuberculosis. Lung cancer is the leading cause of respiratory death, followed by COPD, lower respiratory infections and tuberculosis. More than half of all the deaths from respiratory disease are due to diseases caused by smoking. It is predicted that lung cancer and COPD as causes of death will continue to rise until 2015 and 2030 respectively (**Table 3**) [6].

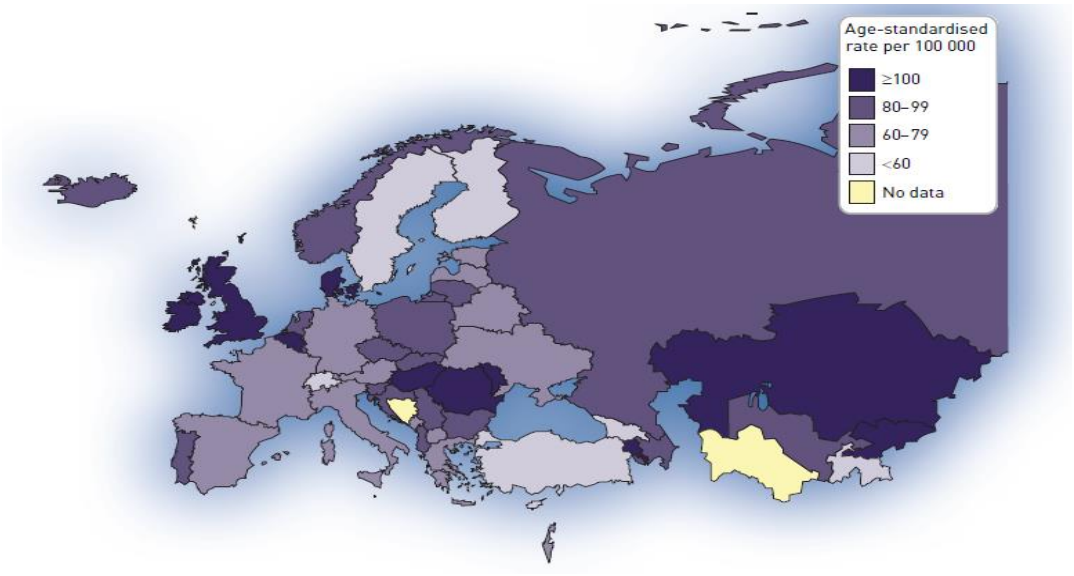

Figure 1. Map of age-standardised mortality rates for all respiratory conditions. Source: World Health Organization World and Europe Detailed Mortality Databases, November 2011 update.

Percentage of deaths in WHO European region	2008	2015	2030
Lower respiratory infections	2.3	2.2	1.9
COPD	2.5	2.7	3.2
Trachea/bronchus/lung cancer	3.9	3.9	4.1
Tuberculosis	0.8	0.7	0.4

Table 3. Data from World Health Organization. World Health Statistics 2011

Meanwhile, lung cancer remains the number one cancer killer for both sexes and is likely to increase faster than any other type, COPD alone affects an estimated 44 million Europeans. This progressive and debilitating disease of the respiratory system, today

largely undiagnosed by physicians and patients alike, is expected to become leading cause of death by 2030.

Within the WHO European Region, in the next two decades, the proportion of deaths caused by respiratory disease is likely to remain stable, at about one-tenth of all deaths (~500.000), with an increase in COPD and lung cancer deaths balancing a decline in deaths from lower respiratory infections and tuberculosis (**Tables 4 and 5**) [5].

Percentage of deaths worldwide	**2008**	**2015**	**2030**
Lower respiratory infections	6.1	5.5	4.2
COPD	5.8	6.6	8.6
Trachea/bronchus/lung cancer	2.4	2.8	3.4
Tuberculosis	2.4	1.6	3.4
Percentage of deaths in WHO European region	**2008**	**2015**	**2030**
Lower respiratory infections	2.3	2.2	1.9
COPD	2.5	2.7	3.2
Trachea/bronchus/lung cancer	3.9	3.9	4.1
Tuberculosis	0.8	0.7	0.4

Table 4. Projected proportion of deaths due to leading respiratory causes. COPD: chronic obstructive pulmonary disease. Source: World Health Organization World Health Statistics 2011**.**

Percentage of DALYs worldwide	**2008**	**2015**	**2030**
Lower respiratory infections	5.4	4.6	3.2
COPD	2.3	2.7	3.8
Trachea/bronchus/lung cancer	0.9	1.0	1.4
Tuberculosis	2.0	1.6	1.1
Percentage of DALYs in WHO European region	**2008**	**2015**	**2030**
Lower respiratory infections	1.5	1.3	1.0
COPD	2.0	2.0	2.2
Trachea/bronchus/lung cancer	2.2	2.2	2.6
Tuberculosis	1.2	1.1	0.6

Table 5. Projected disability-adjusted life-years (DALYs) lost due to leading respiratory causes. COPD: chronic obstructive pulmonary disease. Source: World Health Organization World Health Statistics 2011

In *Italy* respiratory diseases represent the third leading cause of death (after cancer and diseases of the circulatory system), and they account for 12% of all deaths (~70.000). Asthma and COPD account for 55% of all death caused by respiratory diseases.

In Italy, COPD affects about 14% of the older population (65 years or more), and it is the fifth cause of hospital admission in this age group. The prevalence of COPD shows a growing trend that varies from 2.5% in 2005 to 3% in 2013, with estimates significantly higher in men (3.2% in 2005 and 3.6% in 2013) than women (1.8% in 2005 and 2.4% in 2013). There are substantial geographic differences in the prevalence estimation, with higher values in the South and lowest in the North, with no significant differences in gender. The prevalence of COPD shows rising values as age increases, with a significant increase in male reaches the peak in the over 85 (18%) [7].

Both the prevention and treatment of lung diseases will need to be improved. Public health programs are needed to reduce or eliminate cigarette smoking to avoid the inevitable rise in respiratory chronic diseases, such cancers and COPD. Moreover, it is necessary to develop long-term, strategic and integrated policy advice to protect people against significant negative effects of air pollution on human health and the environment. Respiratory illnesses are frequently avoidable. The ability to control and eliminate respiratory diseases worldwide relies on public health measures, which include increasing awareness, education, and capacity. Scientific research is essential to improve knowledge and understanding of pathophysiological processes, which then allows for better diagnoses, treatments, and overall prevention.

CHAPTER 1

Chronic Obstructive Pulmonary Disease (COPD)

1.1. PATHOLOGY

Chronic Obstructive Pulmonary Disease (COPD) is currently the fourth leading cause of death in the world [8], and represents one of the major public health challenge (**Figure 1**). COPD is a life-threatening lung disease that interferes with normal breathing. Many people suffer from this disease for years, and die prematurely from it or its complications.

The primary cause of COPD is tobacco smoke (including second-hand or passive exposure), although in many countries, indoor air pollution (such as solid fuel used for cooking and heating), outdoor air pollution, occupational dusts and chemicals (vapours, irritants and fumes) and frequent lower respiratory infections during childhood are major COPD risk factors [9].

COPD is a disease that it is growing in both industrialized countries and developing countries, with a prevalence of 5% in the general population and it is by far the leading cause of hospitalization in the departments of internal medicine and pulmonology.

According to WHO estimates, 65 million people have moderate to severe COPD. More than 3 million people died of COPD in 2012, which is equal to 6% of all deaths globally that year [10].

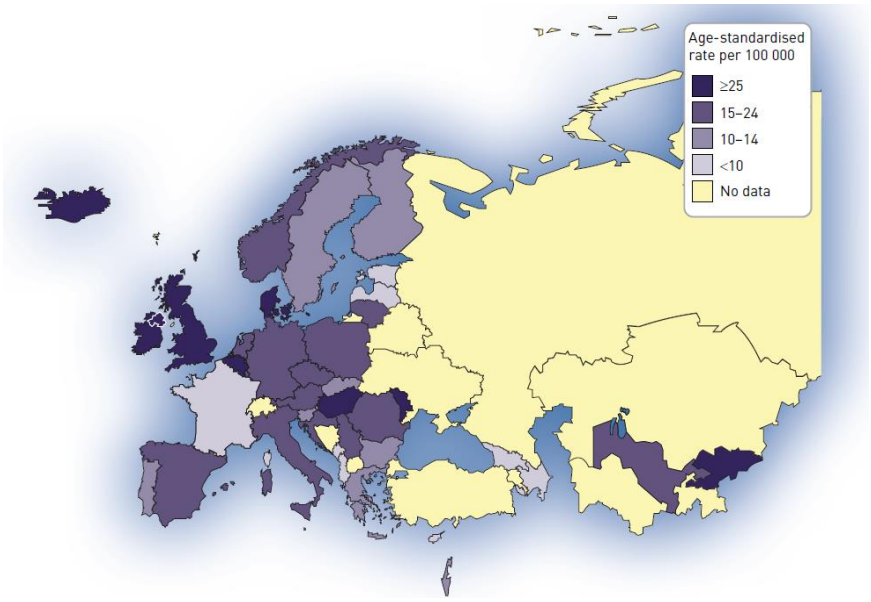

Figure 1. Mortality rate for chronic obstructive pulmonary disease (COPD). Data from World Health Organization World and Europe Mortality Databases, November 2011 update. Data for some countries are missing because mortality data for asthma and COPD are not reported separately.

The Global Burden of Disease Study estimated that COPD will be the third leading cause of death worldwide in 2030. In addition, considering the sum of years lost because of premature mortality and years of life lived with disability (Disability-Adjusted Life Year = DALY), it has been estimated that by 2030 COPD will be the seventh leading cause of DALYs lost worldwide [11].

The increased mortality is mainly driven by the expanding epidemic of smoking, reduced mortality from other common causes of death (e.g. ischemic heart disease, infectious diseases), and aging of the world population [12].

A systematic review and meta-analysis of studies carried out in 28 countries between 1990 and 2004 [13], provides evidences that the prevalence of COPD is appreciably higher in smokers and ex-smokers than in nonsmokers, in those over 40 years of age than those under 40, and in men than in women. Because of increased tobacco use among women in high-income countries and the higher risk of exposure to indoor air pollution (such as biomass fuel used for cooking and heating) in low-income countries, the disease now affects men and women almost equally.

COPD is not curable and it is essential to stop smoking to prevent the progression of the disease. Various forms of treatment can help control symptoms and increase quality of life for people with the illness, for example, medicines that help dilate major air passages of the lungs, improving shortness of breath, such as broncodilators (β2-agonists, anticolinergics, methylxantines), or anti-inflammatory drugs (corticosteroids and phosphodiesterase-4 inhibitors). Usually these drugs are used in combination.

Although in the recent years the scientific community has paid increased attention to COPD, this syndrome remains relatively unknown or ignored by the general population, the public health system and government officials. In 1998, in order to bring more attention to COPD, its prevention and its treatment, a committee of scientists, encouraged by the US National Heart, Lung and Blood Institute, US National Institute of Health (NIH) and the World Health Organization (WHO), has initiated the Global Strategy for the Diagnosis, Treatment and Prevention of COPD (Global Initiative for Chronic Obstructive Lung Disease - GOLD). Among the important goals of this project are, to increase awareness of the burden of COPD and to improve prevention and management of COPD, in order to help millions of people who suffer and die prematurely from COPD or its complications [14].

According to the guidelines adopted by the international scientific community, Chronic Obstructive Pulmonary Disease (COPD) is a "*common preventable and treatable disease characterized by persistent airflow limitation that is usually progressive and associated with an enhanced chronic inflammatory response in the airways and the lung to noxious particles or gases. Exacerbations and comorbidities contribute to the overall severity in individual patients"* [14].

COPD is a syndrome, with a set of medical signs and symptoms that are correlated with each other, essentially characterized by chronic airflow limitation, a variety of pathological changes in the lung (**Figure 2**), some significant extrapulmonary effects, and important comorbidities that may contribute to the severity of the disease in individual patients.

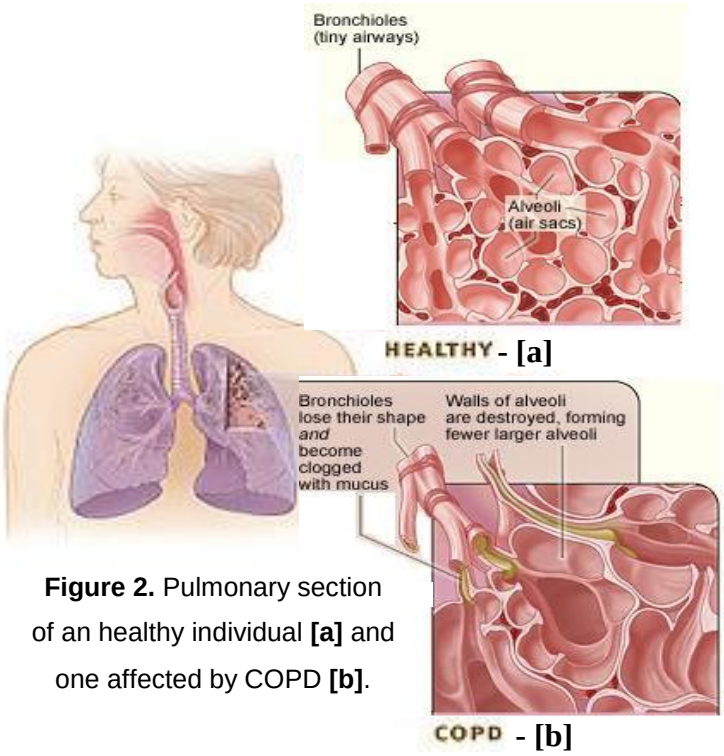

Figure 2. Pulmonary section of an healthy individual **[a]** and one affected by COPD **[b]**.

The chronic airflow limitation, characteristic of COPD, is caused partly by a mixture of small airways disease (obstructive bronchiolitis), parenchymal tissue destruction (emphysema), and disrupt normal repair and defense mechanisms (resulting in small airway fibrosis), the relative contributions of which vary from person to person (**Figure 3**).

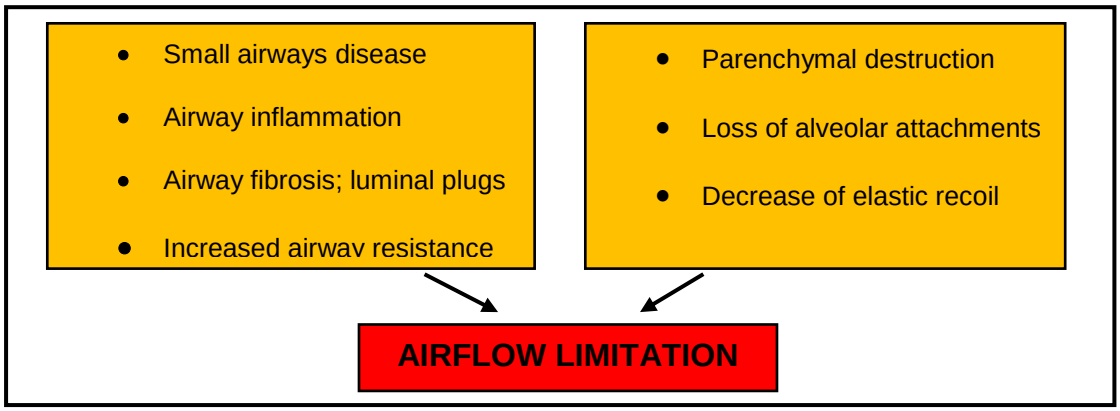

Figure 3. Mechanisms underlying Airflow Limitation in COPD

It is important to point out that emphysema, or destruction of the gas-exchanging surfaces of the lung (alveoli), is a pathological term that is often (but incorrectly) used clinically and describes only one of several structural abnormalities present in patients with COPD. Chronic bronchitis, or the presence of cough and sputum production for at least 3 months in each of two consecutive years, remains a clinically and epidemiologically useful term. However, it is important to point out that chronic cough and sputum production (chronic bronchitis) is an independent disease entity that may precede or follow the development of airflow limitation and may be associated with development and/or acceleration of fixed airflow limitation. Chronic bronchitis also exists in patients with normal spirometry.

The chronic inflammatory response causes structural changes, narrowing of the small airways, and the destruction of the lung parenchyma that leads to the loss of alveolar attachments to the small airways and a reduction in lung elastic recoil. These alterations diminish the ability of the airways to remain pervious during the expiratory phase. COPD clinically manifested as chronic cough, phlegm and progressive shortness of breath on exertion before, and then, in severe cases, even at rest.

Based on these characteristics, the team of experts involved in the GOLD project defined the disease according to spirometric criteria. Spirometry is the most common and reproducible pulmonary function tests, and the best way to measure the extent of airflow limitation. Through this test it was drawn up the "spirometric classification of COPD severity " that includes four stages: mild, moderate, severe, very severe (**Table 1**).

Table 1. Classification of Severity of Airflow Limitation in COPD (Based on Post-Bronchodilator FEV1)	
GOLD 1: **Mild**	FEV1/FVC < 0.70 FEV1 ≥ 80% predicted
GOLD 2: **Moderate**	FEV1/FVC < 0.70 50% ≤ FEV1 < 80% predicted
GOLD 3: **Severe**	FEV1/FVC < 0.70 30% ≤ FEV1 < 50% predicted
GOLD 4: **Very Severe**	FEV1/FVC < 0.70 FEV1< 30% predicted o FEV1 < 50% predicted, with chronic respiratory failure
FEV1: Forced Expiratory Volume in the first second, post-bronchodilator; FVC: Forced Vital Capacity; Respiratory Failure: arterial partial pressure of oxygen (PaO2) less than 8.0 kPa (60 mm Hg) with or without arterial partial pressure of carbon dioxide (PCO_2) greater than 6.7 kPa (50 mm Hg), at sea level.	

Spirometry is often altered in the patient with COPD, even before the onset of major symptoms, so it is essential that it is performed in subjects at risk, even in the absence of symptoms, as a measure of general health. In practice, the basic measure is to perform a forced expiration through the mouth by which a given volume of air is expelled in a determined time. This air volume is expressed by the term FEV1 - Forced Expiratory Volume in the first second, post-bronchodilator administration. In patients affected by COPD the FEV1 value is much less than the theoretical one of an healthy person with the same age, sex, height, race and body size. A normal subject in the first second expels more than 70% of the mobilized air (Vital Capacity), in comparison to a COPD patient, that expels less than 70% of vital capacity, even after inhaled bronchodilators. In conclusion a post-bronchodilator ratio FEV1/FVC < 0.70 confirms the presence of persistent airflow limitation and thus presence of COPD (**Figure 4**) [14].

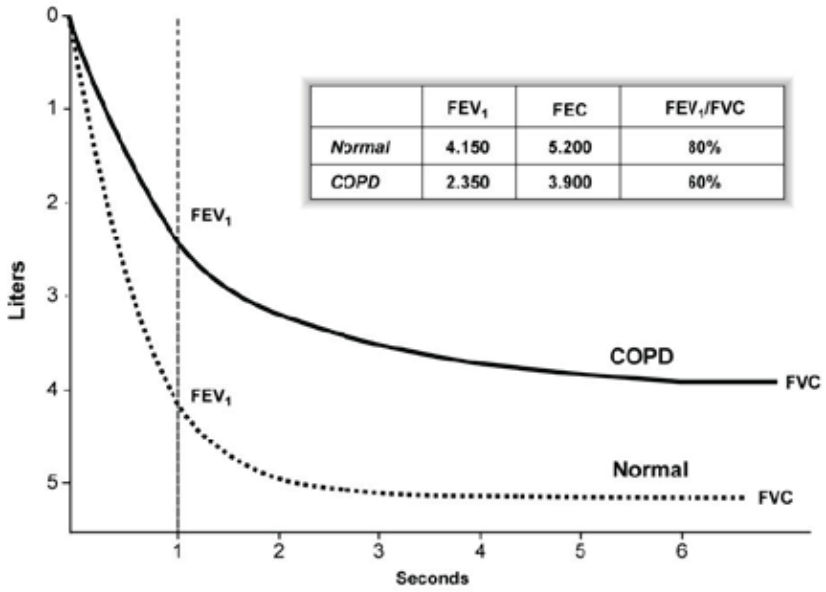

Figure 4. Lung capacity spirogram of a healthy individual and a patient with mild to moderate COPD.

A population study showed that the FEV1/FVC ratio post-bronchodilator exceed the value of 0.70 regardless of age, supporting the use of this fixed ratio in the spirometric classification of COPD severity [15]. However, there are limitations to the use of this value: the aging process affects the lung volume, so the use of this ratio is likely to lead to an overestimation in the diagnosis of COPD in elderly and to an underestimation in young adults, under 45 years, particularly the mild COPD [16].

The impact of the disease on the individual patient depends, not only on the degree of airflow limitation, but also on the severity of the symptoms, especially dyspnea and decreased exercise ability. However, the COPD stages are defined based on the spirometry results, which provide a general indication for defining the initial therapeutic approach.
COPD stages based on GOLD guidelines:

1. **GOLD 1 - MILD**: mild airflow limitation; the symptoms, chronic cough and sputum production may be present or not; at this stage the individual is usually unaware that lung function is impaired.

2. **GOLD 2 - MODERATE**: worsening airflow limitation; progression of symptoms with shortness of breath especially on exertion (exertional dyspnea), cough and sputum production; at this stage patients usually resort to medical care because of respiratory symptoms.

3. **GOLD 3 - SEVERE**: further worsening airflow limitation; increased shortness of breath, reduced exercise capacity, fatigue, and repeated exacerbations that almost always have an impact on the patient's quality of life.

4. **GOLD 4 - VERY SEVERE**: severe airflow limitation or the presence of chronic respiratory failure. The respiratory failure may also lead to effects on the heart, such as right heart failure that may occur, for example, with elevation of jugular venous pressure. At this stage the quality of life is significantly impaired and exacerbations may be life threatening the patient.

COPD often develops in people of middle aged who smoke for a long time, so patients often have co-morbidities related to smoking or aging [17]. COPD itself also has significant extrapulmonary (systemic) effects that lead to comorbid conditions [18]. A Dutch study showed that up to 25% of the population aged 65 and older suffer from two comorbid conditions and up to 17% has three [19]. Weight loss, nutritional abnormalities and skeletal muscle dysfunction are well-recognized extrapulmonary effects of COPD and patients have increased risk of myocardial infarction, angina, osteoporosis, respiratory infection, bone fractures, depression, diabetes, sleep disorders, anemia and glaucoma [20].

COPD has a variable natural history and not all individuals follow the same progress. However, it is usually a progressive disease, especially if patient is continuously exposed to noxious agents. Stopping exposure to these agents, even after the emergence of a significant airflow limitation, may improve lung function and slow or even stop the progression of the disease. Once COPD is developed, and its comorbidities can not be cured and it is necessary continuous treatment, COPD treatment may reduce symptoms, improve quality of life, reduce exacerbations, and possibly reduce mortality in patients.

1.2. PATHOGENESIS

The anatomical and pathological changes characteristic of COPD are observed in the proximal and peripheral airways, in the lung parenchyma, and pulmonary vasculature [21]. These alterations include chronic inflammation, with increased numbers of specific inflammatory cells in various parts of the lung (mostly lymphocytes and macrophages, few neutrophils or eosinophils) (**Figure 5**), and structural changes resulting from repeated damage and subsequent repair attempts. Usually, inflammation and structural changes in the airways increase with disease severity, and persist even after smoking cessation.

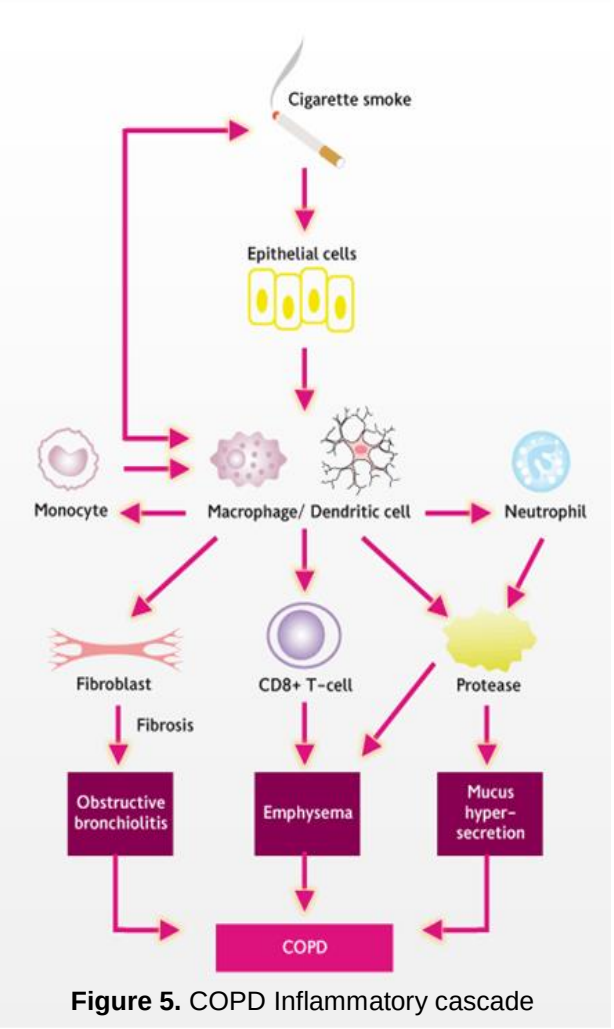

Figure 5. COPD Inflammatory cascade

The inflammation in the respiratory system of COPD patients appears to be an amplification of the inflammatory response to chronic irritants such as cigarette smoke. The mechanism for this abnormal process is not yet understood, but it is supposed to be genetically determined. Some patients can develop COPD without smoking, but, in these patients, the nature of the inflammatory response and the related mechanisms are unknown [22]. Lung inflammation is further amplified by oxidative stress and an excess of proteinases in the lung. Together these factors lead to characteristic pathologic changes in COPD (**Figure 6**).

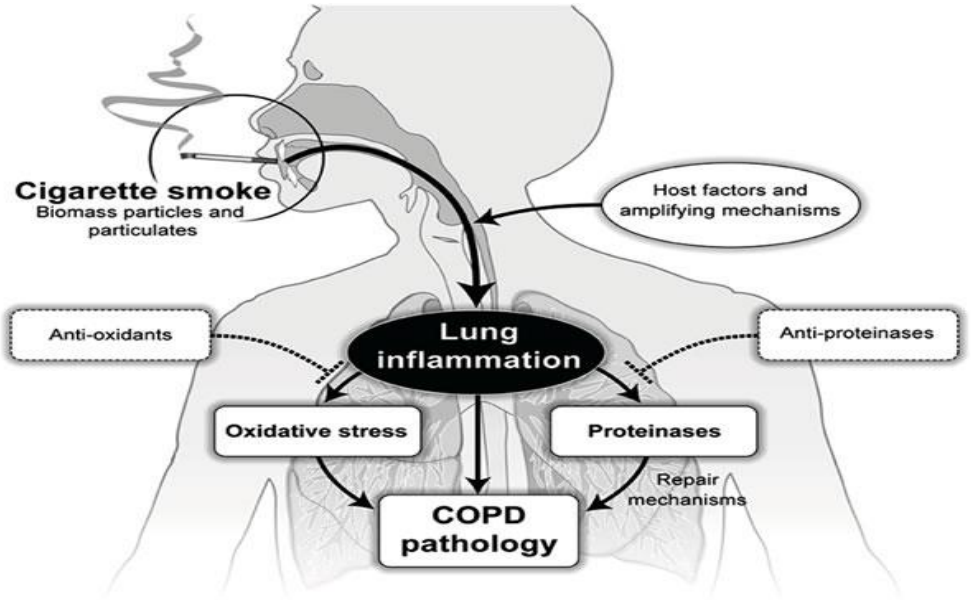

Figura 6. Pathogenesis of COPD

Oxidative stress may be an important amplifying mechanism in COPD [23]. Biomarkers of oxidative stress (e.g., hydrogen peroxide, 8-isoprostane) are increased in the exhaled breath condensate, sputum, and systemic circulation of COPD patients. Oxidative stress is further increased in exacerbations. Oxidants are generated by cigarette smoke and other inhaled particulates, and released from activated inflammatory cells such as macrophages and neutrophils. In COPD patients it is also possible a reduction in endogenous antioxidants, as consequence of reduced activity of transcription factor Nrf2, important regulator of antioxidant genes expression [24].

There is compelling evidence for an imbalance in the COPD patients' lungs between proteases, which break down connective tissue components, and antiproteases, which counteract proteases activity. Several proteases, derived from inflammatory cells and epithelial cells, are increased in COPD patients. Protease-mediated destruction of elastin (a major connective tissue component in lung parenchyma) is believed to be an important feature of emphysema and it is likely to be irreversible.

COPD is characterized by a specific inflammation pattern involving increased numbers of CD8+ (cytotoxic) Tc1 lymphocytes (present only in smokers that develop the disease), neutrophils, macrophages and lymphocytes [25]. These cells release inflammatory mediators and enzymes and interact with structural cells in the airways, lung parenchyma and pulmonary vasculature [26]. A wide variety of inflammatory mediators, which have been shown to increase in COPD patients [27-28], attract inflammatory cells from the circulation (chemotactic factors), amplify the inflammatory process (proinflammatory

cytokines), and induce structural changes (growth factors) [29]. Examples of each type of mediator are listed in **Table 2**.

Table 2. Inflammatory mediators in COPD
CHEMOTACTIC FACTORS: • lipid mediators: eg. leukotriene B4 exerts chemoattractant activity for neutrophils and T lymphocytes • Chemokines: eg. Interleukin-8 (IL-8) exerts chemoattractant activity for neutrophils and monocytes
PROINFLAMMATORY CYTOKINES: eg. tumor necrosis factor-α (TNF-α), IL-1β, IL-6 amplify the inflammatory process and may contribute to some of the systemic effects of COPD
GROWTH FACTORS: eg. the transforming growth factor-β (TGF-β) can cause fibrosis of small airways

1.3. COMORBIDITIES

COPD often coexists with other diseases (comorbidities) that may have a significant impact on prognosis [22] [30-34]. Some of these arise independently of COPD whereas others may be causally related, either with shared risk factors or by one disease actually increasing the risk of another. It is possible that features of COPD, such as systemic inflammation, are shared with other diseases and as such this mechanism represents a link between COPD and some of its comorbidities [35]. This risk of comorbid disease can be increased by the sequelae of COPD (e.g. reduced physical activity).

Comorbidities are common at any severity of COPD [36] and the differential diagnosis can often be difficult. For example, in a patient with both COPD and heart failure an exacerbation of COPD may be accompanied by worsening of heart failure.

The chronic airflow limitation is mainly caused by inhaled particles and gases, the most common of which is cigarette smoking. However, also nonsmokers may develop airflow limitation presenting similar symptoms that can be associated with other diseases, such as asthma, congestive heart failure, lung cancer, pulmonary tuberculosis and other lung diseases.

Asthma and COPD - COPD can coexist with asthma, the other major chronic obstructive pulmonary disease characterized by an underlying inflammation of the airways. The airway inflammation occurs with very different patterns in the two diseases. However, individuals

with asthma who are exposed to noxious agents, may also develop inflammation that is a combination of Asthma-like and COPD-like. In addition, there are epidemiological evidences that, in the long term, asthma alone can lead to the irreversible airflow limitation [37]. Other patients with COPD may have features of asthma such as a mixed inflammatory pattern with increased eosinophils [38].

COPD and pulmonary tuberculosis - In many developing countries both pulmonary tuberculosis and COPD are common. Tuberculosis has proved as an independent risk factor for airways obstruction. For this reason every doctor should be aware of the long-term risk of COPD in patients with tuberculosis, regardless of smoking status, especially in patients from countries with a high rate of tuberculosis [39].

1.4. RISK FACTORS

The identification of risk factors is an important stage in the development of strategies for prevention and treatment of any disease. At the base of major chronic diseases, such as COPD, there are common and modifiable risk factors, including unhealthy diet, tobacco use, alcohol abuse and lack of physical activity, but also non-modifiable risk factors such as age and genetic predisposition. In the last years, environmental factors are becoming increasingly important determinants of COPD.

Identification of cigarette smoking as the most common risk factor for COPD has led to consider smoking cessation programs essential in COPD prevention, as well as an important intervention for patients have already developed the disease. However, although cigarette smoking is the main and better studied risk factor for COPD, it is certainly not the only one. There are epidemiological evidences that even non-smokers may develop chronic airway obstruction [40-42] suggesting there are individual susceptibility factors to disease onset. In other words, of two individuals characterized by the same history of smoking, only one may develop COPD due to differences in the genetic predisposition (inter-individual genetic differences).

Many evidences concerning risk factors for COPD are derived from epidemiological studies to investigate associations rather than cause-and-effect relationships. Population studies on people affected by COPD have been done, with a follow-up until 20 years, but none has monitored the progression of the disease through its entire course, or has

included the pre-and perinatal periods which may be important in shaping an individual's future COPD risk.

Therefore, the current understanding of risk factors (**Table 3**) for COPD in many respects is still incomplete.

Table 3. COPD risk factors
Genetic Factors
Environmental factors (exposure to particles) • Tobacco Smoking • Organic and Inorganic Occupational Dusts • Indoor air pollution caused by heating and cooking with biomass in poorly ventilated dwellings • Outdoor air Pollution
Oxidative Stress
Lung growth and development
Sex
Age
Infections
Comorbidities
Socioeconomic Status
Nutrition

Genetic factors - COPD is a polygenic disease and a classic example of gene-environment interaction. Among people with the same smoking history, not all will develop COPD due to differences in genetic predisposition to the disease, or in how long they live.

The best documented genetic risk factor is the severe hereditary deficiency of alpha-1-antitrypsin [43], an important circulating inhibitor of serine proteases. Premature and accelerated panlobular emphysema development and decline in lung function occur in both smokers and nonsmokers with the severe deficiency, although smoking habit increases considerably the risk. There is significant variability between individuals in the extent and severity of emphysema and the pace of decline in lung function.

Although the alpha-1 antitrypsin deficiency is relevant to only a small part of the world's population (more common in people of Northern European origin) [44], it illustrates the interaction between genes and environmental exposure leading to COPD. This way provides a model of how it is possible to believe that other genetic factors may contribute to COPD onset.

A significant familial risk of airflow limitation has been observed in smoking siblings of patients with severe COPD [45], suggesting that genetic together with environmental

factors could influence this susceptibility. Single genes, such as gene encoding matrix metalloproteinase 12 (MMP12), have been related to decline in lung function [46].

Through genetic linkage analysis, several regions of the genome, that are likely to contain COPD susceptibility genes, have been identified, including chromosome 2. Genetic association studies have discovered a set of genes involved in the pathogenesis of COPD, including tumor growth factor-β1 (TGF-β1), the microsomal epoxide hydrolysis (EPHX1) and tumor necrosis factor-α (TNF-α) [47-49]. However, the results of these genetic association studies are largely inconsistent, and functional genetic variants influencing the development of COPD (other than alpha-1-antitrypsin deficiency) have not yet been identified.

Environmental factors (exposure to particles) - Important factor to consider is the environment in which the individual lives. Of the many environmental exposures that we experience during lifetime, only tobacco smoke, occupational dusts and chemicals in professional environments (vapors, irritants and fumes) are known to cause, alone, COPD [50-53]. Tobacco smoke and occupational exposures appear to act additively to increase the risk of developing COPD.

Across the world, tobacco smoke is by far the main COPD risk factor. Cigarette smokers have a higher prevalence of respiratory symptoms and lung function abnormalities, a greater annual rate of decline in FEV1, and a greater COPD mortality rate than nonsmokers [54]. Passive exposure to cigarette smoke (also known as environmental tobacco smoke or ETS) may also contribute to respiratory symptoms [55] and COPD [56] by increasing the lung's total burden of inhaled particles and gases [57-58]. Smoking during pregnancy may also pose a risk for the fetus, by affecting lung growth and development in utero and possibly the priming of immune system [59-60].

The risk of developing COPD in smokers is dose-related, while the age at which the smoker begins to smoke, the number of smoked cigarettes in pack per year and current smoking status are predictive of COPD mortality. As aforementioned, not all smokers develop clinically significant COPD, which suggests that genetic factors are able to change the individual risk of disease [47].

Occupational exposures, including organic and inorganic dusts and chemical agents and fumes, are an underappreciated risk factor for COPD [61-63]. An analysis of the large U.S. population-based NHANES III (National Health and Nutrition Examination Survey) survey of almost 10,000 adults aged 30-75 years estimated the fraction of COPD

attributable to work was 19.2% overall, and 31.1% among never-smokers [64]. These estimates are consistent with a statement published by the American Thoracic Society that concluded that occupational exposures account for 10-20% of either symptoms or functional impairment consistent with COPD [65].

Wood, animal dung, crop residues, and coal, typically burned in open fires or poorly functioning stoves, may lead to very high levels of indoor air pollution. Evidences continue to grow that indoor pollution from biomass cooking and heating in poorly ventilated dwellings is an important risk factor for COPD [66-72]. Almost 3 billion people worldwide use biomass and coal as their main energy source for cooking, heating, and other household needs, so the population at risk worldwide is very large [69] [73].

High levels of urban air pollution are harmful to individuals with existing heart or lung disease. The role of outdoor air pollution in causing COPD is unclear, but appears to be small when compared with that of cigarette smoking. It has also been difficult to assess the effects of single pollutants in long-term exposure to atmospheric pollution. However, exposure to air pollution from fossil fuel combustion, primarily by car emissions in urban areas, is associated with reduction of respiratory function, and it remains one of the major source of health risk, as confirmed by insertion of outdoor particulate matter (PM) in Group 1 carcinogens (agents certainly carcinogenic to humans) by the International Agency for Research on Cancer (IARC) [74-75]. The relative effects of short-term, high-peak exposures, and long-term, low-level exposures, are yet to be resolved.

In estimating the risk of developing COPD, it is important to think in terms of the total burden of inhaled particles (**Figure 7**).

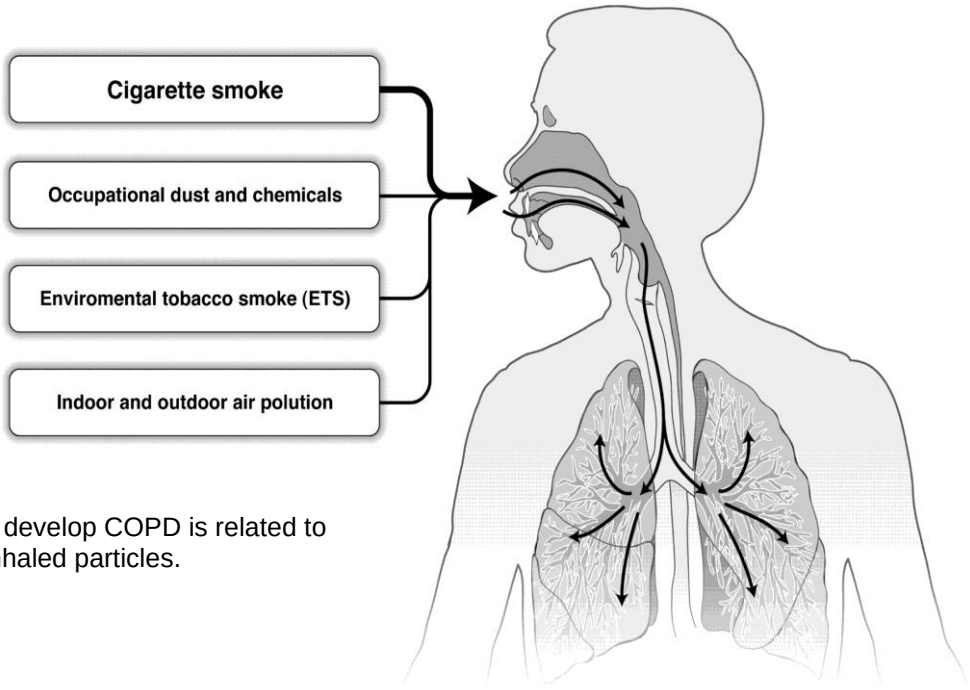

Figure 7. The risk to develop COPD is related to the total amount of inhaled particles.

Oxidative Stress - The lungs are continuously exposed to oxidizing substances, either endogenously produced, starting from phagocytes and other cell types, either exogenously produced, by environmental pollutants or by cigarette smoke. Moreover, intracellular oxidants, such as those derived from the electron transport chain in the mitochondria, are involved in many cellular pathways of signal transduction [76].

Under physiological conditions, the production and detoxification of oxidants are more-or-less balanced, in order to maintain a state of homeostasis (redox homeostasis), but when the balance oxidants/antioxidants shifts in favor of the first (excess of oxidants or depletion of antioxidants), oxidative stress occurs.

Oxidative stress is a pathological condition characterized by excess of oxidants that, through oxidative damage to proteins, lipids, nucleic acids, causes cellular toxic effects, leading to tissue injury and inflammation that contribute to aging and disease (cardiovascular diseases, pulmonary diseases, autoimmune diseases, neural disorders and cancer) [77]. It has been shown that, the generation of ROS and the consequent oxidative stress represent an important toxicological mechanism in respiratory diseases. The mechanism includes both, effects dependent on factors belonging to the particles that come into contact or are deposited on the surface of epithelial cells of respiratory tract (shape, size, solubility, reactivity, catalysis by transition metals and reduction of quinone species), and cell-dependent (ability to increase the endogenous production of ROS, alterations of signal transduction pathways, inflammation) [78].

Lung, as the organ of gas exchanges, is the seminal point of exposure to oxygen and environmental toxicants, so, a huge amount of oxidants contribute to increase oxidative stress, triggering the initiation and progression of diseases like COPD, asthma, cystic fibrosis, idiopathic pulmonary fibrosis and lung cancer.

In the lung, oxidative stress has many negative consequences that include: activation of inflammatory genes, inactivation of antiproteases, stimulation of mucus secretion and increased plasma exudation. Many of these effects are mediated by nitrogen peroxide that is formed by the interaction of superoxide anions ($O_2^{\cdot -}$) and nitric oxide (NO). The nitric oxide is generated by inducible nitric oxide synthase and expressed in the peripheral airways and lung parenchyma of COPD patients. Oxidative stress may also be responsible for reduction of histone deacetylase activity in lung tissue of COPD patients, and this leads to increased expression of inflammatory genes and to reduction in the glucocorticosteroids anti-inflammatory activity [79].

Important consequence determined by oxidative stress, as mentioned above, is the inactivation of antiproteases, and then the alteration of the protease-antiprotease balance (**Figure 8**). The elastin degradation (a major component of the connective tissue in the lung parenchyma) mediated by proteases, is an important feature of emphysema and is likely to be irreversible.

As consequence of free radicals exposure, the body has developed a variety of defense mechanisms against oxidative stress. These include: preventive and repair mechanisms, physical and antioxidant defenses [80]. In COPD patients there is also a decline in Nrf2-regulated antioxidants, as consequence of reduced activity of transcription factor Nrf2 [24].

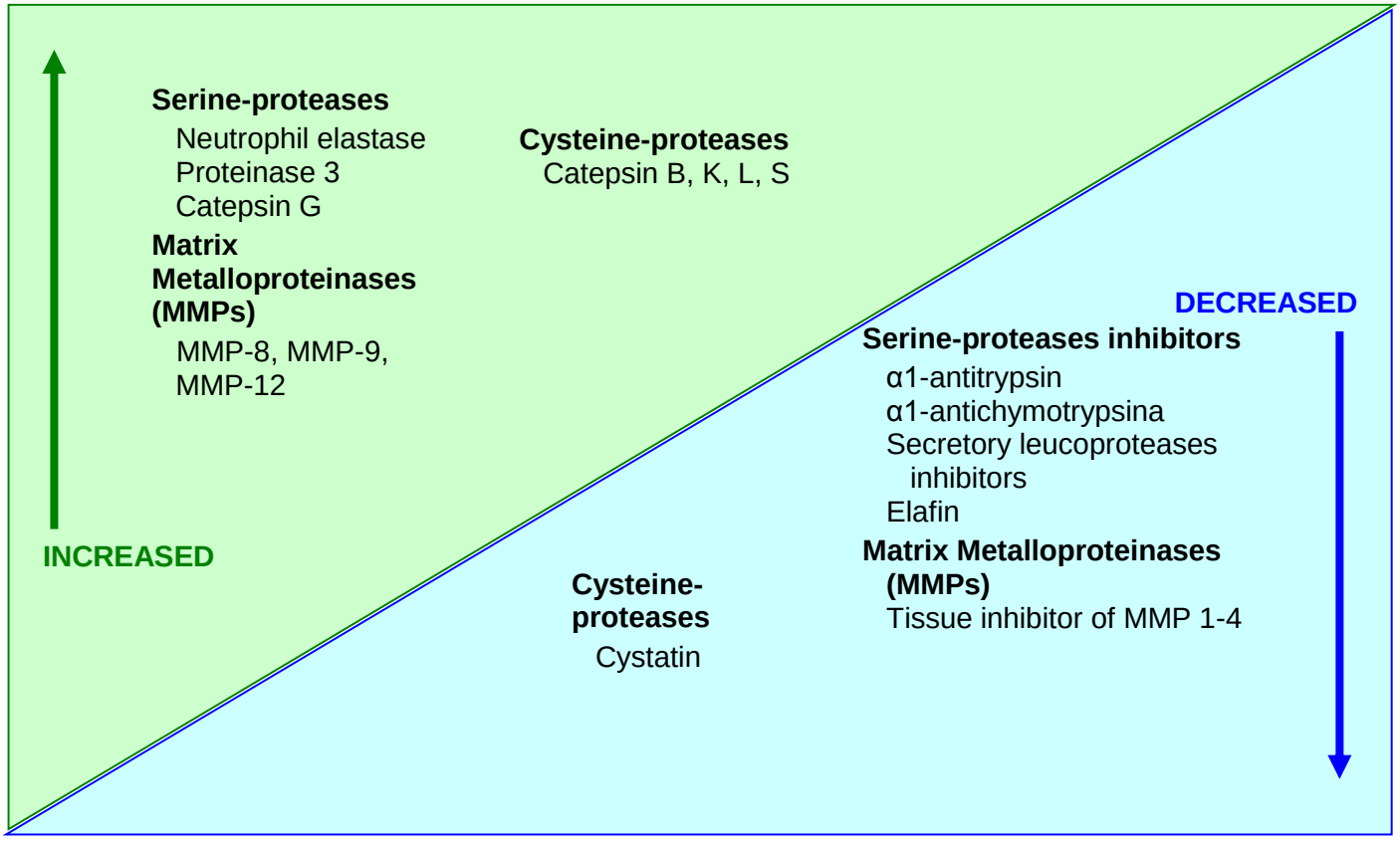

Figura 8. Proteases ed antiproteases involved in COPD.

Lung growth and development - The lung growth is related to processes occurring during pregnancy and birth and to environmental exposures occurring during childhood and adolescence [81-82]. Any factor that affects lung growth during pregnancy and childhood has the potential to increase individual risk for the development of COPD [83]. For example, a large number of studies in meta-analysis have confirmed the association between birth weight and FEV1 in adulthood [84], and several studies have found an effect of early childhood lung infections.

Age and Gender – Age is often listed as a risk factor for COPD. It is unclear if healthy aging as such leads to COPD or if age reflects the sum of cumulative exposures throughout life.

The role of gender in the risk of developing COPD is not yet clear. In the past, most studies showed that COPD prevalence and mortality were higher among men than women, but data from developed countries [85-86] show that the prevalence of the disease is now almost equal in men and women, probably reflecting the changing patterns of tobacco smoking. Some studies have even suggested that women are more susceptible to the effects of tobacco smoke than men [87-90].

Infections - Viral and bacterial infections may contribute to the pathogenesis of COPD, as well as episodes of exacerbation. Several studies have shown that an history of severe respiratory infections during childhood is associated with reduced lung function and increased respiratory symptoms in adults [81] [91]. Susceptibility to infections plays a role in exacerbations of COPD but the effect on the development of the disease is less clear. Tuberculosis has been found to be a risk factor for COPD [39] [92].

Asthma - Asthma can be a risk factor for COPD, although the evidence is not conclusive. An epidemiological study showed that adults with asthma were found to have a twelve-fold higher risk of acquiring COPD over time than those without asthma, after adjusting for smoking [93]. A second study on people with asthma showed that around 20% of subjects developed functional alterations related to COPD and irreversible airflow limitation [94].

Chronic Bronchitis In the seminal study by Fletcher and coworkers, chronic bronchitis was not associated with decline in lung function [95]. However, subsequent studies have found an association between mucus hypersecretion and FEV1 decline [96], and in

younger adults who smoke the presence of chronic bronchitis is associated with an increased likelihood of developing COPD [97-98].

Socioeconomic status - Poverty is clearly a risk factor for COPD but the components of poverty that contribute to this are unclear. Socioeconomic status is inversely proportional to the risk of developing COPD [99], although it is unclear whether this pattern reflects exposure to environmental pollutants, poor nutrition, crowding, poor nutrition, infections or other factors closely related to low socioeconomic status [100].

Nutritional status - The nutritional status as independent risk factor for development of COPD is not completely clear. It is known that malnutrition and weight loss can reduce the length of the respiratory muscles, while animal studies have shown an association between emphysema and starvation [101].

"There is no such thing as an average person, we are all genetically and biologically unique. But when sperm meets egg, our characteristics are not locked in stone. Bad genes do not necessarily cause disease by themselves, and nutrition and environment can alter the outcome."

CHAPTER 2

Population-based case-control study to assess the involvement of microsomal epoxide hydrolase in COPD onset and severity

2.1. METABOLISM OF FOREIGN COMPOUNDS

2.1.1. Introduction

When any exogenous substance (xenobiotic) enters into an organism, it is recognized as foreign and it needs to be metabolized (transformed) to facilitate the elimination.

The term metabolism, or biotransformation, refers to the set of processes by which an exogenous substance is enzimatically transformed by living organisms.

During the course of evolution living organisms have learned how to defend themselves from the toxic molecules, developing enzyme systems, very simple or acting connected each other, that modify the structure of xenobiotics making them easy to eliminate. In "higher organisms", this is achieved through a complex series of biochemical reactions that tend to deprive the substances of those characteristics that make them attractive to elective places of deposit or for the sites of chemical bond, by decreasing the biological half-life and increasing the electric charge and water solubility. The physical property that facilitate the absorption of a xenobiotic (lipophilicity) is modified in order to facilitate the excretion (hydrophilicity) in the urine or faeces; an exception to this general principle is the removal of volatile compounds, which occurs through the exhalation.

The xenobiotics metabolism take place primarily in the liver cells and, to a lesser extent, in other organs such as the kidneys, lungs, gastrointestinal tract, skin and plasma.

The liver is located in a strategic position in order to drain toxic compounds from the body, once they have been absorbed along the gastro-intestinal tract. In fact, the blood, that perfuses the gastrointestinal tract, gathers into the portal vein, which is directly connected with the liver. The liver, therefore, avoids substances to enter immediately into the systemic circulation and consequently avoids molecules distribution in different parts of the body.

The liver has also the ability to convey the toxic metabolites through the bile into the intestine, where they can be excreted through faeces or they can be reabsorbed, heading for an active enterohepatic circulation.

The molecules excreted through the bile can undergo the enzymatic activity (reactions) of the gut microbiota, that gives back to the molecule the original features that enable it to be reabsorbed by the gastrointestinal tract and come back to the liver. This is the case of a large number of substances that are conjugated with glucuronic acid in the liver and that once poured into the intestine undergo the β-glucuronidase reaction.

The chemical modifications resulting from xenobiotic biotransformation may affect the biological properties of xenobiotics in different ways: through elimination of exogenous (but also endogenous) compounds, activation of inactive molecules, and control the duration of a pharmacological activity. For example, some drugs are converted into active metabolites able to exert therapeutic or toxic effect. However, in most cases, biotransformation ends the pharmacological effect of an active drug and reduces the toxicity of a xenobiotic. Enzymes that catalyze the biotransformation reactions are often crucial in the intensity and duration of drug action, and play a critical role in the toxicity and carcinogenesis induced by chemicals.

Xenobiotics, or their reactive metabolites resulting from biotransformation reactions, can form covalent bonds with endogenous macromolecules, such as functional proteins (enzymes), genetic material (DNA) or macromolecules such as tRNA or mRNA. These bonds are irreversible and may damage the cells producing cytotoxic and life-threatening effects or interfering with cell cycle regulation; this can lead to an uncontrolled cell proliferation that can promote a carcinogenic effects.

The electrophilic compounds interact with the target molecules through the formation of intermediates carbocation or transition complexes energetically unstable. These reactions lead to the formation of covalent bonds (alkylation) with molecules that show nucleophiles sites such as phosphoric, aminic, sulfidrilic, hydroxylic, carboxylic, imidazole groups.

In many cases biotransformation enzymes are constitutively expressed, but it has been found that the synthesis of these enzymes can be activated by xenobiotics. Some drugs (e.g. barbiturates), and also molecules that result from environmental pollution, such as polycyclic aromatic hydrocarbons (benzo(a)pyrene, methylcholanthrene) or halogenated pesticides (DDT, polychlorinated biphenyls, dioxins), have the ability to induce the smooth endoplasmic reticulum proliferation, increasing the biotransformation enzymes. This phenomenon, typical in the centrilobular area of hepatocytes, is called enzymatic activity

induction and is believed to be the principal mechanism by which the body detoxifies foreign substances (e.g. Phenobarbital, environmental pollutants- CYTP450). The opposite phenomenon is the enzymatic activity inhibition (eg. Grapefruit juice - CYTP450). In both cases, the toxicological implications are important, because the enzymatic activity induction and the enzymatic activity inhibition can modify the speed of bioinactivation or bioactivation of potentially toxic compounds.

The stereochemical properties impact the interaction between a xenobiotic and the biotransformation enzyme. Many xenobiotics, especially drugs, have one or more chiral centers and exist in two mirror images called: enantiomers or stereoisomers. In some cases the biotransformation of chiral xenobiotics is stereoselective, and this means one stereoisomer is biotransformed faster than its enantiomer.

A further feature that can determine a potential toxicity associated with biotransformation enzymes in the xenobiotics metabolism is the human genetic variability. Both genotypic (genetic polymorphisms) as well environmental and physiological factors influence the expression of biotransformation enzymes (**Figure 1**).

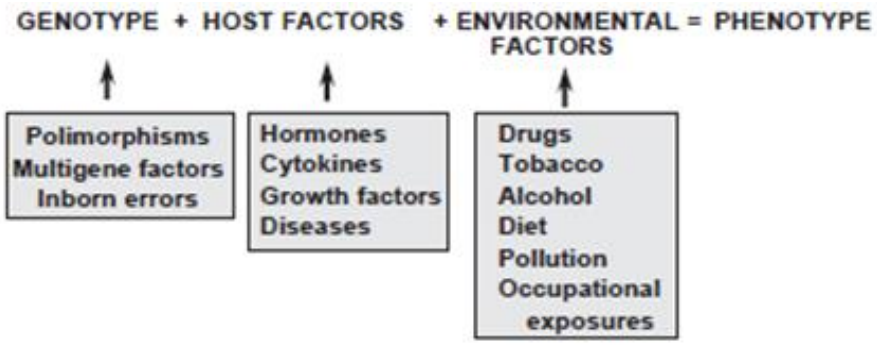

Figure 1. Determinantsof interindividual variability of xenobiotic metabolism.

The structure (in terms of amino acid sequence) of a specific biotransformation enzyme may differ between two individuals, and this feature may be the cause of differences in the speed of xenobiotics transformation.

Several genetic polymorphisms are known to easily explain large part of the different reactions to xenobiotics observed between individuals and between different populations. For example, in the 70s the administration of *debrisoquine*, antihypertensive drug, in a volunteer subject led to a dramatic reduction of the blood pressure. Through studies it was established that the increased hypotensive activity of the drug derived from a reduced

hydroxylation of the *debrisoquine*, and that was dependent, in that subject, on a low activity of the cit. P-450 isoform involved in its biotransformation [102]. Individuals with a genetically determined enzyme deficiency that can lead to a reduced xenobiotics biotransformation, are called slow metabolizers.

Different enzyme isoforms have different physical properties and substrate specificity. To date, for example, in humans up to 21 families, 20 subfamilies and 57 genes of cytochrome P-450 have been described. Out of these CYP 1, 2 and 3 account for 70% of total hepatic CYPs content and are responsible for 94% of drugs metabolism in liver [103].

The xenobiotics biotransformation dependent on a limited number of enzymes that have a wide substrate specificity, since they must be able to react on a wide variety of substrates.

The enzyme systems involved in the biotransformation processes are called: Phase I and Phase II reactions. In some cases, however, the produced metabolites are more toxic than the parent compound and the set of these reactions is called bioactivation reactions or phase III reactions.

2.1.2. Biotransformation reactions and related enzymes: distribution and localization

The enzymes for xenobiotics biotransformation are widely distributed in the body and they are present in different subcellular compartments. In vertebrates, the liver is the main site of biotransformation, and consequently presenting a high concentration of enzyme systems. Other tissues, such as those involved in the major routes of exposure to xenobiotics: skin, lungs, nasal mucosa, eye, gastrointestinal system, kidney, adrenal gland, pancreas, spleen, heart, brain, ovary, testicles, placenta, plasma, erythrocytes, platelets, intestinal microflora have biotransformation activity, however their metabolizing ability is somewhat limited, and in general their contribution to detoxification is low.

At the subcellular level, enzymes (and their cofactors) involved in biotransformations are mainly located in the membrane of smooth endoplasmic reticulum (microsomes) or in the soluble fraction of the cytoplasm (cytosol), while smaller amounts are found in the mitochondria, nuclei and lysosomes.

Biotransformation enzymes are therefore described as cytosolic or microsomal to indicate their specific subcellular localization. Phase I reaction enzymes are predominantly microsomal, this is because most of the xenobiotics are fat-soluble, so they easily dissolve in the lipid bilayer of the cell membranes where the interaction between the xenobiotic and

biotransformation enzymes takes place. The Phase II reaction enzymes interact with hydrophilic substrates and they are generally cytosolic.

The reactions catalyzed by enzymes for xenobiotics biotransformation reactions are generally divided into four categories: hydrolysis, reduction, oxidation and conjugation (**Figure 2**).

The reactions of hydrolysis, reduction and oxidation, called Phase I reactions, expose or introduce a functional group (-OH, -NH2, -SH or -COOH) into the xenobiotic and they usually determine only a modest increase of hydrophilicity. Most Phase I reactions consist in oxidation reactions catalysed by two groups of monooxygenases, i.e. cytochrome P450-depending monooxygenases and flavin monooxygenases (FMN), as well as reductions catalysed by P450 reductase, other reductases and hydrolases (**Table 1**).

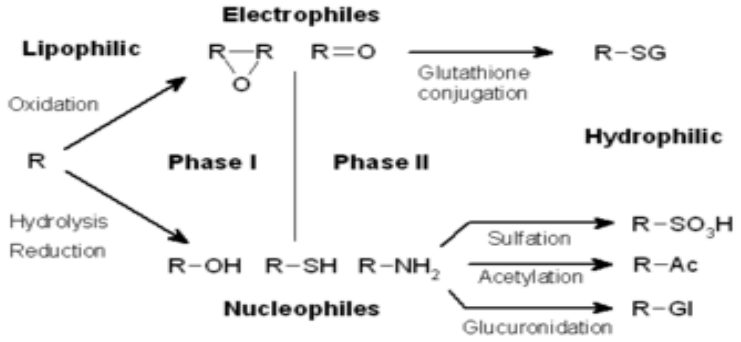

Figure 2. Phases I and II of the metabolism of a lipophilic xenobiotic.

Table 1. Main Phase I reactions and related enzymes		
REACTION	**ENZYME**	**LOCALIZATION**
Function Mixed Oxidase	Cyt. P-450	Microsomes
Function Mixed Oxidase	FMO	Microsomes
Oxidases/Dehydrogenases	Various	Cytosol/non-microsomal
Co-oxidations	Prostaglandin H Synthase	Cytosol/non-microsomal
Reductases	Cyt. P-450	Microsomes
Reductases	Various	Cytosol/gut microbiota
Hydrolases	Various	Cytosol/microsomal

The conjugation reactions, called Phase II reactions (**Figure 2**), consist in conjugation of products of Phase I transformation with endogenous molecules which determine a

substantial increase in hydrophilicity of the xenobiotic and making it easily removable through the urine, bile, faeces.

The most important conjugation reactions are those with glucuronic acid, sulfuric acid, amino acids, and with glutathione. Also methylation and acetylation are conjugation reactions, although they generally result in a decreased hydrophilicity of the substrate. Phase II xenobiotic metabolizing enzymes are mostly transferases and include: UDP glucuronosyltransferases (UGTs), sulfotransferases (SULTs), N-acetyltransferases (NATs), glutathione S-transferases (GSTs) and various methyltransferases (mainly thiopurine S methyl transferase (TPMT) and catechol O-methyl transferase (COMT).

This conjugation process requires energy, therefore, availability of highly energetic molecules such as ATP, both for substrate and co-factors activation.

2.1.3. Cytochrome P450

The cytochrome P450 (CYP450) is particularly studied. The term P450 is derived from the spectrophotometric peak at the wavelength of the absorption maximum of the enzyme (450 nm) when it is in the reduced state and complexed with CO.

The cytochrome P450 constitutes a superfamily of enzymes presents in some prokaryotes and in all eukaryotes, and that has evolved and diversified during the transfer of primordial life from the aquatic to the terrestrial environment. During the evolutionary process, these enzymes specialized from the metabolism of endogenous substances, to metabolize xenobiotics that were present in plants and who could potentially create an hazard if ingested by a more complex organism.

The cytochromes P-450 are heme proteins (containing ferroprotoporfirina IX) and they constitute a class of isoenzymes of molecular weight in the range 45-60 kDa. The cytochrome P450 system is actually a complex of two enzymes inserted into phospholipidic matrix of smooth endoplasmic reticulum: the NADPH-cytochrome P450 reductase and cytochrome P-450, existing in different enzymatic isoforms.

The oxidation via the microsomal system is characterized by two substrates: the molecular oxygen and the exogenous or endogenous compound. The complex is called mixed-function oxidases because, from the oxigen molecule activated an atom is reduced to water and the other one is inserted into the substrate, oxidizing it.

Cytochrome P450 is a transmembrane protein located in the smooth endoplasmic reticulum and it is attached to a type "channel" structure. In this way, the cytochrome P-

450 may interact with the substrates that access to the channel with relative low specificity but high concentration.
In presence of enzyme inducers the amount of cytochrome P-450 increases, also because of the concomitant proliferation of smooth endoplasmic reticulum, thus offering more targets to the different molecular species subject to biotransformation.
Although the cytochrome P-450 is classified as an oxidase it also has reductase activity. The activity of the cytochrome P-450 is inhibited by carbon monoxide.

2.1.4. Hydrolases

The hydrolases are a class of enzymes that react with compounds which contain an ester bond and are classified into: arilesterasi, that hydrolyze aromatic esters, carboxylesterase that hydrolyze aliphatic esters, cholinesterase that hydrolyze esters in which the alcohol component is choline, and acetylcholine esterase that hydrolyze esters in which the acid component is constituted by acetic acid. In particular, the epoxide hydrolases play a crucial role in the detoxification of electrophilic epoxides, that otherwise might bind to proteins and nucleic acids, causing cellular toxicity and genetic mutations. Indeed, the epoxide hydrolases, which are virtually localized in all tissues, catalyze the hydration of aliphatic epoxides and arene oxides to their corresponding trans-1,2-dihydrodiol, compounds less electrophilic than the original ones.
In some cases, however, the epoxide hydrolase may contribute to the bioactivation of xenobiotics, since the activity of these enzymes is stereoselective with respect to the formation of diols. One example is the combined activity of the oxidases and the epoxide hydrolases on benzo[a]pyrene (PAH), which involves the stereoselective formation of metabolites whose activity can be mutagenic (**Figure 3**). Benzo[a]pyrene undergoes epoxidation that can occur in three different ways with consequent formation of benzopyrene 4,5-oxide, 7,8-oxide and 7,8-dihydrodiol-9,10-epoxide. In the latter product the benzyl hydroxide in position 7 and the epoxide oxygen take on a trans position which makes the compound itself less attackable from epoxide hydrolases. The tumorigenic activity of this product is more powerful than all other stereoisomers and seems to depend on the ability of the carbon atom C10 to act as carbocation on the nucleophilic components of DNA.

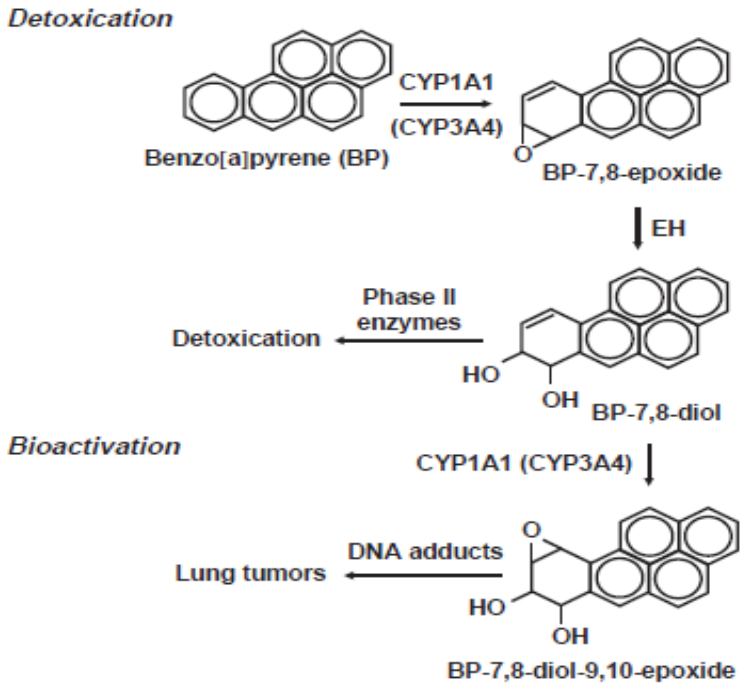

Figure 3. Role of P450 in the bioactivation of the pre-carcinogen benzo[a]pyrene. Benzo[a]pyrene (BP) ismetabolis ed by P450 enzymes (CYP1A1 and CYP3A4) to BP-7,8-epoxide, which is subsequently converted into BP-7,8-diol by epoxide hydrolase (EH), and into BP-7,8-diol-9,10-epoxide by CYP1A1. BP-7,8- diol-9,10-epoxide isa reactive metabolite that covalently interactswith DNA.

In mammals there are five distinct forms of epoxide hydrolases: microsomal (mEH or EPHX1), soluble (sEH or EPHX2), cholesterol, the LTA4 hydrolases and epossiline hydrolases. The last three forms hydrolyze exclusively endogenous epoxides, they have a high substrate specificity and have no role in the metabolism of oxides xenobiotics. In contrast, the microsomal (mEH) and soluble (sEH) forms hydrolyze a wide variety of substrates, including many alkene epoxides and arene oxides. These two forms generally share the same cellular localization with the enzymes of the Cytochrome P-450 family, often responsible for the production of toxic epoxides. This likely ensures the rapid detoxification of alkene epoxides and arene oxides generated during oxidative biotransformation of xenobiotics.

The epoxide hydrolase is one of many inducible enzymes in liver microsomes, and its induction is invariably associated with cytochrome P-450.

2.2. PULMONARY METABOLISM OF FOREIGN COMPOUNDS

2.2.1. Introduction

While the liver has been recognized as the major site of drug and xenobiotic metabolism, increased attention is also paid to the metabolism of xenobiotics by extrahepatic tissues, in particular, those tissues, such as lung, intestine, and skin, which are markedly influenced by the environment, dietary status, and exposure to other chemicals.

Inhalation represents one of the major routes by which the body enters in contact with gases, as well as solids and liquids suspended in the air. The very large surface area of the alveoli (about 70 m^2), besides being ideally suited for the function of gas exchange, also facilitates the penetration into the body of potentially toxic agents, and since the entire cardiac output passes through the lungs, all chemicals present in the circulation must also traverse the lungs. The lung, therefore, is a primary target organ for toxic inhaled compounds, and many of these chemical substances pose a risk to the lung as they include specific pneumotoxins and carcinogens.

Occupational, accidental or prolonged exposure to a great variety of exogenous chemicals may result in acute or delayed injury to cells of the respiratory tract. Some examples of harmful organic chemicals include polycyclic aromatic hydrocarbons (PAHs), aromatic amines, halogenated compounds, aliphatic compounds, aldehydes, and ketones. Many of those compounds can be found in significant concentrations in the air of urban and industrial settings (either the gas/vapour state or adsorbed onto respirable particles), and in cigarette smoke [104-106]. Not surprisingly, many of those foreign chemicals, and also biological agents to which the airways are exposed, have been implicated in a wide variety of diseases of the respiratory tract, for example, lung cancer (tobacco smoke, benzo(a)pyrene, nitrosamines, polonium-210, chromates, nickel and arsenic); chronic bronchitis and emphysema (cigarette smoking and air pollution); diffuse pulmonary fibrosis (busulfan, bleomycin, nitrofurantoin, methysergide, paraquat, methylphenylethylhydantoin, and diphenylhydantoin); and phospholipidoses (chlorphentermine).

The lung has a significant capability of biotransforming many foreign compounds with the aim of reducing its potential toxicity by Phase I and Phase II reaction enzymes.

While much of what is known about the xenobiotic metabolizing enzyme systems comes from studies on the liver, comparable work on the lung emphasizes the similarities rather than the diversities of this enzyme system in different tissues.These differences may, in

part, be due to the presence of different isozymes of cytochrome P-450.
It is difficult to assess the contribution of pulmonary metabolism to the overall metabolism of a compound. In most cases, in vitro enzymic activities of liver are significantly higher than those of lung, but these differences may be offset in vivo by other factors such as blood flow and distribution.

2.2.2. Lung Toxicity

The mechanisms by which xenobiotics cause damage to pulmonary tissue is a complex and partially characterised issue. Complexity arises because of the heterogeneity of the lung, containing over 40 different cell types, and the remarkable variety in cell functionality [107].
Functions range from gas exchange by epithelial alveolar cells, secretory cells with cilia, designed to move foreign particles up to tracheobronchial tract, to endothelial cells that line the pulmonary vasculature, providing a junction between bloodstream and respiratory cells. Each of these cells, and the function they sustain, is a potential target for toxic action. The most susceptible lung cells are capillary endothelial cells, pulmonary alveolar macrophages, non-ciliated bronchiolar epithelial cells (Clara cells), ciliated bronchiolar epithelial cells, and type I and type II alveolar epithelial cells [105] [108].
The cellular heterogeneity of the lung presents enormnous difficulties to the isolation of all the many cell types in sufficient yield and viability required for metabolic studies. Another issue that make more complex understanding mechanisms involved in xenobiotics-induced pulmonary tissue damage is the limited knowledge about the potential toxicity of many chemicals present in our environment. A significant number of chemicals produced in the range 2–100 ton/year and used in industrial processes are insufficiently known in terms of their potential toxicity. Among them, there are many compounds for which the available toxic information and potential human health risks associated with their inhalation is almost inexistent. Awareness on this problem has been raised by the European Union, by promoting the REACH-program (http://ec.europa.eu/environment/chemicals/reach/reach).
Althought a complete understanding of how a compound may induce cell damage is lacking, there is a cumulative experimental evidence of the role of xenobiotic metabolism as a cause of lung toxicity.

In general, biotransformation reactions are beneficial, helping the pulmonary tissues to eliminate foreign compounds. Sometimes, however, these enzymes transform an otherwise harmless substance into a reactive form. Results of several studies indicate that P450-mediated oxidations frequently result in the generation of more reactive, and frequently more toxic, intermediates (i.e. electrophiles, pro-carcinogens), a process known as metabolic bioactivation (**Figure 4**). Thus, many compounds that elicit toxic injury to the lung are not intrinsically pneumotoxic, but cause damage to target cells following metabolic activation. Classic examples are the activation of benzo[a]pyrene, which is a constituent of tobacco smoke and combustion products, or N-nitrosamines into reactive forms capable of binding to DNA and eventually leading to cancer formation. As the resulting intermediates of biotransformation are highly reactive and unstable, they tend to exert toxicity in situ rather than in distant tissues.

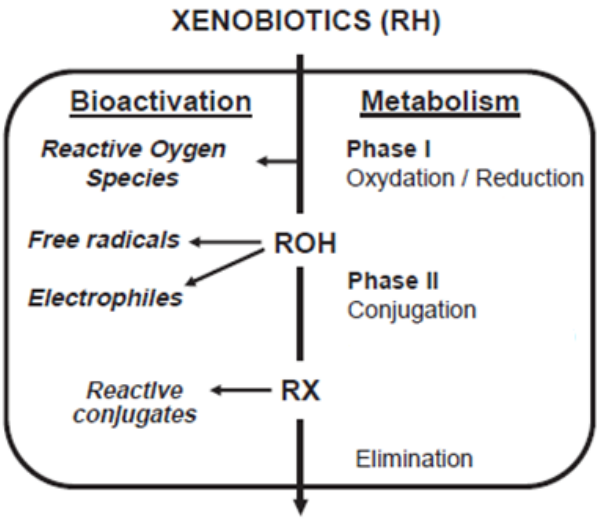

Figure 4. Metabolism and bioactivation of xenobiotics. Phase I reactionscan generate more reactive metabolitesthan the parent compound. Phase II reactions tend to render more water-soluble and less active metabolites, however, bioactivation can also occurs. GST: glutathione S transferase; UGT: UDP glucuronyltransferase; EH: epoxide hydrolase; ST: sulphotransferase; NAT: N acetyltransferase.

The xenobiotic metabolic activation may take place in the lung or in another tissue such as liver. The possible contribution of extrapulmonary metabolic activation of chemicals to metabolites that are toxic to the lung will depend, in part, on the relative stability of such metabolites and the inherent susceptibility to toxicity of the lung compared to other tissues. Alternatively a stable, proximate, toxic metabolite may be formed in an extrapulmonary site, transported to the lung, and then metabolized to the ultimate toxic form. Finally, the

lung may be responsible for the formation of the toxic metabolite from the parent chemical (**Figure 5**).

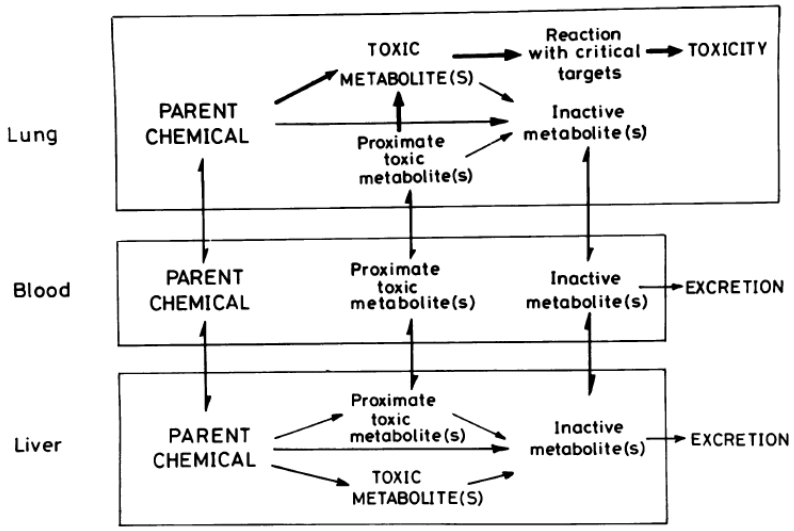

Figure 5. Toxicity mediated by reactive metabolites formed in the lung either from the parent chemical or from proximate toxic metabolite. If the toxic metabolite is chemically very reactive, it may have to be generated in situ in the lung in order to exert toxicity. Depending on the metabolic capability of the tissue, the metabolic activation by the parent chemical may be completely carried out in the lung. Alternatively, part of the metabolic activation may be carried out in other tissues, such as the liver, but the ultimate toxic metabolites are formed in situ in the lung.

The site and importance of the pulmonary injury ultimately depends on factors such as the concentration of the reactive agent within lung, the existence of an adequate pulmonary detoxication pathway, and the bioactivation to a more toxic species. These factors also determine which specific type of lung cells will be preferentially damaged [109]. Toxicity in the target cell occurs when metabolic activation is followed by inappropriate detoxification of the reactive metabolite, which is normally achieved by Phase II reactions. In such cases, toxicity reflects the unbalance between activation and detoxification reactions [110]. Some of the activating and deactivating enzymes and their cofactors are shown in **Table 2**. Obviously, the relative importance of these will differ for different chemicals. It is also important to note that many of these enzyme activities may be altered by various environmental factors such as air pollution, cigarette smoking and diet, thus potentially affecting the pulmonary metabolism of some chemicals and, thereby, possibly affecting their toxicity.

Assessment of the potential toxicity of new chemicals for man is still largely based on data obtained from studies *in vitro* and *in vivo* with experimental animals. However, the well-known species differences in biotransformation enzymes raises concerns about the suitability of animal data for predicting lung toxicity in humans as a result of bioactivation

reactions. The development of human relevant in vitro models (i.e. cell lines from human pulmonary origin), can notably contribute to better understanding the basis of chemical-induced lung toxicity in man and, in particular, the role of pulmonary biotransformation enzymes in the bioactivation/detoxication processes.

Table 2. Balance of activating and deactivating enzymes and their cofactors.

Cytochrome P-450	NADH-cytochrome b5 reductase
Prostaglandin synthetase	Xanthine oxidase
Flavin-containing monooxygenase	Glutathione
	Glutathione peroxidase
	Glutathione S-transferase
NADPH-cytochrome P-450 reductase	UDP-glucuronosyltransferase
Catalase	Vitamin E
Superoxide dismutase NAD(P)H	Ascorbic acid

2.3. GENETIC SUSCEPTIBILITY TO COPD

2.3.1. Genetic polymorphisms

The existence of variations in the DNA sequence among different individuals - the so-called inter-individual genetic variability - is a phenomenon widely appreciated, proved and quantifiable in its qualitative and quantitative aspects thanks to the completion of the human genome sequencing, announced in 2000 by the Celera Genomics Group (The Human Genome Project).

Currently, it is believed that about 80% of the genes in humans contain sequence variations among individuals, that means, that genes are present in the form of different allelic variants. The main types of sequence variation in the genome are: insertions/deletions (ins/del) and single nucleotide polymorphisms (SNP - Single Nucleotide Polymorphisms) (**Figure 6**).

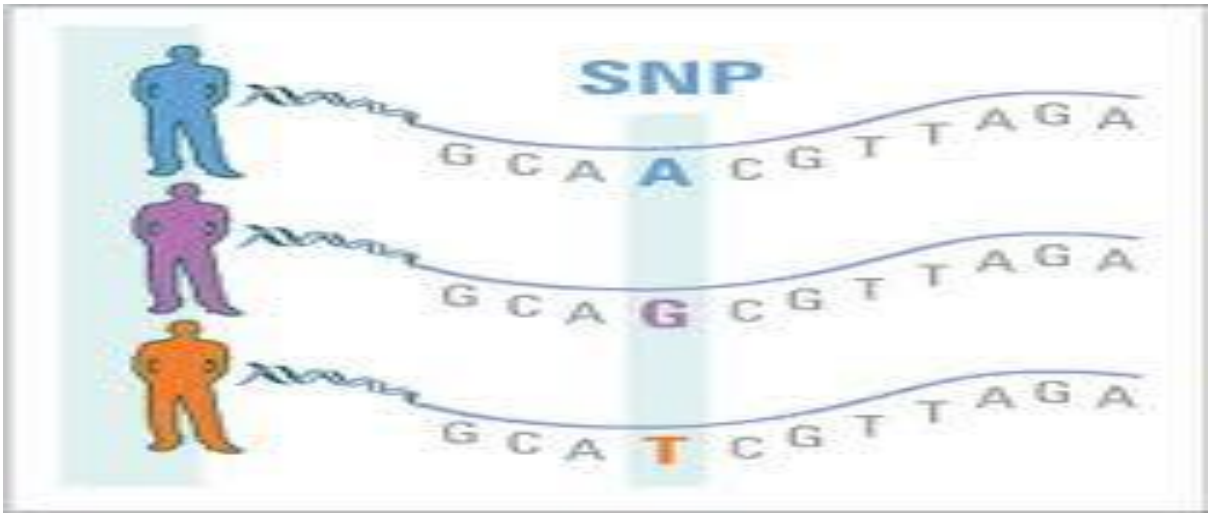

Figure 6. Single Nucleotide Polymorphism.

SNPs consist of a single nitrogenous base variation in a DNA sequence, so two individuals may have in the same position of their respective genomes, two different bases [111]. So far, more than 3.1 million SNPs have been characterized, and they are responsible for 90% of the genetic variability observed between individuals.

SNPs are classified into three groups, according to the position they occupy in the genome (**Figure 7**):

- **cSNP -** Variations in the coding regions, called exons; these SNPs may have different functional effects according to the involved nucleotide. If any change does not occur in the amino acid sequence of the protein, we talk about synonymous SNP, whereas if the nucleotide substitution changes the amino acid codon, it is called non-synonymous SNP, which can have effects on the structure, stability and function of the encoded protein; sometimes the cSNP may also lead to the introduction of a stop-codon, which leads to production of a truncated protein, generally inactive.
- **pSNP -** It is a SNP in perigenic regions. It affects the regulatory regions, such as promoters, enhancers, and splicing junctions. The possible effects include alterations in the protein expression, (as a consequence of the effects (direct action) on transcription, stability and translatability of the mRNA) and, sometimes, variations in the structure of the protein by interference with splicing mechanisms.
- **rSNP -** The random SNPs are located in intragenic regions, non-coding, which represent 90% of the whole genome. These SNPs have no direct effect on the protein but, considering the phenomenon of linkage disequilibrium, they can be employed for the identification of genes involved in different pathologies. The linkage disequilibrium is a key phenomenon for genome association studies in the human (associations between single-nucleotide polymorphisms and traits like major diseases), so, assuming that the association between the two is high, the presence of a given SNP can predict the presence of a second SNP associated with the onset of certain pathologies [112-113].

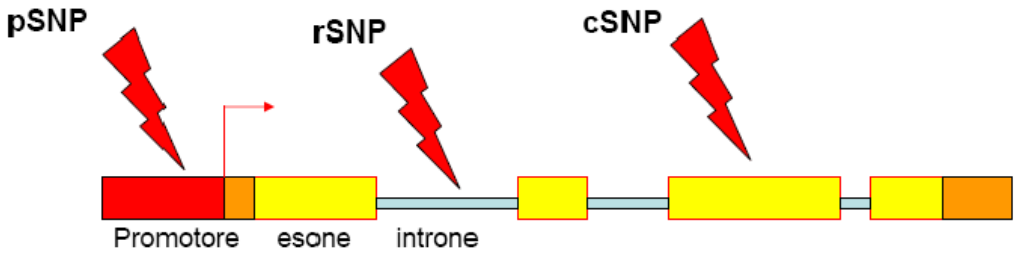

Figure 7. SNPs classification based on location inside genome.

2.3.2. Microsomal epoxide hydrolase (EPHX1)

Human microsomal epoxide hydrolase (EPHX1) is an evolutionarily highly conserved biotransformation enzyme expressed in nearly all tissues and localized mainly in the microsomal fraction of the endoplasmic reticulum of eukaryotic cells.

EPHX1 was the first characterized among the known epoxide hydrolases and it was first purified from rabbit liver by Watabe and Kanehira (1970). Human EPHX1 was then characterized by Oesch (1974) in human liver. Human EPHX1 gene orthologues have been found in 127 organisms. Humans possess two EPHX enzymes, namely microsomal EPHX1 and soluble EPHX2.

EPHX1 is an important part of microsomal defense mechanisms against toxicity of xenobiotics and accumulating knowledge suggests that the enzyme also has essential physiological roles. EPHX1 has a broad substrate selectivity and does play an important role in the detoxification of many reactive epoxide intermediates [114]. It tipically catalyzes the hydrolysis of epoxides to trans-dihydrodiols [115], and it is responsible for the detoxification of a wide variety of suspected genotoxins [116].

In certain instances, the initial trans-dihydrodiol metabolites are further activated by subsequent P450 catalysis to form highly electrophilic and reactive dihydrodiol-epoxides that, in a stereoselective manner, form covalent adducts with DNA [117]. Thus, EPHX1 is important for its dual functional role in detoxication as well as bioactivation processes. In particular there is great interest in EPHX1 because of its potential involvement in the bioactivation of carcinogenic polycyclic aromatic hydrocarbons [118].

2.3.2.1 EPHX1 gene

Human EPHX1 gene is located on chromosome 1 (1q42.12), consists of 9 exons, separated by 8 introns, and spans about 35 kb [119-122]. Exons 2–9 of EPHX1 encode three transcription variants differing in the 5′-untranslated region, while each translated protein product has 455 amino acids.

The regulation of EPHX1 gene expression is complex. Human EPHX1 expression in the liver is selectively driven by the proximal E1 promoter, but an alternative promoter region (E1-b promoter) drives expression in other tissues from both adult and fetal sources [123]. The gene sequence contains several Sp1/Sp3 (transcription factors) binding sites and there are two DNAseI hypersensitive sites (HS-1 and HS-2) in the intronic region between

E1b and E1 [124]. These elements take part in cell- and tissue-specific transcriptional regulation of EPHX1. The complexity of EPHX1 gene regulation also derives from a vast and diverse array of transcriptional factors binding to regulatory sequences (**Figure 8**).

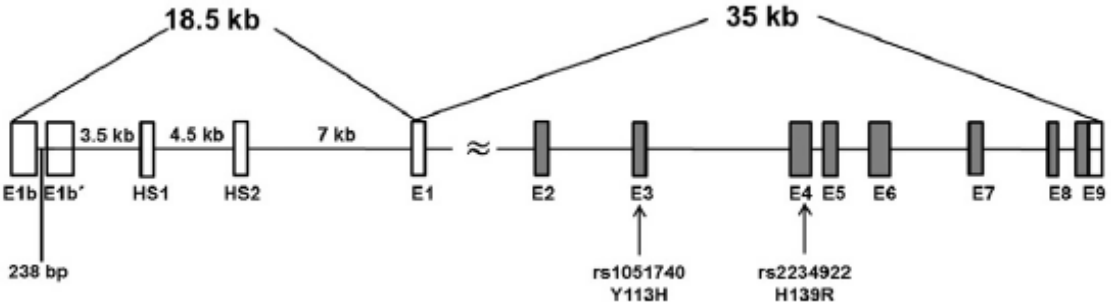

Figure 8. EPHX1 gene sequence and regulatory elements on chromosome 1 at position 1q42.12. E=exons, HS=DNAseI hypersensitivity sites, kb=kilobases, rs=refence SNP ID number. Coding exons are marked in gray.

Gene expression of EPHX1 in most tissues and anatomical compartments was demonstrated by microarray gene expression analysis and RNA sequencing (www.genecards.org). Human liver and skin express the highest EPHX1 transcript and protein levels. EPHX1 expression is tissue- [125], age-, and sex-specific [126], but also shows high inter-individual variation among humans [127-128]. EPHX1 transcripts were found in human primary bronchial epithelial cells, but not in alveolar macrophages [129]. Dysregulation of EPHX1 expression has been linked to several human pathologies including cancer. So, delineating the regulatory mechanisms of EPHX1 gene expression is key to understand the role of EPHX1 in human disease pathology and for predicting organ-specific toxicities.

Deleterious mutations and more common gene sequence variations such as single nucleotide polymorphisms (SNPs) can affect the physiological function of the protein product, and, in concert with environmental exposures, may have consequences for disease development or progression, especially in the lungs.

There are 142 EPHX1 gene variations currently listed in the National Cancer Institute dbSNP database (http://www.ncbi.nlm.nih.gov/SNP), of which several may have clinical significance (http:// www.ncbi.nlm.nih.gov/clinvar/).

The complexity of EPHX1 gene regulation, its expression pattern, and the presence of functional genetic variability suggest that individuals may considerably differ in the capacity of EPHX1 to metabolize diverse substrates with potential consequences for disease

pathophysiology. Transformation of this information into clinical application is, however, hindered by the lack of the crystal structure of human EPHX1 and by the complexity of unexplored relationships between its genotype and phenotype.

2.3.2.2. EPHX1 protein structure and enzyme function

EPHX1 is a member of the α/β hydrolases enzyme family, and comparisons of homologies among microsomal epoxide hydrolases from phylogenetically different organisms suggest their origin from a common ancestor [130-132]. The N-terminal part anchors the EPHX1 protein into the membrane, while the C-terminus contains catalytic residues. Although the three dimensional structure of human EPHX1 has not been characterized so far, the crystal structure of its orthologue from Aspergillus niger is available [133-134]. Deciphering the crystal structure of human microsomal EPHX1 is very important for further elucidation of structure-function relationships and prediction of mechanistic implications of EPHX1 gene variants.

EPHX1 appears to play an important role in organ-specific human physiology, and it is generally accepted that, in contrast to EPHX2 and other epoxide hydrolases, EPHX1 is more oriented toward the metabolism of xenobiotics compounds than endogenous substrates and has mostly a detoxifying function.

The mechanism of EPHX1 generally follows a mechanism similar to that of EPHX2, with the attack of the oxirane ring to yield an alkyl-enzyme intermediate followed by subsequent hydrolysis of the intermediate by water [135]. The EPHX1 catalytic cycle comprises a so-called catalytic triad, consisting of a His^{431}, Asp^{226}, and a Glu^{404} [136-137], that consists of fast nucleophilic attack of the substrate by EPHX1-Asp^{226} residue forming an enzyme-substrate ester intermediate and subsequent hydrolysis of the complex by water [138].

EPHX1 plays a dual role in the biotransformation of xenobiotics. While it detoxifies certain carcinogenic compounds, e.g., butadiene, benzene, and styrene [139], it can also activate procarcinogens such as polycyclic aromatic hydrocarbons [140-141].

EPHX1 has a broad substrate specificity [142] [116]. Typical substrates include toxic and procarcinogenic compounds, such as epoxide derivatives of 1,3-butadiene, benzene, aflatoxin B1, chrysene, nitropyrene, naphthalene, and anthracene, as well as commonly used anticonvulsant drugs, such as phenytoin and carbamazepine.

The most common environmental compound metabolized by EPHX1 are epoxide derivatives of polycyclic aromatic hydrocarbons (benzo[a]pyrene 4,5-oxide). The

dihydrodiol products of EPHX1 metabolism have been implicated as ultimate reactive carcinogens that are responsible for polycyclic aromatic hydrocarbon-initiated carcinogenesis. The importance of EPHX1 is underscored by data obtained from a EPHX1 knockout mouse model that show reduced carcinogenicity of 7,12-dimethylbenz[a]anthracene in knockout versus control animals [143].

EPHX1 may also play an important role in the endocannabinoid signaling pathway [144] and modulate, through its regulation, energy metabolism and immunity.

Enzyme induction and inhibition by both xenobiotics and endogenous substrates are an important phenomenon that may influence drug–drug interactions or disrupt important physiological processes.

Mouse and rat EPHX1 were shown to be readily inducible by xenobiotics in several animal studies [145-146]. EPHX1 expression was induced by phenobarbital, β-naphthoflavone, benzanthracene, and trans-stilbene oxide in human fetal hepatocytes in vitro [147]. Several polycyclic aromatic hydrocarbons [148] were shown to induce EPHX1 in precision-cut liver slices prepared from fresh human liver.

Inhibitors of EPHX1 have been developed and characterized, and divalent heavy metals were shown to inhibit EPHX1 enzymatic activity [149]. The most potent of the inhibitors was Zn^2+ and Hg^2+.

Enzyme stability is a potential source of variability in estimating the in vivo activity of EPHX1. The phenomenon of varying stability of polymorphic variants has been documented with other biotransformation proteins, including the soluble form of human epoxide hydrolase, EPHX2 [150]. Inherent allelic differences in protein stability may lead to altered rates of clearance of epoxide species in vivo. The relationship between EPHX1 protein stability and epoxide metabolism in vivo remains unclear, although it is likely that potential differences in enzyme stability, together with polymorphisms in the 5-flanking region affecting transcriptional rates [151], may combine to modify metabolism and clearance of epoxides. Results from several studies suggest that interactions between specific polymorphic loci, such as between EPHX1 and the cytochrome P450s [152], and/or between EPHX1 and the glutathione-S-epoxide transferases [153], will likely determine unique genotypes that are most highly susceptible to chemically-initiated diseases.

Further studies conducted on large population samples will required to thoroughly address these gene–gene interaction determinants.

Some investigators [154] provided evidence about substrate-specific variation for EPHX1 activity among different species, supporting the hypothesis that individual EPHX1 variants may possess unique substrate preferences and associated activity differences.

There exist certain well-characterized genetic polymorphisms in human EPHX1 [155-156]. The coding region of EPHX1 presents with two prominent genetic polymorphisms. The first, within exon 3, results in the substitution of Tyr with His at amino acid position 113; another, within exon 4, codes for the substitution of a His with Arg at amino acid position 139. In vitro cDNA expression studies indicate that EPHX1 enzymatic activity is decreased by approximately 50% in subjects with the His 113 allele (slow allele) and is increased by at least 25% in subjects with the Arg 139 allele (fast allele). The rare occurrence of both mutations together produces an enzyme with normal activity [156]. These data, together with results from additional studies [151] [128], suggest that differences in protein stability among the variant EPHX1 proteins may factor into the basis of observed interindividual differences in EPHX1 phenotype. Additionally, seven other 5'-flanking region genetic polymorphisms have been described [157], and may also impact EPHX1 gene transcriptional activity and resulting cellular phenotype.

2.3.2.3. EPHX1 and human diseases

The presence of inherited genetic variability affecting EPHX1 activity or dysregulation of its expression may contribute to the development of human diseases.

Mutations in EPHX1 may cause preeclampsia [158-159], hypercholanemia [160], and are suspected to contribute to fetal hydantoin syndrome [161] and diphenylhydantoin toxicity.

The most frequently studied SNPs Tyr113His (T337>C) and His139Arg (A416>G) were previously used as markers to predict EPHX1 activity [162]. However, their effect on enzyme activity in vitro is modest towards cis-stilbene oxide, none towards benzo[a]pyrene-4,5-epoxide, and was not confirmed in human liver microsomes [156] [163]. A detailed study of mouse brains has also shown that EPHX1 contributes to the cerebral metabolism of epoxyeicosatrienoic acids which could interfere with neuronal signal transmission [164], vasodilation, cardiovascular homeostasis, and inflammation [165]. A significant association of the low EPHX1 activity diplotype harboring the rs1051740 and rs2234922 SNPs with alcohol dependence was recently found [166] supporting the previously suggested role of EPHX1 genotype in the risk of alcoholic liver disease [167]. From the reviewed information it can be concluded that there is a

convincing link between EPHX1 dysregulation and neurological pathologies, including both degenerative disorders such as Alzheimer's disease and various forms of drug-dependence.

Despite considerable research on EPHX1-related physiological and pharmacological consequences for human health, most investigations involving EPHX1 have focused on its contribution to gene-environmental susceptibility to genotoxicity and carcinogenesis using both human and animal model studies. Studies on gene knockout mice models (EPHX1-null; EPHX1−/−) showed lack of bioactivation of 7,12-dimethylbenz[a]anthracene to the carcinogenic metabolite 3,4-diol-1,2-oxide by the EPHX1−/− mice consequently supporting the role of EPHX1 in bioactivation of certain polycyclic aromatic hydrocarbons [143].

Polymorphisms in EPHX1 may lead to differences in host-mediated bioactivation of procarcinogens resulting in differential susceptibility to cancers of various tissues. Studies suggested that the presence of EPHX1 SNPs may significantly affect the risk of lung, upper aerodigestive tract, breast, bladder, and ovarian carcinomas [168-175]. Numerous human epidemiological studies have examined the role of the polymorphism in EPHX1 and tumor formation [176-180]. These data suggest that mEH genotype is associated with altered risk of several types of cancers and pulmonary disease.

The most convincing evidence is currently available for lung and colorectal cancers, for which environmental exposures and gene–environment interactions are proposed to play major etiological roles, but the relevance of EPHX1 genetic variability for susceptibility to colorectal carcinoma remains an open question.

More convincing evidence exists in respect to exposure-related lung carcinoma risk. A recent meta-analysis on EPHX1 exon 3 SNP Tyr113His (rs1051740) has suggested an association of the His allele with increased lung carcinoma risk in Asian, but not Caucasian populations [181]. Another meta-analysis confirmed that this SNP may be a risk factor for lung carcinoma in Asians, but observed its protective effect in Caucasians as well [174]. Interestingly, genetically predicted (estimated using rs1051740 or rs2234922 SNPs) low EPHX1 activity was associated with an increased risk of developing tobacco-related cancer in smokers among 47,089 individuals from the Danish general population [182]. A further study reported that subjects exposed to environmental tobacco smoke and carrying low EPHX1 activity alleles had a significantly increased lung carcinoma risk [183]. Thus, the evidence for a link of tobacco exposure, EPHX1 genetic variability, genetic damage [184-185], and lung carcinoma risk seems particularly strong.

Besides cancers, there are interesting parallels with non-malignant diseases. A significant correlation between the two functional polymorphisms, rs1051740 and rs2234922, of the EPHX1 gene and the enzyme activity and the individual's susceptibility to chronic obstructive pulmonary disease (COPD) was noted. COPD is more frequent in smokers and together with the above discussion of EPHX1 and lung carcinogenesis, it seems that EPHX1 plays a pivotal role in protecting the lung against environmental exposures.

A comprehensive meta-analysis reports that EPHX1 113 mutant homozygote was significantly associated with an increased risk of COPD in Caucasian individuals, and the 139 mutant heterozygote was significantly associated with dicreased risk of COPD in Asian populations, but not in Caucasian populations. Pooled analyses revealed that, similarly to lung cancer, the slow and extremely slow EPHX1 enzyme activity were associated with an increased risk of COPD, while the fast enzyme activity was not associated with dicreased risk of COPD. The stratified analysis demonstrated this association in Caucasian, but not in Asian individuals [186]. A number of studies and meta-analysis have assessed the association between EPHX1 polymorphisms and COPD in different populations, however, the results are still inconsistent and controversial.

Genetic variability of EPHX1 is associated with several pathological phenotypes and may in concert with environmental exposures contribute to the development of malignancies, especially in the lungs.

2.4. AIM OF THE STUDY

Pathogenesis of COPD is still poorly understood, but is generally accepted that the pathogenic triad of oxidative stress, protease–antiprotease imbalance, and inflammation is relevant in disease onset and progression.

Lung damage can be attributed to an imbalance in the endogenous protease/antiprotease equilibrium, promoting tissue hydrolysis; examples of such imbalance include genetically determined alfa-1-antitrypsin deficiency, and the overexpression of elastases and collagenases that mimics the development of pulmonary emphysema [187-188]. The oxidant/antioxidant theory postulates that an excess of oxidants and free radicals in the lungs promotes cellular and tissue damage and it is the major initiator of the disease process [189-190]. Inflammation is not a separate entity by itself, but is integrally related to oxidative stress and protease–antiprotease imbalance.

Cigarette smoke (CS), occupational exposure to solvents, and other chemicals and environmental pollutants are rich source of oxidants and highly toxic electrophiles can serve as a trigger or activator of oxidative stress and inflammation, inducing severe macromolecular, cellular, and tissue damage, cell death, and inhibition of cell repair, through direct cytotoxic effects, promotion of primary genotoxic events, or generation of reactive oxygen intermediates [191-192]. CS is certainly the main risk factor for COPD, but, although it accounts for ~80-90% of COPD cases worldwide, only a small proportion of smokers (15-20%) develop symptomatic disease [193]. This phenomenon, together with the familial clustering of patients with early-onset COPD [194], strongly suggests that COPD is a complex disease involving the interaction of genetic and environmental factors.

As the only well-defined genetic factor of COPD, alfa-1-antitrypsin deficiency, is rare in worldwide populations, other genetic factors must be involved in the susceptibility and development of COPD.

Polymorphisms in the genes controlling xenobiotic metabolism (hence oxidant-anti-oxidant balance) may explain some of the observed differences in susceptibility to various diseases caused by environmental factors, including COPD [195-197].

The microsomal epoxide hydrolase gene, EPHX1, is a good candidate for several reasons. First, it is strongly expressed in the lung bronchial epithelial cells, but downregulated in COPD [198]. Secondly, the enzyme product is a critical biotransformation enzyme that plays a dual role in the detoxification and activation of exogenous chemicals and smoking-induced reactive substances, such as epoxides and polycyclic aromatic hydrocarbons

(PAHs), which may cause oxidative stress [199] [116]. Finally, there are two well-characterised variants of the EPHX1 gene which have been shown to alter enzyme activity considerably [200]. This might account for some of the variety in susceptibility to COPD among smokers. Polymorphisms of the EPHX1 gene may be an important risk factor in lung disease associated with oxidative stress consistent with the direct effects of cigarette-smoke components.

Four distinct EPHX1 alleles exist, which arise because of the presence or absence of two point mutations in the gene. Among 11 polymorphic loci found in human EPHX1, two genetic polymorphisms have been reported within the coding region of the EPHX1 gene: the TAC to CAC transition in exon 3 (rs1051740), which changes tyrosine (Tyr) residue 113 to histidine (His), and the CAT to CGT transition in exon 4 (rs2234922), which changes His residue 139 to arginine (Arg). In vitro cDNA expression studies indicate that EPHX1 enzymatic activity is decreased by approximately 50% in subjects with the His 113 allele (slow allele) and is increased by at least 25% in subjects with the Arg 139 allele (fast allele). The rare occurrence of both mutations together produces an enzyme with normal activity [15]. Based on the polymorphism of EPHX1 gene, the population can be classified into four groups of putative EPHX1 phenotypes: normal, fast, slow and very slow. The genetic characteristics of these subgroups are: normal—homozygous wild type for both exon 3 and exon 4, or heterozygous for both exon 3 and exon 4; fast—at least one mutation in exon 4 and no exon 3 mutation; slow—heterozygous for exon 3 and homozygous for exon 4; very slow—homozygous mutation type for exon 3 [192] [200].

A number of studies have assessed the association between EPHX1 polymorphisms and COPD in different populations, however, the results are inconsistent and inconclusive.

Aim of this study is to investigate, in a population based case-control study, whether aforementioned polymorphisms of EPHX1 gene had any bearing on individual susceptibility to the development of chronic obstructive pulmonary disease (COPD) and on the severity of the disease. Associations between disease group and specific genotypes and phenotypes will be assessed. The results of this study will provide a contribution to delineate the gentic signature responsible for COPD onset and progression.

2.5. MATERIALS and METHODS

2.5.1. STUDY POPULATION

Subjects were enrolled consecutively among outpatients who were undertaking respiratory function tests at the Pneumology Unit of the Sant'Orsola-Malpighi Hospital, Bologna, from October 2010 to July 2012. Patients are usually sent by the General Practitioners for a first diagnosis of COPD and subsequent checks.

A case was defined as patient diagnosed with COPD (spirometry with post-bronchodilator ratio: FEV1/FVC<0.70), and it was classified according to GOLD guidelines (GOLD project) in: Mild (GOLD 1), Moderate (GOLD 2), Severe (GOLD 3) and Very Severe (GOLD 4). A control was defined as healthy subject without COPD or any other respiratory disease. In order to increase the number of potential controls we included subjects from Blood Transfusion Service, a group of healthy subjects with the common feature to be not affected by COPD. The study population includes 443 subjects: 229 affected by COPD and 214 healthy controls.

This study was approved by the competent local ethics committee (protocol number: RE69/2015/U/OssN).

2.5.2. SOCIO-DEMOGRAPHIC AND CLINICAL VARIABLES

The COPD population has been well characterized by Pandolfi et al. in 2015, in order to assess the role of socio-demographic, lifestyle and clinical factors as predictors of acute events [201].

Comprehensive socio-demographic, lifestyle and clinical data were collected by physician interviewers through the use of a predefined questionnaire during a routine clinical consultation. In particular, in addition to socio-demographic and lifestyle characteristics, the following information were collected: age, gender, educational status, smoking status (including n. packs of cigarettes/year) and physical activity. Moreover, for each participant a deprivation index was attributed. The deprivation index was developed by Caranci et al. using variables from the 2001 General Census of Population and Housing [202]. Five traits that represented the multidimensionality of the social and material deprivation concept were considered: low level of education, unemployment, non-home ownership, one-parent

family and household overcrowding. The index is calculated by summing standardized indicators [202].

The following clinical characteristics were collected for each participant: Charlson index, Fraction Exhaled Nitric Oxide (FeNO), PaO_2, $PaCO_2$, FVC, FEV1, FEV1/FVC (%), FVC (% of total) and FEV1 (% of total). The Charlson Comorbidity Index contains 19 categories of comorbidity [203]. In this study this index is expressed in 3 categories: no comorbidity, one comorbidity and two or more comorbidities. FeNO levels were evaluated using a Niox chemiluminescence analyser (Aerocrine AB, Solna, Sweden). According to the American Thoracic Society (ATS) guideline, the subjects inhaled nitric oxide free air to total lung capacity and then exhaled at a constant flow rate against a valve connected to the nitric oxide analyzer [204]. The mean value of FeNO levels obtained in two tests was used. The measurements of PaO_2 and $PaCO_2$ were evaluated using arterial blood gas (ABG) analysis. FEV1 and FVC were obtained by spirometry (Model N 403; Monaghan, Littleton, CO), with the spirometer calibrated daily.

In addition, two anthropometric characteristics were collected: BMI and waist circumference. BMI was determined from weight and height measured at the time of the first visit, and categorized into four groups: underweight (<18.5kg/m^2), normal (18.5–24.9kg/m^2), overweight (25–29.9 kg/m^2) and obese (>30kg/m^2).

2.5.3. GENETIC ANALYSIS

2.5.3.1. DNA extraction

The DNA was extracted from cell pellet obtained by arterial and venous blood sample, starting from a sample volume of 200 µL, after removal of plasma by centrifugation. Given the small amount of the starting sample, the extraction was performed using spin columns of the QIAamp® DNA Mini Kit (Qiagen™, Hilden, Germany), a silica-membrane-based nucleic acid purification.

Kit contents:

1. QIAamp mini spin columns, extractive spin columns containing a silica resin
2. Collection tubes;

3. Proteinase K, lyophilized dissolved in 1.2 mL of solvent with 0.4% sodium azide, at the time of kit opening;
4. Buffer AL;
5. Buffer AW1, in concentrated solution, it has been diluted with 25 mL of absolute ethanol at the opening time;
6. Buffer AW2, in concentrated solution, it has been diluted with 30 mL of absolute ethanol at the opening time;
7. Buffer AE (elution buffer).

Experimental Procedure - To 200 µL of arterial or venous blood (**Figure 9**), treated with the common anticoagulants (heparin or EDTA) and deprived of plasm, were added 20 µL of Proteinase K, which lyses the cell components making DNA accessible. The sample was shaken well to ensure the homogeneity of the solution and centrifuge briefly to collect all of the solution at the bottom of the tube. 200 µL of Buffer AL were added to promote cell lysis and, after stirring at the vortex for 15 seconds, the samples were incubated in the heating block at 56 °C for at least 10 minutes, allowing the Buffer AL to work. After incubation, the samples were briefly centrifuged to collect the drops formed on the tube wall, then I added 200 µL of cold absolute ethanol (4°C), to facilitate DNA precipitation. After shaking well for 15 seconds, the solution (about 600 µL) was transferred into the appropriate column (QIAamp spin columns) inserted into a collection tube, and it was centrifuged at 8000 rpm for one minute. The column contains a resin of silica gel with a high affinity for the DNA which is retained while the other components pass through the resin into the collection tube. The column was washed with 500 µL of Buffer AW1 and centrifuge at 8000 rpm for one minute: the DNA remains bound to the resin, the collection tube is discarded, and the column is inserted into a new collection tube. At this point, the DNA was washed with 500 µL of Buffer AW2, then centrifuged at 1400 rpm for three minutes. AW1 and AW2 are saline buffers for washing the DNA extracted from contaminants, proteins and other cellular components present in solution. After centrifugation, the column was transferred into a new collection tube. I added 200 µL of Buffer AE (elution baffer) and the column was incubated at room temperature for five minutes. Finally, the column was centrifuged at

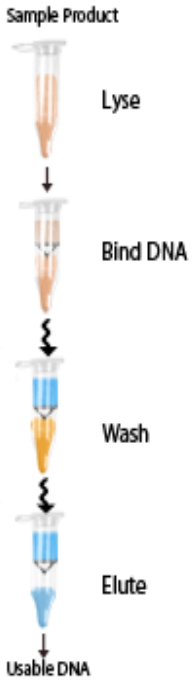

Figure 9. Experimental Procedure.

8000 rpm for one minute and the eluate was collected and transferred into sterile vial suitably encoded. The DNA has a greater affinity for the buffer AE respect to the resin silica column and this allows that the nucleic acid itself is detached from the resin and elute in the collection tube.

The extraction using commercial kits allows to extract DNA from minimal sample volumes (200 µL), with short experimental time, allowing you to process many samples simultaneously, but with low yields (proportionate to the amount of starting biological material).

2.5.3.2. DNA quantification

The dosage of the DNA was measured using the NanoVue® technology (**Figure 10**), based on the principle of classical spectrophotometry, whereby nucleic acids absorb ultraviolet light and absorption is directly proportional to the concentration. The absorption spectrum of DNA ranges between 230 and 290 nm, but the absorbance is read at 260 nm, the wavelength at which DNA has maximum absorption of UV-light.

Figura 10. Spectrophotometer NanoVue®

The NanoVue is an innovative UV-visible spectrophotometer, capable of working with micro-volumes of sample, from 0.5 to 5 µL, and at high concentrations (linearity range: 2-3700 ng). Quantification is accurate and fast. Modern NanoVue technology uses the surface tension exerted by small volumes when placed between two adjacent surfaces (**Figure 11**). This surface tension is developed by the reading plates of the instrument on which are directly loaded 1 or 2 µL of sample. The reading plates are connected to two optical fibers and the light source of the instrument is made up of a xenon lamp. The sample concentration and purity are directly calculated by the software and displayed on the instrument interface.

Figura 11. Surface tension exerted by small volumes.

The nucleic acid concentration (ng/µL) is calculated by the following formula:

[Nucleic acid ng/µL] = (Abs260 - Abs280) x K

K is the factor of reading, specific for each type of nucleic acid
(DsDNA = 50; ssDNA = 37; RNA = 40).
The purity determination is very important. The proteins are the main source of contamination for extracted DNA sample. For this reason, the absorbance is read also at 280 nm, the wavelength at which the proteins absorb UV-light. The Abs 260/Abs 280 ratio provides a measure of the purity of the extracted nucleic acid sample: a pure DNA should have a ratio of approximately 2. In general, DNA solutions with a ratio greater than 1.6 are considered to have a good degree of purity for analysis of SNPs.

2.5.3.3. Genotype analysis

The analysis of the SNPs was carried out using two different methods: Polymerase chain reaction (PCR) analysis associated with restriction enzyme (RFLP: Restriction Fragment Length Polymorphism) and Real-Time PCR with TaqMan probes (Applied Biosystems™, Foster City, USA).

PCR-RFLP - The PCR reaction was carried out with a BioRad thermocycler (BioRad Laboratories™, Herculres, CA, USA) in a final volume of 10 µL, containing 1 µL of DNA template (10 ng/µL) and 9 µL of PCR buffer containing 2 mM magnesium chloride, 1x buffer 10x, 0.30 µM of each primer, 5% dimethyl sulphoxide (DMSO), 0.11 mM of dNTPs, and 0.03 U/µL of AmpliTaq® Gold Polymerase (Applied Biosystem™) that catalyzes the amplification reaction.
The amplification program, performed with thermocycler (**Figure 12**) is characterized by alternation of three different temperature segments for 30-40 cycles:

- **Denaturation**: 95°C for 30 seconds: separation of the two strands of DNA;
- **Annealing**: 50-60°C for 30 seconds: specific temperature for each primer (depending on the length and the ratio GC/AT) that determines the pairing of primers with the respective complementary regions within the denatured DNA strands;
- **Elongation**: 72°C for 30 seconds, that allows DNA synthesis by Taq polymerase using the single strand as a template.

At the end of the 30/40 cycles, the temperature of 72 °C is kept for 5 minutes, to allow the elongation of the final amplified fragments. This results in the exponential amplification of the DNA segment of interest.

Figura 12. Thermocycler for polymerase chain reaction (PCR).

After successful amplification, the analysis is performed by cutting the portion of the amplified DNA containing the SNP of interest with restriction enzyme. This involves the consequent formation of fragments of different lengths that are separated by electrophoresis (180V, for 30-35 minutes), through a non-denaturing 8% polyacrylamide gel containing TBE buffer (Tris/Borate/EDTA, 0·09 mol/L Tris-borate and 0·002 mol/L edetic acid). The gels were prepared just before use, using 5 mL of 8% polyacrylamide, 50 µL of ammonium persulfate and 5 µL of tetramethylethylenediamine. After the electrophoresis, the gels were dipped in a dilute solution of ethidium bromide, planar molecule which intercalates between the bases of DNA. The DNA, intercalated by ethidium bromide, absorbs ultraviolet light (260-360 nm) and consequently emits fluorescent light (590 nm). The emitted light is detected by the system CHEMIDOC™ MP imaging system (BIO-RAD) tool with digital camera through which captures an image of the gel, which is transferred directly to the analysis software dedicated “ImageLab”.

The human genome is diploid, so, as result of the cleavage reaction with restriction enzyme, it is possible to discern three different situations on the scanned image:

- Homozygous for the common allele wild-type (Ho wt);
- Heterozygosity (He) in which one allele has the SNP while the other is wt;
- Homozygous for the SNP (Ho SNP), in which both alleles exhibit the polymorphism

The gel allow to identify, for the same SNP, three different fragments:

- uncut/cut homozygous (aa)
- heterozygous with both fragments (aA or Aa)
- cut/uncut homozygous (AA)

In this study, the SNP EPHX1 exone 4 rs2234922 was analyzed by PCR-RFLP. The table below (**Table 3**) shows the sequences of specific primers for the amplification reaction, the annealing temperature, the size of the amplified fragment, and the restriction enzyme used with the relative cutting conditions (**Figure 13**).

<table>
<tr><td rowspan="4">EPHX1

Exone 4 A139>G

His139Arg (H139R)

rs2234922</td><td colspan="2">Primer Forward: AGG GTG GCA GGA CTC AAT

Primer Reverse: AGG GCA GAT GAC TTC AAA AAC</td></tr>
<tr><td colspan="2">Thermocycler steps:

• 95°C for 5 min
• 95°C for 30s (denaturation)
• 57°C for 30s (annealing)
• 72°C for 30s (elongation) } 34 cycles
• 72°C for 7 min (elongation)</td></tr>
<tr><td colspan="2">Restriction Enzyme: RsaI (o Afa I) 37°C o/n (16h)

Cutting Sequence: 5’…G T▼ A C…3’

3’…C A▲ T G…5’</td></tr>
<tr><td>Fragments Pattern</td><td>Omozigote Wild Type (AA): 285 bp

Eterozigote (AG): 131 bp + 154 bp + 285 bp

Omozigote SNP (GG): 131 bp + 154 bp</td></tr>
</table>

Table 3 - PCR-RFLP analysis for EPHX1 exone 4 rs2234922 polymorphism

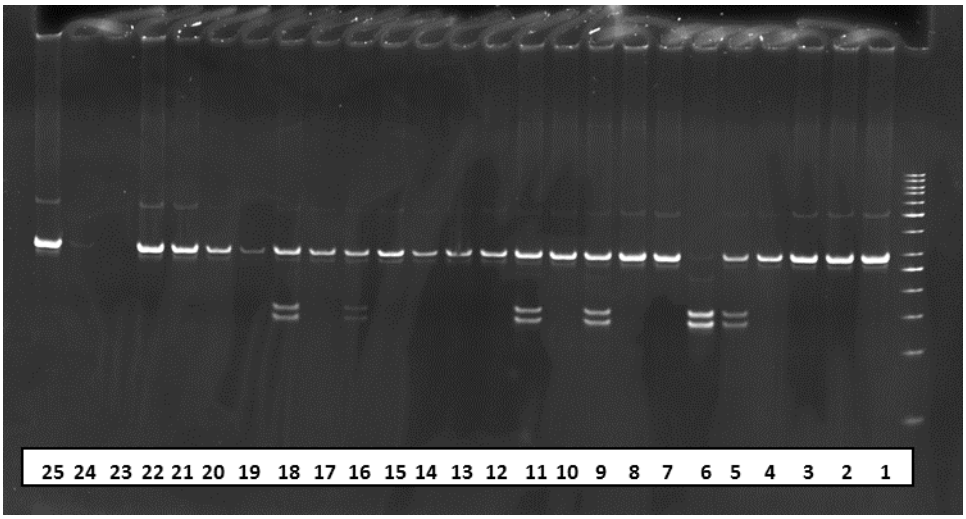

Figure 13. Result from PCR-RFLP of EPHX1 exone 4 rs2234922 polymorphism; samples: 1-4, 7, 8, 10, 12-15, 17, 19-22, 25 Ho WT; 5, 9, 11, 16, 18 He; 6 Ho SNP.

Real-time PCR - The Real-Time PCR allows to determine the presence of a SNP in the target sequence, using fluorescent oligonucleotide probes (Taqman, Applied Biosystem) able to hybridize specifically to the sequence of interest (**Figure 14**). In particular, in the allelic discrimination analysis to determine the presence of polymorphism, the Real-Time PCR technique involves two fluorescent oligonucleotid probes, each having a complementary sequence to one of the two alleles: a probe pairs with the wild type allele, the other with the SNP allele. The two probes are differently labeled on 5' end with two different fluorophores reporters: VIC for the wt (wild type) allele and FAM for the SNP allele, or vice versa.

TaqMan probes are short oligonucleotides (about 20-30 bp) characterized by having linked at the 3' molecule minor groove binder (MGB) which binds the minor groove of DNA, thus increasing the affinity of the probes for the DNA

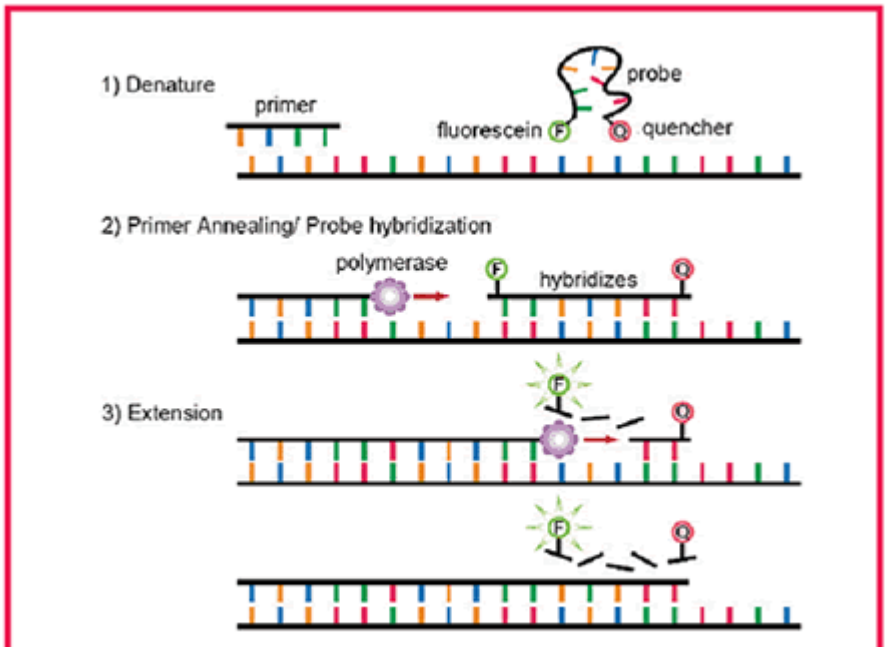

Figure 14. Application of TaqMan format for allelic discrimination.

itself. The probes are "dual-labeled," because in addition to being labeled the 5' end with the fluorophore reporter (Vic or Fam), the 3' end has a quencher, which "switches off" the fluorescence of the reporter, absorbing photons (Förster energy transfer type) when they are near (distance of 20 to 30 bases). The probe binds very specifically the complementary DNA sequence in the region between the forward and reverse primers used in the annealing step for the amplification reaction. Subsequently, during the extension phase, the probes are cut by the 5'-3' exonuclease activity of the Taq Polymerase. Once the probe is cut by Taq polymerase, the released reporter, no longer suffering influence from the quencher, it is capable of emitting fluorescence. The exponential amplification of the target sequence during PCR is accompanied by a corresponding increase in the signal emitted by the fluorophore. This analysis system is highly specific, in fact the two probes do not interfere with each other and the signal is output only when there is the correct pairing of the probe to the target sequence.
Real-Time PCR has several advantages compared to PCR-RFLP. First of all, enormous material and time saving. With Real-Time PCR results are ready in few minutes, immediately after the amplification process, so restriction enzyme and electrophoresis are unecessary;
The allelic discrimination reaction was performed in a volume of 10 µL containing:

- DNA at a concentration of 10 ng/µL;
- SNP Genotyping Probe 20X (or 40X), containing two primers and the specific probe for the SNP in study (Applied Biosystem™, Foster City, CA, USA);
- TaqMan® Universal Master Mix II, no Uracil N-Glycosylase (UNG) containing the components of the PCR reaction: AmpliTaq Gold® DNA Polymerase Ultra Pure, dNTPs with dUTP, ROX™ Passive Reference, Optimized buffer components (Applied Biosystem™, Foster City, CA, USA);
- Nuclease-free water.

The 10 µL are pipetted in 96-well plate, and at least 3 wells are free of DNA template (NTC) and serve as negative controls.
The following table (**Table 4**) shows the sequence of the labeled probe, for the SNP EPHX1 exone 3 rs1051740 analyzed with Real Time-PCR.

GENE e SNP	PROBE SEQUENCE
EPHX1 **Exone 3 T113>C** **Tyr113His (Y113H)** **rs1051740**	GAAGCAGGTGGAGATTCTCAACAGA **[Cvic/Tfam]** ACCCTCACTTCAAGACTAAGATTGA

Table 4 - REAL TIME-PCR analysis for EPHX1 exone 3 rs1051740 polymorphism

The experimental procedure, performed on the platform Real-Time 7900HT System (Applied Biosystem™), consist in three steps:

1. reading of the basal fluorescence due to the components of the starting mixture (Pre-read);
2. amplification reaction (consisting of denaturation at 95 °C for 10 minutes, followed by 40 cycles at 92 °C for 15 seconds and 1 minute at 60 °C);
3. fluorescence signal detection (VIC and/or FAM), which is subtracted from the initial signal (Post-read).

The instrument, through the dedicated software Applied Biosystem program, after the analysis subtracts the background signal (pre-read) from the final reading and automatically elaborates the chart that enables to distinguish the genotype of the analyzed samples. The presence of VIC flourescence signal indicates homozygosity for one allele, the FAM flourescence signal indicates homozygous for the other one; the presence of the fluorescence from both the probes, indicates the status of heterozygosity. At the end of analysis the instrument processes the chart (**Figure 15**).

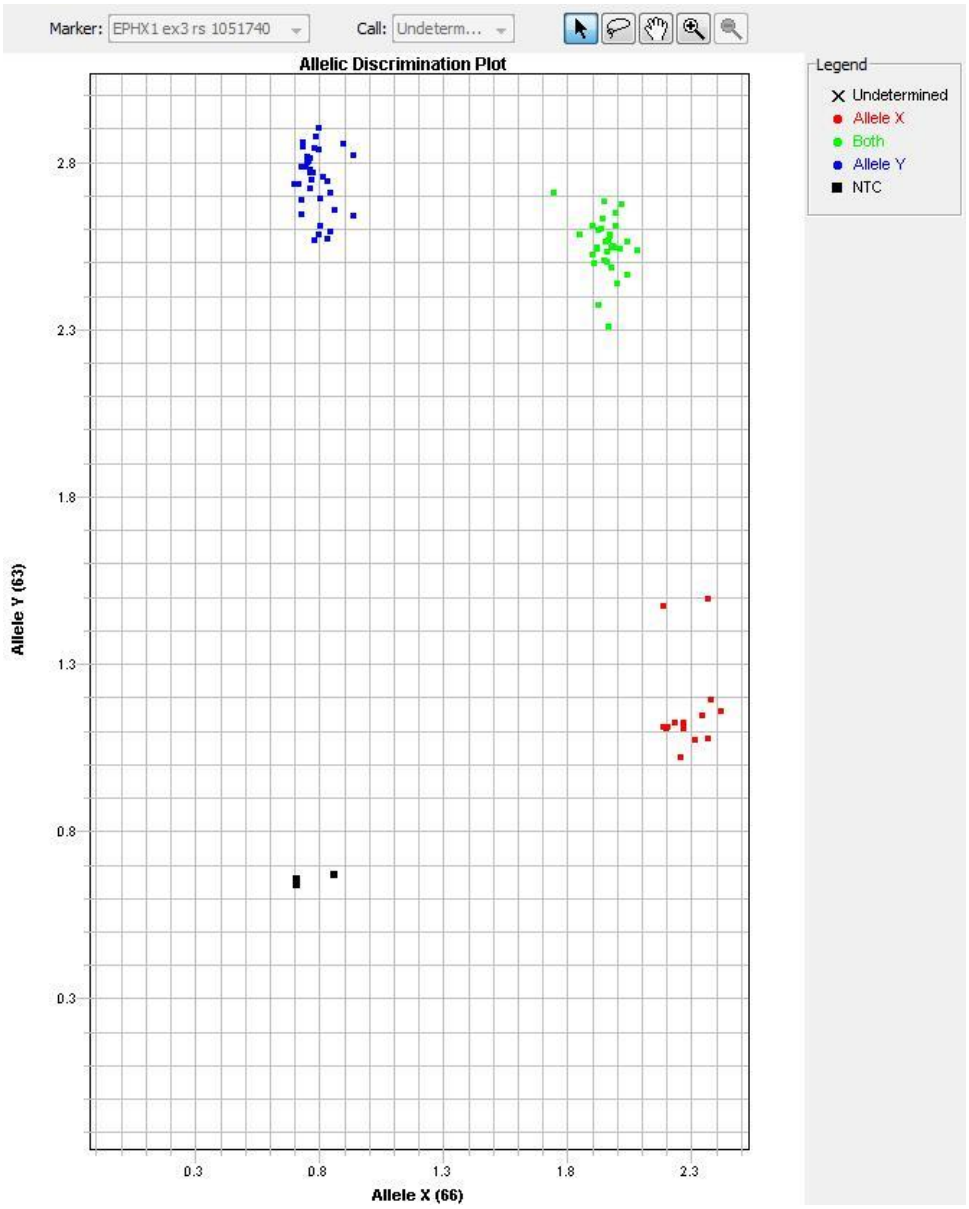

Figura 15. Result from REAL TIME-PCR of EPHX1 exone 3 rs1051740 polymorphism; blue dot represents Homozygous Wild Type (allele Y, 63, TT), green dot represents Heterozygosity (Both, TC), red dot represents Homozygous SNP (allele X, 66, CC), black dot represents blank (NTC).

2.5.3.4. Phenotype analysis

Based on the polymorphism of EPHX1 gene, the population can be classified into four groups of putative EPHX1 phenotypes: normal, fast, slow and very slow. The genetic characteristics of these subgroups are: normal—homozygous wild type for both exon 3 and exon 4, or heterozygous for both exon 3 and exon 4; fast—at least one mutation in exon 4 and no exon 3 mutation; slow—heterozygous for exon 3 and homozygous for exon 4; very slow—homozygous mutation type for exon 3 [192] [200] (**Table 5**).

		EXON 4 (A>G) His139Arg		
		Ho wt = 0	**He = 1**	**Ho SNP = 2**
EXON 3 (T>C) Tyr113His	**Ho wt = 0**	N (0 - 0)	F (0 - 1)	F (0 - 2)
	He = 1	S (1 - 0)	N (1 - 1)	S (1 -2)
	Ho SNP = 2	VS (2 - 0)	VS (2 - 1)	VS (2 - 2)
Ho wt=homozygous wild type; He=heterozygous; Ho SNP=homozygous SNP; N= normal; F=fast; S=slow, VS=very slow				

Table 5. Four groups of putative EPHX1 phenotypes: normal, fast, slow and very slow.

2.5.3.5. STATISTICAL ANALYSIS

Continuous variables are presented as mean ± standard deviation (SD), while categorical variables as absolute frequency (relative frequency).

Student T Test, analysis of variance (ANOVA), Pearson's chi-square and Fisher's exact tests were used to compare variables between COPD cases and controls and among COPD stages as appropriate. Same tests were used, as appropriate, to assess association between genotype/phenotype and gender and anthropometric characteristics (BMI and waist circumference).

Genotype and phenotype distribution among cases and controls, and among COPD stages was evaluated with Pearson's chi-square and Fisher's exact tests.

Logistic regression analysis was applied to assess the relationship between genotype/phenotype and COPD. Only in the COPD population, logistic regression analysis was performed to study the association between genotype/phenotype (outcome 1: death, outcome 2: hospitalization for respiratory causes) and acute events. The association

between genotype/phenotype and COPD stages (mild= reference category) was evaluated with multinomial regression model. All multivariate analysis were adjusted for age at blood draw and sex. The results of models are presented as odds ratio (OR) and 95% confidence interval (95% CI). All P-values are based on 2-sided tests and P-values<0.05 were considered significant. Statistical analysis was performed using statistical package Stata Intercooled for Windows, version 12.0.

For each analyzed polymorphism we calculated the allele frequency (q). The Hardy-Weinberg equilibrium (HWE) was applied to ensure that the frequency of the genotype observed was in accordance with the expected. The chi-square test was applied to check for differences in the genotype distribution observed in comparison with the expected.

A P-value <0.05 was considered statistically significant.

2.6. RESULTS and DISCUSSION

2.6.1. SOCIO-DEMOGRAPHIC, LIFESTYLE, CLINICAL AND ANTHROPOMETRIC CHARACTERISTICS OF THE STUDY POPULATION

229 patients (129 male and 100 female; mean age 73.74±9.46 years) affected by COPD, and 214 healthy controls (120 male and 94 female; mean age 47.94±14.12) were enrolled in the study (**Table 6**).

According to the GOLD Guideline COPD patients were classified into four severity stages as follows: 44 mild (COPD, GOLD1), 68 moderate (COPD, GOLD2), 52 severe (COPD, GOLD3) and 65 very severe (COPD, GOLD4). **Table 7** shows the results regarding social and lifestyles characteristics observed in the COPD population, and it shows that more than 60% were ex-smokers and more than 50% turned out to be deprived or very deprived. Significant differences within COPD stage, in terms of smoking status, were detected.

Table 8 provides the details of clinical and anthropometric characteristics of the COPD population. There were non-significant differences in BMI (body mass index) and waist circumference among COPD stage. On the contrary, the stage was significantly associated with the values of all clinical tests (spirometry and arterial blood gas analysis) and with presence of comorbidities. The highest percentage of patients (42.2%) who had two or more comorbidities was observed in the group suffering from very severe COPD.

Table 6. Demographic characteristics of study population	**CONTROLS**		**COPD**		**p-value**
	n	**%**	**n**	**%**	
n° SUBJECTS	214		229		
AGE, mean ± sd*	47.94 ± 14.12		73.74 ± 9.46		>0.001
GENDER					
male	120	56.07	129	56.33	
female	94	43.93	100	43.67	0.957
***information not available for all subjects**					

Table 7. Social and lifestyle characteristics in COPD population	COPD GOLD STAGES										
	MILD		MODERATE		SEVERE		VERY SEVERE		TOTAL		p-value
	n	%	n	%	n	%	n	%	n	%	
n° SUBJECT	44	19.21	68	29.69	52	22.71	65	28.38	229		
AGE, mean ± sd*	73.80 ± 9.06		74.15 ± 11.77		72.83 ± 7.86		74.03 ± 8.30		73.74 ± 9.46		0.8816
GENDER											
male	21	47.73	36	52.94	32	61.54	40	61.54	129	56.33	
female	23	52.27	32	47.06	20	38.46	25	38.46	100	43.67	0.402
SMOKING STATUS*											
never smoker	15	34.09	22	32.35	7	13.46	6	9.38	50	21.93	
smoker	9	20.45	7	10.29	8	15.38	8	12.5	32	14.04	
ex-smoker	20	45.45	39	57.35	37	71.15	50	78.13	146	64.04	0.003
DEPRIVATION INDEX*											
very rich	9	21.95	11	16.92	9	18.00	9	14.75	38	17.51	
rich	8	19.51	8	12.31	4	8.00	6	9.84	26	11.98	
medium	3	7.32	12	18.46	10	20.00	11	18.03	36	16.59	
deprivated	9	21.95	13	20.00	10	20.00	9	14.75	41	18.89	
very deprivated	12	29.27	21	32.31	17	34.00	26	42.62	76	35.02	0.73
*information not available for all subjects											

Table 8. Clinical and anthropometric characteristics in COPD population	COPD GOLD STAGES										
	Mild		Moderate		Severe		Very Severe		TOTAL		p-value
	n	%	n	%	n	%	n	%	n	%	
BMI*											
underweight	2	4.55	0	0.00	3	5.77	3	4.69	8	3.52	
normal	17	38.64	16	23.88	17	32.69	25	39.06	75	33.04	
overweight	17	38.64	32	47.76	21	40.38	22	34.38	92	40.53	
obese	8	18.18	19	28.36	11	21.15	14	21.88	52	22.91	0.337
WAIST CIRCUMFERENCE (cm)	96.4 ± 12.5		101.6 ± 12.3		101.0 ± 14.6		100.1 ±15.0		100.0 ± 13.7		0.39
CHARLSON INDEX*											
no comorbidity	32	72.73	33	49.25	24	46.15	20	31.2	109	48.02	
one comorbidity	3	6.82	16	23.88	9	17.31	17	26.6	45	19.82	
two or more comorbidity	9	20.45	18	26.87	19	36.54	27	42.2	73	32.16	0.003
FeNO (ppm)*	16.7 ± 5.9		19.5 ± 6.7		20.1 ± 7.2		27 ± 10.3		21.1 ± 8.6		>0.001
PaO_2 (mmHg)*	79.72 ± 8.89		73.83 ± 10.02		69.88 ± 10.09		71.10 ± 14.80		73.12 ± 12.16		>0.001
$PaCO_2$ (mmHg)*	38.34 ± 4.12		40.37 ± 5.56		41.81 ± 6.90		49.70 ± 10.50		43.04 ± 8.72		>0.001
FVC (L)*	2.80 ± 0.84		2.19 ± 0.78		2.04 ± 0.62		1.61 ± 0.62		2.20 ± 0.82		>0.001
FEV1 (L)*	1.88 ± 0.58		1.27 ± 0.38		1.03 ± 0.29		0.71 ± 0.27		1.18 ± 0.56		>0.001
FEV1/FVC (%)*	67.59 ± 6.63		59.93 ± 11.14		51.86 ± 12.91		45.50 ± 11.80		55.60 ± 13.62		>0.001
FVC (% of total)*	102.93 ± 19.51		81.28 ± 14.51		69.62 ± 16.25		57.10 ± 17.80		76.04 ± 23.21		>0.001
FEV1 (% of total)*	87.80 ± 13.49		61.39 ± 7.54		44.77 ± 9.64		32.80 ± 12.15		54.68 ± 22.28		>0.001

*information not available for all subjects

FeNO=Fraction Exhaled Nitric Oxide; PaO_2=partial pressure oxygen; $PaCO_2$=partial pressure carbon dioxide; FVC=Forced Vital Capacity; FEV1=Forced Expiratory Volume in 1 second.

2.6.2. GENOTYPE and PHENOTYPE IN RELATION TO GENDER AND ANTHROPOMETRIC CHARACTERISTICS (BMI, WAIST CIRCUMFERENCE)

ASSOCIATION BETWEEN GENOTYPE AND GENDER AND ANTHROPOMETRIC CHARACTERISTICS (BMI and waist circumference)

Table 9. Genotype distribution among male and female in the study population.

	MALE		FEMALE		
	n	**%**	**n**	**%**	**p-value**
EPHX1 rs1051740*					
Ho wt	120	48.19	102	52.85	
He	110	44.18	77	39.90	
Ho SNP	19	7.63	14	7.25	0.618
EPHX1 rs2234922*					
Ho wt	163	65.99	131	68.23	
He	78	31.58	55	28.65	
Ho SNP	6	2.43	6	3.13	0.749
*information not available for all subjects					
Ho wt: homozygous wild type; He: heterozygous; Ho SNP: homozygous SNP					

In the study population the genotype distribution among males and females (**Table 9**) is mostly similar for each analyzed SNP and any statistically significant difference was observed, even by merging He and Ho SNP into a single group (data not shown).

Table 10. Genotype distribution among the 4 classes of BMI in COPD group.

	BODY MASS INDEX								
	UNDERWEIGHT		NORMAL		OVERWEIGHT		OBESE		
	n	**%**	**n**	**%**	**n**	**%**	**n**	**%**	**p-value**
EPHX1 rs1051740*									
Ho wt	5	62.50	38	50.67	48	52.17	26	50.00	
He	3	37.50	33	44.00	41	44.57	23	44.23	
Ho SNP	0	0.00	4	5.33	3	3.26	3	3.26	0.971
EPHX1 rs2234922*									
Ho wt	7	87.50	49	67.12	57	61.96	35	67.31	
He	1	12.50	23	31.51	32	34.78	15	28.85	
Ho SNP	0	0.00	1	1.37	3	3.26	2	3.85	0.780
*information not available for all subjects									
Ho wt: homozygous wild type; He: heterozygous; Ho SNP: homozygous SNP									

In the COPD group the genotype distribution among the four classes of BMI (**Table 10**) for each analyzed SNP did not show any statistically significant difference, even by merging He and Ho SNP, or oveweight and obese, into a single group (data not shown).

Table 11. Association between genotype and waist circumference in COPD group.

	WAIST CIRCUMFERENCE (cm)	
	mean ± sd	**p-value**
EPHX1 rs1051740*		
Ho wt	100.128 ± 14.750	
He	100.162 ± 12.485	
Ho SNP	98.600 ± 14.089	0.8589
EPHX1 rs2234922*		
Ho wt	99.449 ± 12.957	
He	101.465 ± 15.556	
Ho SNP	102.167 ± 89.98	0.4962
*information not available for all subjects		
Ho wt: homozygous wild type; He: heterozygous; Ho SNP: homozygous SNP		

In the COPD group the association between genotype and waist circumference (**Table 11**), for each analyzed SNP, did not show any statistically significant difference, even by merging He and Ho SNP into a single group (data not shown).

ASSOCIATION BETWEEN PHENOTYPE AND GENDER AND ANTHROPOMETRIC CHARACTERISTICS (BMI and waist circumference)

Table 12. Phenotype distribution among male and female in the study population.

	MALE		FEMALE		
	n	**%**	**n**	**%**	**p-value**
Phenotype*					
normal	92	48.17	195	44.52	
fast	31	16.23	78	17.81	
slow	54	28.27	132	30.14	
very slow	14	7.33	33	7.53	0.594
*information not available for all subjects					
NORMAL: homozygous wild type for both exon 3 and exon 4, or heterozygous for both exon 3 and exon 4; FAST: at least one mutation in exon 4 and no exon 3 mutation; SLOW: heterozygous for exon 3 and homozygous for exon 4; VERY: homozygous mutation type for exon 3					

In the study population the phenotype distribution among males and females (**Table 12**) did not show any statistically significant difference, even by merging slow and very slow phenotypes into a single group (data not shown).

Table 13. Phenotype distribution among the 4 classes of BMI in COPD group.

	BODY MASS INDEX								
	UNDERWEIGHT		NORMAL		OVERWEIGHT		OBESE		
	n	%	n	%	n	%	n	%	p-value
Phenotype*									
normal	4	50.00	50	54.35	45	42.86	23	40.35	
fast	1	12.50	14	15.22	22	20.95	11	19.30	
slow	3	37.50	23	25.00	34	32.38	20	35.09	
very slow	0	0.00	5	5.43	4	3.81	3	5.26	0.806
*information not available for all subjects									
NORMAL: homozygous wild type for both exon 3 and exon 4, or heterozygous for both exon 3 and exon 4; FAST: at least one mutation in exon 4 and no exon 3 mutation; SLOW: heterozygous for exon 3 and homozygous for exon 4; VERY: homozygous mutation type for exon 3									

In the COPD group the phenotype distribution among the four classes of BMI (**Table 13**) did not show any statistically significant difference, even by merging slow and very slow phenotypes, or oveweight and obese, into a single group (data not shown).

Table 14. Association between phenotype and waist circumference in COPD group.

	WAIST CIRCUMFERENCE (cm)	
	mean ± sd	p-value
Phenotype*		
normal	97.451 ± 14.506	
fast	102.149 ± 16.269	
slow	99.633 ± 13.437	
very slow	94.250 ± 16.608	0.2369
*information not available for all subjects		
NORMAL: homozygous wild type for both exon 3 and exon 4, or heterozygous for both exon 3 and exon 4; FAST: at least one mutation in exon 4 and no exon 3 mutation; SLOW: heterozygous for exon 3 and homozygous for exon 4; VERY: homozygous mutation type for exon 3		

In the COPD group the association between phenotype and waist circumference (**Table 14**) did not show any statistically significant difference, even by merging slow and very slow phenotypes into a single group (data not shown).

2.6.3. CASE-CONTROL STUDY

GENOTYPE ANALYSIS COMPARING COPD PATIENTS WITH CONTROLS

The genotype distribution of EPHX1, into the group of COPD patients and the control group (**Table 15**), is in Hardy-Weinberg equilibrium for all the analyzed SNPs (data not shown).

Table 15. A. Genotype distribution among cases and controls in the study population and assessment of COPD risk; **B.** same analyses merging He and Ho SNP.

A.	COPD		CONTROLS			Model unadjusted		Model adjusted**	
	n	%	n	%	p-value	OR (95% CI)	p-value	OR (95% CI)	p-value
EPHX1 rs1051740*									
Ho wt	118	51.53	104	48.83		1.000		1.000	
He	101	44.10	86	40.38		1.035(0.701-1.529)	0.862	1.122(0.610-2.066)	0.711
Ho SNP	10	4.37	23	10.80	0.036	0.383(0.174-0.842)	0.017	0.440(0.121-1.596)	0.212
EPHX1 rs2234922*									
Ho wt	150	66.08	144	67.92		1.000		1.000	
He	71	31.28	62	29.25		1.099(0.729-1.657)	0.651	1.613(0.835-3.118)	0.155
Ho SNP	6	2.64	6	2.83	0.892	0.96(0.303-3.045)	0.945	0.583(0.086-3.936)	0.580
*information not available for all subjects; **adjusted for age at blood draw and sex									
Ho wt: homozygous wild type; He: heterozygous; Ho SNP: homozygous SNP; OR: odds ratio; CI: confidence interval									

B.	COPD		CONTROLS			Model unadjusted		Model adjusted**	
	n	%	n	%	p-value	OR (95% CI)	p-value	OR (95% CI)	p-value
EPHX1 rs1051740*									
Ho wt	118	51.53	104	48.83		1.000		1.000	
He+Ho SNP	111	48.47	109	51.18	0.634	0.898(0.618-1.304)	0.570	1.001(0.558-1.800)	0.995
EPHX1 rs2234922*									
Ho wt	150	66.08	144	67.92		1.000		1.000	
He+Ho SNP	77	33.92	68	32.08	0.686	1.087(0.730-1.619)	0.681	1.491(0.789-2.819)	0.219
*information not available for all subjects; **adjusted for age at blood draw and sex									

Considering the SNP rs1051740, the univariate analyses show a significant difference in the genotype distribution among cases and controls: 51.5% of COPD patients is wt vs 48.8% in the control group, 44.10% is He vs 40.4% in control group and 4.4% is Ho SNP vs. 10.8% in control group. Note that the univariate association and the unadjusted model give a significant result, but this result is not more significant when adjusted for sex and age (multivariate logistic regression analysis), so we can not attribute this significant result to the genotype since there is a difference by sex and age. The difference that is observed

may be due to gender difference, or age difference between cases and controls. Any significant results was observed even by merging He and Ho SNP into a single group (**Table 15 B**).

Although any results is statistically significant, considering both SNPs, in adjusted model genotypes He show a tendency to increase the COPD risk compare to wt, while Ho SNP, especially for rs1051740, seems to protect from COPD risk.

GENOTYPE ANALYSIS IN RELATION TO COPD SEVERITY

The genotype distribution of EPHX1 (**Table 16**), in COPD patients according to the four stages of disease severity, is in Hardy-Weinberg equilibrium for all the analyzed SNPs in each stage, with exception of mild stage for SNP rs1051740 (data not shown).

Table 16. A. Genotype distribution among different COPD stages; **B.** Assessment of COPD risk among different stages of severity.

A.	**MILD**		**MODERATE**		**SEVERE**		**VERY SEVERE**		
	n	**%**	**n**	**%**	**n**	**%**	**n**	**%**	**p-value**
EPHX1 rs1051740									
Ho wt	23	52.27	36	52.94	25	48.08	34	52.31	
He	21	47.73	27	39.71	25	48.08	28	43.08	
Ho SNP	0	0.00	5	7.35	2	3.85	3	4.62	0.658
EPHX1 rs2234922*									
Ho wt	27	61.36	49	72.06	38	73.08	36	57.14	
He	16	36.36	18	26.47	11	21.15	26	41.27	
Ho SNP	1	2.27	1	1.47	3	5.77	1	1.59	0.160
*information not available for all subjects									
Ho wt: homozygous wild type; He: heterozygous; Ho SNP: homozygous SNP									

B.	Model unadjusted		Model adjusted**	
	OR (95% CI)	p-value	OR (95% CI)	p-value
MODERATE vs MILD				
EPHX1 rs1051740				
Ho wt	1.000		1.000	
He+Ho SNP	0.974(0.456-2.080)	0.945	0.920(0.427-1.983)	0.831
EPHX1 rs2234922				
Ho wt	1.000		1.000	
He+Ho SNP	0.616(0.275-1.378)	0.238	0.629(0.28-1.412)	0.262
SEVERE vs MILD				
EPHX1 rs1051740				
Ho wt	1.000		1.000	
He+Ho SNP	1.183(0.530-2.642)	0.682	1.114(0.494-2.511)	0.795
EPHX1 rs2234922				
Ho wt	1.000		1.000	
He+Ho SNP	0.585(0.247-1.386)	0.223	0.568(0.238-1.357)	0.203
VERY SEVERE vs MILD				
EPHX1 rs1051740				
Ho wt	1.000		1.000	
He+Ho SNP	0.999(0.464-2.148)	0.997	0.999(0.458-2.177)	0.997
EPHX1 rs2234922				
Ho wt	1.000		1.000	
He+Ho SNP	1.191(0.543-2.613)	0.663	1.181(0.533-2.618)	0.682
*information not available for all subjects; **adjusted for age at blood draw and sex				
Ho wt: homozygous wild type; He: heterozygous; Ho SNP: homozygous SNP; OR: odds ratio; CI: confidence interval				

The genotype distribution among different COPD stages (**Table 16 A**) did not show any statistically significant difference, even by merging He and Ho SNP in a single group (data not shown).

Since there are not subjects with genotype Ho SNP and mild stage (reference category) for the SNP rs105170, and there is only 1 subject with genotype Ho SNP for the SNP rs2234922, the multinomial regression analysis to assess the risk of developing more severe COPD at different stages of disease severity was carried out by merging genotype He and Ho SNP into a single group (**Table 16 B**). The analysis did not show any statistically significant result.

PHENOTYPE ANALYSIS COMPARING COPD PATIENTS WITH CONTROLS

Table 17. Phenotype distribution among COPD patients and controls in the study population and assessment of COPD risk;

	COPD		CONTROLS			Model unadjusted		Model adjusted**	
	n	%	n	%	p-value	OR (95% CI)	p-value	OR (95% CI)	p-value
Phenotype*									
normal	106	46.7	89	42.18		1.000		1.000	
fast	42	18.5	36	17.06		0.980(0.578-1.659)	0.939	1.284(0.566-2.912)	0.550
slow	69	30.4	63	29.86		0.920(0.591-1.432)	0.711	0.857(0.430-1.708)	0.660
very slow	10	4.41	23	10.9	0.080	0.365(0.165-0.808)	0.013	0.421(0.115-1.545)	0.192
*information not available for all subjects; **adjusted for age at blood draw and sex									
NORMAL: homozygous wild type for both exon 3 and exon 4, or heterozygous for both exon 3 and exon 4; FAST: at least one mutation in exon 4 and no exon 3 mutation; SLOW: heterozygous for exon 3 and homozygous for exon 4; VERY: homozygous mutation type for exon 3; OR: odds ratio; CI: confidence interval									

In the study population the phenotype distribution among cases and controls did not show any statistically significant difference, even merging slow and very slow phenotypes into a single group (data not shown). Also the multivariate logistic regression analysis didn't show any statistically significant result.

PHENOTYPE ANALYSIS IN RELATION TO COPD SEVERITY

Table 18. A. Phenotype distribution among different COPD stages; **B.** Assessment of COPD risk within the different stages of severity

A	MILD		MODERATE		SEVERE		VERY SEVERE		
	n	%	n	%	n	%	n	%	p-value
Phenotype*									
normal	22	50.00	34	50.00	18	34.62	32	50.79	
fast	9	20.45	10	14.71	10	19.23	13	20.63	
slow	13	29.55	19	27.94	22	42.31	15	23.81	
very slow	0	0.00	5	7.35	2	3.85	3	4.76	0.374
*information not available for all subjects									
NORMAL: homozygous wild type for both exon 3 and exon 4, or heterozygous for both exon 3 and exon 4; FAST: at least one mutation in exon 4 and no exon 3 mutation; SLOW: heterozygous for exon 3 and homozygous for exon 4; VERY: homozygous mutation type for exon 3; OR: odds ratio; CI: confidence interval									

B	Model unadjusted		Model adjusted**	
	OR (95% CI)	p-value	OR (95% CI)	p-value
MODERATE vs MILD				
Phenotype*				
normal	1.000		1.000	
fast	0.719(0.252-2.051)	0.537	0.718(0.252-2.045)	0.536
slow+very slow	1.195(0.504-2.829)	0.686	1.122(0.469-2.683)	0.796
SEVERE vs MILD				
Phenotype*				
normal	1.000		1.000	
fast	1.358(0.454-4.059)	0.584	1.359(0.452-4.084)	0.585
slow+very slow	2.256(0.901-5.653)	0.082	2.227(0.88-5.636)	0.091
VERY SEVERE vs MILD				
Phenotype*				
normal	1.000		1.000	
fast	0.993(0.362-2.722)	0.989	0.941(0.337-2.629)	0.908
slow+very slow	0.952(0.388-2.333)	0.914	0.929(0.375-2.303)	0.873
*information not available for all subjects; **adjusted for age at blood draw and sex				
NORMAL: homozygous wild type for both exon 3 and exon 4, or heterozygous for both exon 3 and exon 4; FAST: at least one mutation in exon 4 and no exon 3 mutation; SLOW: heterozygous for exon 3 and homozygous for exon 4; VERY: homozygous mutation type for exon 3; OR: odds ratio; CI: confidence interval				

In the COPD group the phenotype distribution among the various COPD stages did not show any statistically significant difference (**Table 18. A**), even by merging slow and very slow phenotypes into a single group (data not shown).

Since there are not subjects with very slow phenotype and mild stage (reference category), the multinomial regression analysis was carried out by merging slow and very slow phenotypes into a single group (**Table 18. B**). The univariate and multivariate analysis did not show any statistically significant result in regard to the risk of developing more severe COPD at different stages of disease severity. Anyway, the slow+very slow phenotype group shows a tendency to increase the risk to develop severe COPD than normal phenotype, compare to mild stage.

2.6.4. GENOTYPE AND PHENOTYPE ANALYSIS IN RELATION TO ACUTE EVENTS (mortality and hospitalization for respiratory causes)

GENOTYPE ANALYSIS IN RELATION TO DEATH IN COPD GROUP

Table 19. Genotype distribution among dead and not dead COPD patients and assessment of death risk;

	DEAD								
	YES (n=93)		NO (n=136)			Model unadjusted		Model adjusted*	
	n	%	n	%	p-value	OR (95% CI)	p-value	OR (95% CI)	p-value
EPHX1 rs1051740									
Ho wt	47	50.54	71	52.21		1.000		1.000	
He	40	43.01	61	44.85		0.991(0.576-1.705)	0.973	0.989(0.561-1.746)	0.971
Ho SNP	6	6.45	4	2.94	0.442	2.266(0.607-8.463)	0.224	2.266(0.582-8.818)	0.238
EPHX1 rs2234922*									
Ho wt	57	61.96	93	68.89		1.000		1.000	
He	33	35.87	38	28.15		1.417(0.800-2.508)	0.232	1.552(0.852-2.827)	0.151
Ho SNP	2	2.17	4	2.96	0.456	0.816(0.145-4.597)	0.817	0.564(0.094-3.379)	0.530
*adjusted for age at blood draw and sex									
Ho wt: homozygous wild type; He: heterozygous; Ho SNP: homozygous SNP; OR: odds ratio; CI: confidence interval									

The univariate analysis did not show any statistically significant difference in the genotype distribution among dead and not dead COPD patients, even by merging He and Ho SNP in a single group (data not shown). Regarding the multivariate analysis, the association between genotype and risk of death did not show any statistically significant result, even by merging He and Ho SNP in a single group (data not shown). Anyway, Ho SNP and He in SNP rs1051740 and SNP rs2234922, respectively, show a tendency to increase the risk of death compare to wt in COPD patients

GENOTYPE ANALYSIS IN RELATION TO HOSPITALIZATION IN COPD GROUP

Table 20. A. Genotype distribution among hospitalized - at least one time for respiratory causes - and never hospitalized COPD patients, and assessment of risk of hospitalization; **B.** same analyses merging He and Ho SNP.

A	HOSPITALIZATION								
	YES (n=69)		NO (n=160)			Model unadjusted		Model adjusted*	
	n	%	n	%	p-value	OR (95% CI)	p-value	OR (95% CI)	p-value
EPHX1 rs1051740									
Ho wt	29	42.03	89	55.63		1.000		1.000	
He	35	50.72	66	41.25		1.627(0.906-2.925)	0.103	1.571(0.862-2.862)	0.140
Ho SNP	5	7.25	5	3.13	0.101	3.069(0.829-11.357)	0.093	3.075(0.824-11.475)	0.095
EPHX1 rs2234922									
Ho wt	49	73.13	101	63.13		1.000		1.000	
He	16	23.88	55	34.38		0.6(0.312-1.152)	0.125	0.588(0.300-1.149)	0.120
Ho SNP	2	2.99	4	2.50	0.298	1.031(0.182-5.821)	0.973	0.873(0.151-5.045)	0.879
*adjusted for age at blood draw and sex									
Ho wt: homozygous wild type; He: heterozygous; Ho SNP: homozygous SNP; OR: odds ratio; CI: confidence interval									

B	HOSPITALIZATION								
	YES (n=69)		NO (n=160)			Model unadjusted		Model adjusted*	
	n	%	n	%	p-value	OR (95% CI)	p-value	OR (95% CI)	p-value
EPHX1 rs1051740									
Ho wt	29	42.03	89	55.63		1.000		1.000	
He+Ho SNP	40	57.97	71	44.38	0.063	1.729(0.977-3.060)	0.060	1.679(0.937-3.010)	0.082
EPHX1 rs2234922									
Ho wt	49	73.13	101	63.13		1.000		1.000	
He+Ho SNP	18	26.87	59	36.88	0.168	0.629(0.335-1.179)	0.148	0.610(0.321-1.162)	0.133
*adjusted for age at blood draw and sex									
Ho wt: homozygous wild type; He: heterozygous; Ho SNP: homozygous SNP; OR: odds ratio; CI: confidence interval									

The univariate analyses and the multivariate analysis (**Table 20 A**) did not show any statistically significant result regarding the genotype distribution among hospitalized and not hospitalized COPD patients and the association between genotype and risk of hospitalization, respectively, even by merging He and Ho SNP in a single group (**Table 20 B**). Anyway, considering the SNP rs1051740 in multivariate analysis, genotypes with at least one allele variation (He, Ho SNP and He+Ho SNP) show a tendency to increase the risk of hospitalization in COPD patients compare to wt. Note that, regarding the SNP rs1051740, merging He and Ho SNP (**Table 20 B**), the univariate analysis, the unadjusted model, and the adjusted model, show a borderline not significant trend with p=0.063,

p=0.060 and p=0.08 respectively, that underline how SNP rs1051740 could be involved in the risk of hospitalization in the COPD group.

PHENOTYPE ANALYSIS IN RELATION TO DEATH IN COPD GROUP

Table 21. Phenotype distribution among dead and not dead COPD patients and assessment of death risk;

	DEAD								
	YES (n=93)		NO (n=136)			Model unadjusted		Model adjusted*	
	n	%	n	%	p-value	OR (95% CI)	p-value	OR (95% CI)	p-value
Phenotype*									
normal	40	43.48	66	48.89		1.000		1.000	
fast	19	20.65	23	17.04		1.363(0.661-2.81)	0.401	1.357(0.636-2.897)	0.430
slow	27	29.35	42	31.11		1.061(0.569-1.977)	0.853	1.003(0.524-1.921)	0.993
very slow	6	6.52	4	2.96	0.495	2.475(0.658-9.309)	0.180	2.429(0.619-9.537)	0.203
*adjusted for età al prelievo and sex									
NORMAL: homozygous wild type for both exon 3 and exon 4, or heterozygous for both exon 3 and exon 4; FAST: at least one mutation in exon 4 and no exon 3 mutation; SLOW: heterozygous for exon 3 and homozygous for exon 4; VERY: homozygous mutation type for exon 3; OR: odds ratio; CI: confidence interval									

The univariate analysis did not show any statistically significant difference in the phenotype distribution among dead and not dead COPD patients, even by merging slow and very slow phenotypes into a single group (data not shown). Regarding the association between phenotype and risk of death, also the multivariate analysis did not show any statistically significant result, even by merging slow and very slow phenotypes into a single group (data not shown). Anyway, fast and very slow phenotypes shows a tendency to increase the risk of death compare to normal phenotype in COPD patients.

PHENOTYPE ANALYSIS IN RELATION TO HOSPITALIZATION IN COPD GROUP

Table 22. A. Phenotype distribution among hospitalized - at least one time for respiratory causes - and never hospitalized COPD patients, and assessment of risk of hospitalization; **B.** same analyses merging slow and very slow phenotypes.

A	HOSPITALIZATION								
	YES		NO			Model unadjusted		Model adjusted*	
	n	%	n	%	p-value	OR (95% CI)	p-value	OR (95% CI)	p-value
Phenotype*									
normal	27	40.30	79	49.38		1.000		1.000	
fast	9	13.43	33	20.63		0.798(0.339-1.878)	0.606	0.696(0.285-1.697)	0.425
slow	26	38.81	43	26.88		1.769(0.920-3.403)	0.087	1.591(0.817-3.100)	0.172
very slow	5	7.46	5	3.13	0.094	2.926(0.786-10.891)	0.109	2.821(0.752-10.584)	0.124
*adjusted for età al prelievo and sex									
NORMAL: homozygous wild type for both exon 3 and exon 4, or heterozygous for both exon 3 and exon 4; FAST: at least one mutation in exon 4 and no exon 3 mutation; SLOW: heterozygous for exon 3 and homozygous for exon 4; VERY: homozygous mutation type for exon 3; OR: odds ratio; CI: confidence interval									

B	HOSPITALIZATION								
	YES		NO			Model unadjusted		Model adjusted*	
	n	%	n	%	p-value	OR (95% CI)	p-value	OR (95% CI)	p-value
Phenotype*									
normal	27	40.30	79	49.38		1.000		1.000	
fast	9	13.43	33	20.63		0.798(0.339-1.880)	0.606	0.696(0.285-1.697)	0.426
slow+very slow	31	46.27	48	30.00	0.057	1.890(1.008-3.542)	0.047	1.720(0.908-3.257)	0.096
*adjusted for età al prelievo and sex									
NORMAL: homozygous wild type for both exon 3 and exon 4, or heterozygous for both exon 3 and exon 4; FAST: at least one mutation in exon 4 and no exon 3 mutation; SLOW: heterozygous for exon 3 and homozygous for exon 4; VERY: homozygous mutation type for exon 3; OR: odds ratio; CI: confidence interval									

The univariate analyses and the multivariate analysis (**Table 22 A**) did not show any statistically significant result regarding the phenotype distribution among hospitalized and not hospitalized COPD patients and the association between phenotype and risk of hospitalization, respectively.

Note that the univariate association and the unadjusted model show a border line not significant p-value (p=0.057) and a significant p-value (p=0.047), respectively, by merging slow and very slow phenotypes into a single group (**Table 22 B**), with the percentage of slow+very slow phenotype higher in hospitalized patients than in not hospitalized. Anyway, this result is not more significant when adjusted for sex and age (multivariate logistic regression analysis), so we can not attribute this significant result to the phenotype since there is a difference by sex and age. The difference that is observed may be due to gender or age difference inside the COPD group.

2.7. CONCLUSION

In this study, the socio-demographic, lifestyle and clinical factors of the population affected by COPD show a population consisted mostly of men, ex-smokers, not practicing any physical activity, obese or overweight, and with regard to the deprivation index, the majority of patients were deprived or very deprived, regardless of COPD stage.

Results from previous studies show that smoking, aging, gender, and socio-economic factors are well established risk factors for COPD development [205] [201]. A systematic review and meta-analysis of studies carried out in 28 countries between 1990 and 2004 [206], provide evidence that the prevalence of COPD is appreciably higher in smokers and ex-smokers than in nonsmokers, in those over 40 years of age than those under 40, and in men than in women.

This study shows a significant association between age and COPD risk (**Table 6**), but this is because the control subjects enrolled are much younger than cases.

Taking into account the COPD GOLD stages, a significant association between the smoking status and severity of disease was detected. Smoking certainly represents the main risk factor for COPD and the risk of developing COPD among smokers is dose-related, while the age at which they start smoking, the number of cigarettes smoked, and current smoking status are predictive of COPD mortality. In the COPD study population can be observed that while the distribution of smokers in the four stages remains almost constant, the number of ex-smokers increases, while that of non-smokers decreases with increasing severity of the disease (**Table 7**).

The role of sex in the risk of developing COPD is not yet entirely clear. In the past, most of the studies reported a higher incidence of COPD and related mortality in men than women. Also in the our study population regression analysis showed a higher incidence of the disease in men than women, but association between gender and COPD risk was not significant. In fact, as can be seen from **Table 7**, we see that as the degree of disease severity increases, decreases the number of females and increases that of males. Anyway, based on WHO analyses, because of increased tobacco use among women in high-income countries and the higher risk of exposure to indoor air pollution (such as biomass fuel used for cooking and heating) in low-income countries, the disease now affects men and women almost equally.

COPD often coexists with other diseases and the scientific literature highlights that they may significantly impact on prognosis. **Table 8** shows the highest percentage of patients

with two or more comorbidities suffer from very severe COPD and the analyses confirms that the Charlson index is a risk factor associated to COPD severity.

According to the literature, FeNO values are normal or mildly increased in stable COPD [207] and measurement of FeNO represents a non-invasive marker that may be useful to detect exacerbations and inflammation reduction in small airway disease [208]. In this study population FeNO and spirometric values are significantly associated with the severity of COPD.

Although some studies highlighted a role of low BMI as an important risk factor for acute events, in particular showing that underweight and low skeletal muscle mass are significant determinants of mortality in COPD [209-211]. In our COPD population any significant association was observed between COPD stage and BMI, as well waist circumference. The heterogeneous distribution of underweight among patients with different characteristics (e.g. deprivation) and the sample size may explain the not significant results of BMI as a risk factor in the bivariate analyses.

Previous studies have examined the association between socio-economic status and COPD health outcomes but results are controversial, possibly due to the different accessibility to health care. Eisner et al. [212] found that socio-economic status represents a risk factor for adverse COPD health outcomes. In contrast, in the present study the deprivation index does not influence disease evolution, probably because the accessibility to the Italian National Health Service, countervails the effects associated to socio-economic status.

COPD is more frequent in smokers and it seems that EPHX1 plays a pivotal role in protecting the lung against environmental exposures. Genetic variability of EPHX1 is associated with several pathological phenotypes and may in concert with environmental exposures contribute to the development of malignancies, especially in the lungs. Several studies and meta-analysis have assessed the association between EPHX1 polymorphisms and COPD in different populations, however, the results are still inconsistent and controversial. In our study population, the statistical analysis did not show any significant result about the potential relationship between analyzed EPHX1 SNPs, and related phenotypes, and gender, BMI, waist circumference and the risk to develop COPD and disease severity. Moreover, any statistically significant result in the COPD group was observed in regard to the associations between analyzed EPHX1 SNPs, and related phenotypes, and acute events (mortality and hospitalization for respiratory causes).

In contrast with literature, the 113 mutant homozygote (rs1051740) shows a tendency to protect from COPD risk (**Table 15 A**), not to increase the COPD risk.

Limitation of this study are the small sample size and the huge age difference between cases and controls, consequently it is not possible to exclude that predictors investigated in the present study might result significantly associated with the outcomes under investigation in larger studies.

CHAPTER 3

Pilot study about the application of stable isotope-resolved metabolomics to explore tissue glycolytic pathway alterations induced by chronic cigarette smoke exposure in emphysema mouse model

3.1 INTERMEDIARY METABOLISM: ENERGY SOURCE FOR THE CELL

The word metabolism comes from the greek term “*μεταβολή*” (“*metabolē*”, "*change*") which means "transformation".

Metabolism is the set of life-sustaining chemical transformations within the cells of living organisms that convert nutrients (the raw material required for sustenance of the living beings), in energy or chemically complex cellular substances.

The metabolism consists of hundreds of enzymatic reactions organized in separate paths. These metabolic pathways involve consecutive transformations of substrates in end products through the formation of many chemical intermediates. The metabolism is sometimes referred by the term “intermediary metabolism” to emphasize this aspect of the process. In the metabolic maps (point = chemical intermediate, line = enzyme) almost all the major reactions of intermediary metabolism of carbohydrates, lipids, amino acids, nucleotides and their derivatives are represented (**Figure 1**).

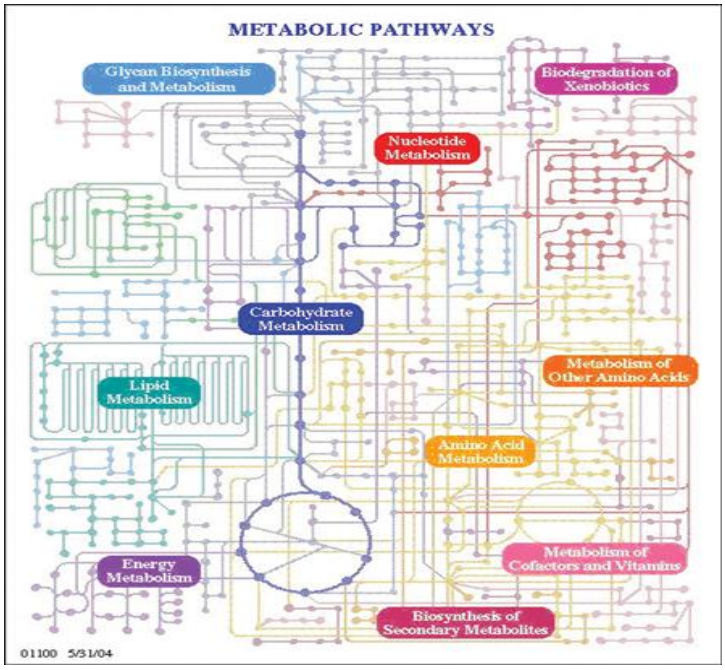

Figure 1. Metabolic Map

Many metabolic pathways (about 80%) tend to proceed only in one direction (essentially irreversible reactions under physiological conditions). However, many intermediates are subject to a variety of fates. In these cases the chosen metabolic pathway entails an important choice of adjustment. Thus, each substrate is directed along a particular metabolic pathway in response to a regulative choice adopted in response to the temporary energetical or nutritional needs of the cell (or organism).

All organisms show a marked similarity in terms of the major metabolic pathways, according to the hypothesis that all living organisms descend from a common ancestral form.

All the forms of nutrition and almost all metabolic pathways have evolved in primitive prokaryotes before the appearance of eukaryotes, a billion years ago. For example, glycolysis, the metabolic pathway through which energy is released from glucose and stored in ATP under anaerobic conditions, it is common to almost all cells. For this reason glycolysis is supposed to be the anciest among the metabolic pathways and it has been originated before the onset of significant traces of oxygen in the atmosphere. All organisms, including those able to synthesize their own glucose, are able to degrade the glucose and to synthesize ATP via glycolysis. Other important metabolic pathways are widely distributed in all living organisms.

3.1.1. CATABOLISM AND ANABOLISM

The metabolism fulfills two fundamentally different purposes: the production of energy which supplies the vital processes, and the synthesis of the molecules necessary for the structure and function of the cells. To accomplish these goals, metabolism consists mainly of two opposing processes: catabolism and anabolism. The catabolic pathways produce energy, while the anabolic pathways require energy.

Catabolism involves the oxidative degradation of complex nutrient molecules (carbohydrates, lipids, proteins) obtained from both the environment and the cellular reserves. The degradation of these molecules through the catabolism leads to the formation of more simple molecules such as lactic acid, ethanol, carbon dioxide, urea and ammonia. The catabolic reactions are generally exoergonic, and often the energy released is captured in form of ATP (free energy of ATP hydrolysis = -30.5 kJ / mol).

Since catabolism is oxidative, part of the chemical energy can be stored through the reduction of coenzyme NAD+ (nicotinamide adenine dinucleotide) and NADP+

(nicotinamide adenine dinucleotide phosphate) forming NADH and NADPH, respectively, which have very different metabolic roles. The reduction of NAD+ to NADH accompanies many oxidative reactions which occur during the catabolism, especially during glycolysis with 2 mole NADH produced for each mole of glucose metabolized to pyruvate (e.g. glyceraldehyde-3-phosphate oxidation to 1,3-bisphosphoglycerate). In aerobic cells, the NADH oxidation can be coupled to the ADP phosphorylation, and so the NADH reoxidation to NAD+ is used to generate more ATP via the mitochondrial electron transport chain. In contrast, the NADPH is the source of the reducing power necessary to carry out the reductive biosynthetic reactions. The oxidation of NADPH is therefore a feature of anabolism.

The anabolism is the process of synthesis during which the different and complex biomolecules (proteins, nucleic acids, polysaccharides and lipids) are assembled starting from simple precursors. These biosynthesis involve the new covalent bonds formation and require energy input to allow these endoergonic chemical processes. ATP is produced by catabolism to provide this energy. Moreover, the NADPH is an excellent electron donor for the anabolic reductive reactions (**Figure 2**).

Catabolism and anabolism occur simultaneously within the cell and, despite the divergent roles, the cell is able to simultaneously manage the catabolism and anabolism since the products of one provide substrates for the other one. First, the cell keeps under close and separate control both anabolism catabolism, so that the metabolic needs are fulfilled in an immediate and tidy way. Second, contrasting metabolic pathways are often located in different subcellular compartments. The isolation of opposite activities within separate compartments, prevents interferences between them. For example, the enzymes responsible for the catabolism of fatty acids are localized in the mitochondria (beta-oxidation), while the biosynthesis of fatty acids takes place in the cytosol.

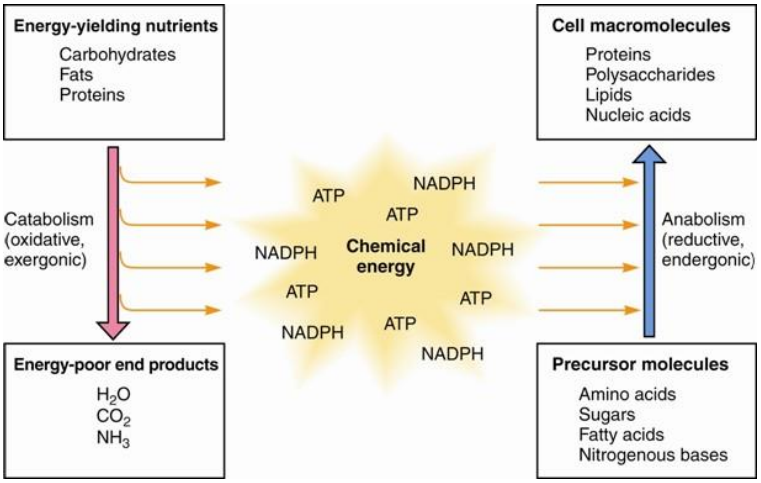

Figure 2. Energy relationships between the pathways of catabolism and anabolism. Oxidative and exoergonic pathways of catabolism release free energy and reducing power that are captured in the form of ATP and NADPH, respectively. Anabolic processes are endoergonic, consuming chemical energy in the form of ATP and using NADPH as a source of high energy electrons for reductive purposes**.**

ATP and NADPH represent the two primary cellular products with high energy. In heterotrophs, the catabolic pathways have the main purpose to release free energy, so that it can be captured in the form of high-energy phosphoanidridic bonds in ATP. In turn, the ATP provides the energy that allows the multiple activities common to all living cells: the synthesis of complex biomolecules, the osmotic work involved in the transport of substances within the cell, the work required by the cell motility and muscle contraction. These activities are all powered by the release of energy due to hydrolysis of ATP to ADP and P_i.

Into the cells it is created an energy cycle in which the ATP has the function of energy carrier from the catabolism to the processes that require energy.

The substrates of catabolism (proteins, carbohydrates and lipids) are good sources of chemical energy, because the carbon atoms in these molecules are relatively reduced (**Figure 3**). During the catabolic oxidative reactions these substrates release reducing equivalents, often in the form of hydride ion (a proton coupled with two electrons, H:-, the dehydrogenation). These hydride ions are transferred (in enzymatic reactions catalyzed by dehydrogenase) from the substrates to molecules of NAD+, which are reduced to NADH (e.g.: the dehydrogenation reaction catalyzed by alcohol dehydrogenase where Ethyl Alcohol is oxidized to acetaldehyde and a hydride ion is transferred to NAD+ that becomes NADH). A second proton, which appears in the equation of the total reaction such as H+ is involved in these reactions (NADH + H+). The NADH is reoxidized to NAD+ when its

reducing equivalents are transferred to electron acceptors which are part of the mitochondria metabolic apparatus. The final oxidizing agent (the final electron acceptor) is the oxygen which is reduced to H_2O.

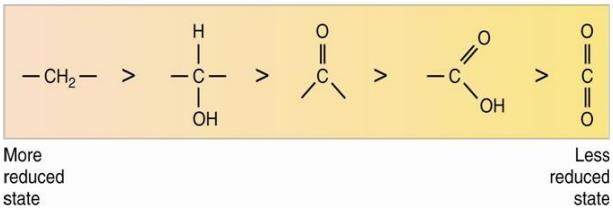

Figure 3. Comparison of the state of reduction of carbon atoms in biomolecules: -CH2 (fats) > CHOH- (carbohydrates) > C=O (carbonyls) > CO2 (carbon dioxide, the final product of catabolism)

Oxidation reactions are exoergonic, and the released energy is coupled to the formation of ATP in a process called *oxidative phosphorylation*. The system NAD+/NADH can be seen as a shuttle system that transports electrons, released by catabolism of substrates, to the mitochondria where they are finally transferred to oxigen, the final metabolic acceptor. During this process the released free energy is trapped in ATP.

Mitochondrial membranes are impermeable to NADH which, therefore, must be transferred into the mitochondrial matrix via "hydrogen shuttle" mechanisms. The shuttle mechanisms for the transfer of reducing equivalents from cytoplasm to mitochondria are the glycerol-3-phosphate pathway in which dihydroxyacetone phosphate is reduced to glycerol-3-phosphate in the cytoplasm and reoxidized in the mitochondria, and the other one is the malate-aspartate shuttle which requires influx of malate and efflux of asparate from the mitochondrial space.

The NADH cycle plays an important role in the transformation of the chemical energy of carbon compounds in the energy present in chemical phosphoanidridic bonds (ATP). These energy transformations from one form into another are known as “energy transduction”. Oxidative phosphorylation is a cellular mechanism of energy transduction.

While catabolism is basically an oxidative process, anabolism, on the contrary, is a reductive process.

The biosynthesis of complex cellular components starts at the level of intermediates that come from degradative pathways of catabolism. For example, when the hydrocarbon chains of fatty acids are assembled from units of acetyl-CoA, activated hydrogen atoms are necessary for reducing the carbonyl carbons (C=O) of acetyl-CoA into groups -CH2-, in all positions along the chain. The reducing equivalents necessary for the reductive

processes are provided by NADPH, the common source of hydrogens for the reductive biosynthesis. NADPH is formed when the NADP+ is reduced by the electrons, in the form of hydride ions. In heterotrophic organisms, these electrons are removed from the fuel molecules by specific dehydrogenases for NADP+. In these organisms NADPH can be seen as a carrier of electrons from catabolic reactions to anabolic reactions (**Figure 4**).

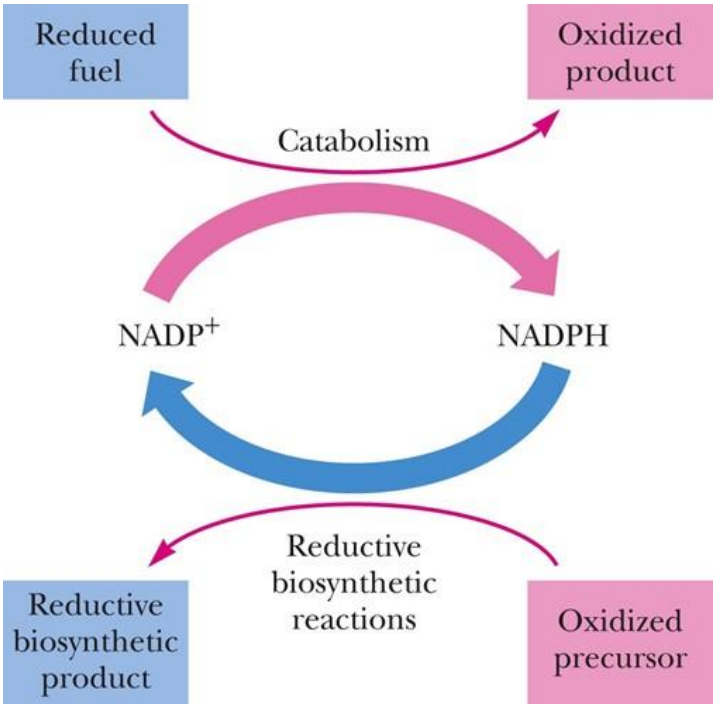

Figure 4. Transfer of reducing equivalents fron catabolism to anabolism via the NADPH cycle.

Nicotinamide coenzymes (also known as pyridine nucleotides) are electron carriers and are involved in many and important redox reactions catalyzed by enzymes (reductive biosynthesis, detoxification reactions, generation of ATP). The ratios of NAD+/NADH and NADP+/NADPH determine the intracellular redox state of cell, which influences the thermodynamic driving force of many reactions in vivo and reflects both the metabolic activities and the health of cells.

3.1.2. GLUCOSE: THE MAIN CELLULAR ENERGY SOURCE

The name "glucose" comes from the Greek word *γλυκος*, meaning "sweet wine, must". Glucose (**Figure 5**) is a sugar (carbohydrate) with the molecular formula $C_6H_{12}O_6$, has six carbon atoms and it is classed as a hexose. It is used as an energy source in most organisms, from bacteria to humans, through either aerobic respiration, anaerobic respiration, or fermentation.

Glucose is the human body's key source of energy and within the cell the major pathways for catabolism of glucose include the glycolytic and pentose phosphate pathways. These reactions produce lactate and CO_2 as major end products and generate glycerol-3-phosphate, ribose and pyruvate which can be utilized as intermediates for synthesis of lipids and nucleic acids, transamination to amino acids, and oxidation via the Krebs cycle. The catabolism of glucose also generates reduced pyridine nucleotides (NADPH and NADH), reducing potential which is essential in the extramitochondrial compartment for reductive biosynthesis and after transfer into the mitochondria, can be utilized for energy generation via the electron transport chain. Finally, the catabolism of glucose results in synthesis of high energy compounds (ATP).

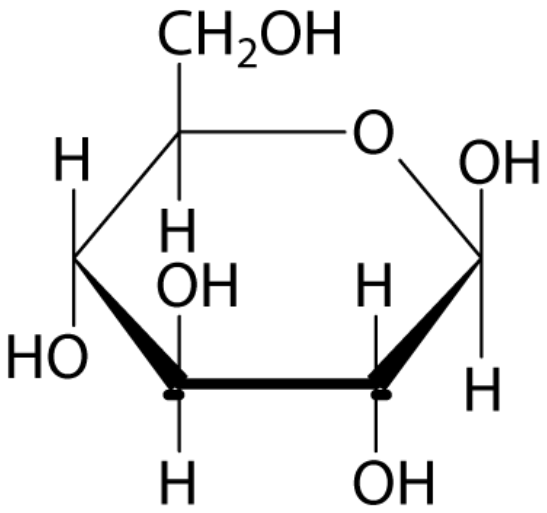

Figure 5. Molecule of glucose

3.1.3. GLYCOLYSIS

Almost all living cells perform a metabolic process known as *glycolysis*, sequential oxidative degradation of glucose, and other simple sugars.

Glycolysis (**Figure 6**) is a metabolic pathway carried out in the cytosol of cells in anaerobic condition.

Millions of years ago, living beings evolved in an oxygen-free environment and glycolysis likely was premature and important metabolic pathway to extract energy from nutrient molecules. It played a central role in the anaerobic metabolism during the first two billion years of biological evolution on Earth.

Currently, the organisms are still using glycolysis to provide the precursors of the aerobic metabolic pathways (the tricarboxylic acid cycle), and as a short term energy source when oxygen is present in limited amount.

Most of the steps of this pathway (the first pathway to be elucidated) were discovered in the first half of the twentieth century by biochemical German Otto Warburg, G. Embden and O. Meyerhof (glycolysis is also called Embden-Meyerhof metabolic pathway).

Glycolysis has two phases. The first one, the glucose is converted into two molecules of glyceraldehyde-3-phosphate through five reactions; the second one, five subsequent reactions convert the two molecules of glyceraldehyde 3-phosphate into two molecules of pyruvate. The phase one consumes two molecules of ATP, the final stages result in the production of four molecules of ATP. The net balance is 4 - 2 = 2 molecules of ATP produced per molecule of glucose.

Metabolic control of the glycolytic pathway can be achieved by agents that exert regulation over the long or over the short term. Long-term regulation occurs chiefly through the effect of hormones (e.g. insulin, glucagone) and other mediators on the enzymes involved in glucose uptake and metabolism. Short-term control occurs by regulation of enzyme activity through changes in concentration of important reactants and modifiers. Two important glycolytic regulators of the second class are the cellular ATP concentration (ATP/ADP ratio, the energy state of the cell) and the cellular NAD+ concentration (the NAD+/NADH ratio, redox state of the cell). In many cells and tissues, glycolytic flux increases in response to ATP depletion (assuming sufficient ATP for glucose phosphorylation) and decreases as NAD+ is depleted. Reoxidation of the cytoplasmic pyridine nucleotide is essential to permit glycolysis to proceed. NAD+ can be regenerated through utilization of

NADH in production of lactate from pyruvate or production of glycerol-3-phosphate from dihydroxyacetone phosphate.

The provision of mitochondrial (Krebs cycle) substrate can also have a regulatory effect on glycolysis. This effect is not due to alteration of redox ratio, but most likely reflects increased citrate synthesis by the mitochondria with subsequent inhibition of cytosolic phosphofructokinase.

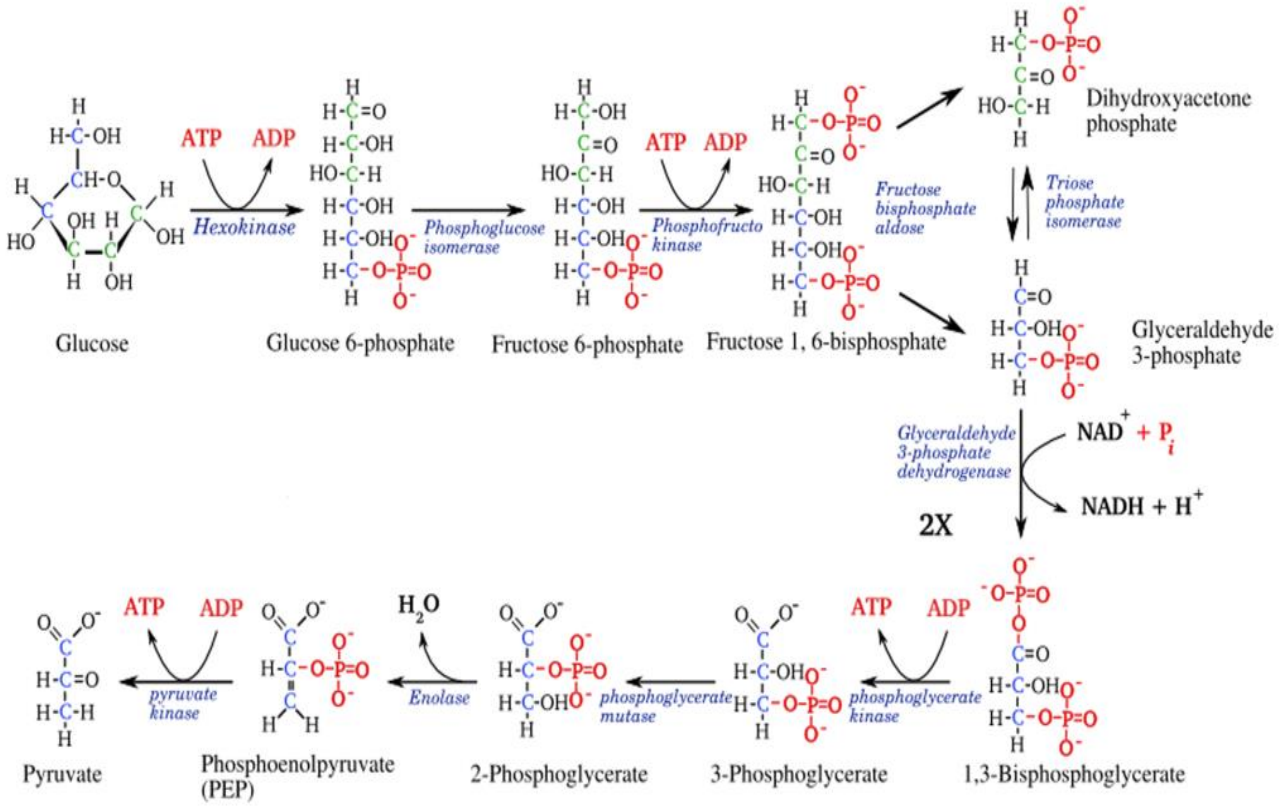

Figure 6. Glycolysis

3.1.4. PENTOSE PHOSPHATE PATHWAY

The cells require a constant supply of NADPH for reductive biosynthesis. Most of this demand is met by a metabolic pathway that starts from glucose, known as the pentose phosphate pathway (**Figure 7**). In addition to supplying the NADPH for biosynthetic purposes, this pathway produces ribose-5'-phosphate, essential for the nucleotides and nucleic acids synthesis, whereas several metabolites can be directed to glycolysis.

The pentose phosphate pathway begins with the glucose-6-phosphate (six carbon sugar) and produces sugars with three-, four-, five-, six- and seven-carbon. Two subsequent oxidative reactions lead to the reduction of NADP+ to NADPH and the release of CO_2. The five subsequent non-oxidative reactions produce a variety of carbohydrates, some of which can enter into glycolytic pathway.

The pentose phosphate pathway enzymes are localized in the cytosol of the cells, which is the site of fatty acid synthesis and also detoxification reactions, two ways strictly dependent on NADPH for reductive reactions. Moreover, the pentose cycle enzymes are particularly abundant in the cytoplasm of the liver, adipose tissue and lung cells, whereas are lacking in the muscle, where glucose-6-phosphate is used mainly to obtain energy by glycolysis and TCA cycle.

The use of glucose-6-phosphate depends on the cellular demands of ATP, NADPH and ribose-5-P.

Glucose-6-phosphate is shared between glycolysis and the pentose phosphate pathway. The entry in one or other metabolic pathway depends on the energy needs (ATP/AMP ratio) of the cell and the relative concentrations of NADP+ and NADPH (NADP+/NADPH ratio). Whether within the cell are occurring reductive reactions or biosynthesis with consumption of NADPH, NADP+ levels increase. The glucose-6-phosphate dehydrogenase (the pentose phosphate pathway key enzyme) is activated allosterically by NADP+, resulting in activation of pentose phosphate pathway. Whether, on the other hand, the levels of NADP+ decrease, the pentose phosphate pathway is slowed and glucose-6-phosphate is used for the glycolysis.

Glucose-6-phosphate can be used as substrate either in glycolysis either in pentose phosphate pathway and within the cell the choice of one pathway rather than the other is determined based on the cellular metabolic needs of energy and biosynthesis. ATP can be produced in abundance if the glucose-6-phosphate is addressed to glycolysis. On the other hand, if it is required NADPH and ribose-5-phosphate, glucose-6-phosphate can be

directed toward the pentose phosphate pathway. The molecular basis of this regulatory decision depends on the enzymes that metabolize glucose-6-phosphate in glycolysis and in pentose phosphate pathway. In glycolysis, the fosfoglucoisomerase converts glucose-6-phosphate into fructose-6-phosphate, which is used by phosphofructokinase (highly regulated enzyme) to produce fructose-1,6-bisphosphate. In the pentose phosphate pathway, glucose-6-phosphate dehydrogenase (also highly regulated) produces gluconolactone from glucose-6-phosphate. The fate of the glucose-6-phosphate is therefore determined in large part by the activity of phosphofructokinase (PFK) and glucose-6-phosphate dehydrogenase (G6PDH). PFK is inhibited by an increased ATP/AMP ratio and by citrate. So, when the energy charge is high, the glycolytic flow is reduced. The glucose-6-phosphate dehydrogenase, on the other hand, is inhibited by high levels of NADPH and also by fatty acids biosynthesis intermediates. Both of these compounds indicate that requests biosynthetic were met. In this case, the glucose-6-phosphate dehydrogenase and the the pentose phosphate pathway are inhibited. If the levels of NADPH go down, the pentose phosphate pathway is restarted and NADPH and ribose-5-phosphate are produced for biosynthetic purposes. However, even when it is operated this latter choice, the cell must still be able to cope with the demands of ribose-5-phosphate and NADPH (such as ATP). Depending on the entity of these demands, the glycolysis and the pentose phosphate pathway reactions can be combined in new ways to increase the synthesis of the required metabolites.

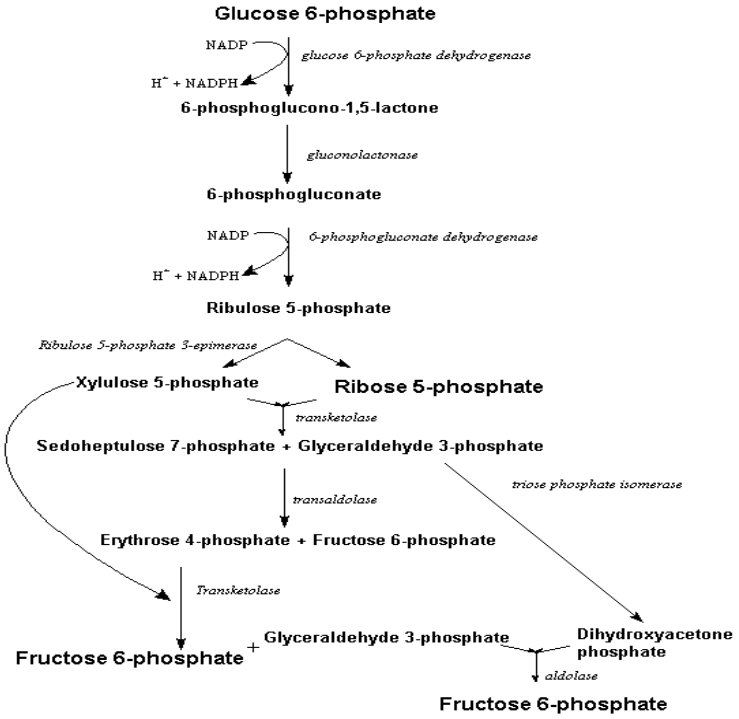

Figure 7. Pentose Phosphate Pathway

In summary the Pentose Phosphate Pathway has three main functions:

1. Supply the cell with NADPH in order to:
    - Provide reducing power for biosynthetic reactions;
    - Serve as a biochemical reductant (e.g. maintaining glutathione levels);
    - Be utilized by the cytochrome P450 monooxygenase system;
    - Serve as electron source for reduction of ribo- to deoxyribonucleotides, for DNA synthesis;
2. Convert hexoses into pentoses (which are essential components of ATP, CoA, NADP+, FAD, RNA and DNA);
3. Enable the complete oxidative degradation of pentoses by converting them into hexoses and trioses which can then enter the glycolytic pathway.

3.1.5. LUNG INTERMEDIARY METABOLISM

The lung is a metabolically active organ that is engaged in secretion, clearance and other maintenance functions that require reducing potential, energy and substrates for biosynthesis. Alterations in lung intermediary metabolism may depress amine clearance, alter lung permeability, and influence the lung response to oxidant stress.

Based on studies on rat perfused lung tissue, lung metabolic requirements are met in part through uptake and catabolism of glucose which represents the major fuel utilized by lung tissue. Glucose is catabolized in the lung by cytoplasmic and mitochondrial pathways that are responsive to regulatory mechanisms that are qualitatively similar to those in other tissues [213].

In addition to generating carbon substrates for further oxidation or for biosynthetic reactions, the catabolism of glucose generates reducing equivalents which in turn are used for reductive biosynthesis, detoxification reactions, and generation of ATP via the mitochondrial electron transport chain.

Cytoplasmic reducing equivalents are generated as NADH during glycolysis and NADPH from the reactions of the pentose shunt pathway. Mitochondrial reducing equivalents, which are generated as NADH and reduced flavins ($FADH_2$, $FMNH_2$) from reactions including pyruvate dehydrogenase and Krebs cycle, are linked directly to the mitochondrial electron transport chain.

Reactions that generate NADPH in the cytoplasm include the pentose pathway (glucose-6-phosphate dehydrogenase and 6-phosphogluconate dehydrogenase), conversion of malate to pyruvate by malic enzyme, and conversion of isocitrate to a-ketoglutarate by isocitric dehydrogenase (IDH1). Therefore, the major source of NADPH in the lung cytoplasm is assumed to be the pentose pathway. The major mitochondrial sources of NADPH are NADP+-linked isocitric dehydrogenase (IDH2, IDH3) and nicotinamide nucleotide transhydrogenase (NNT).

The lung, portal of entry into the body and organ of gas exchanges, is the seminal point of exposure to oxidants and many environmental toxicants. Therefore, reducing and detoxification reactions have a key role in the lung homeostasis.

Generation of NADPH appears to be of primary importance in protection of the lung tissue against oxidative damage and xenobiotics. Several studies have shown that oxidants and toxic free radicals [213-215] stimulate pentose cycle activity in order to meet the increased demand for cytoplasmic reducing equivalents. Indeed, the elimination of toxic free radicals, by their further reduction to water, requires reducing equivalents generated intracellularly from intermediary metabolism.

NADPH is the major biological reductant utilized for biosynthetic reactions, and to maintain the redox status of the cell by regenerating thiol-based redox couples, GSH and thioredoxin, thus protecting the cell from oxidative damage. This reducing power is also utilized in double-bond reduction in fatty acid biosynthesis, which is involved in surfactant synthesis, as well as in detoxification reactions (e.g. NADPH-cytochrome P450 reductase).

Regarding energy consumption, lung tissue per se is a relatively modest consumer of energy in comparison to muscles of respiration or other working tissues [216]. Nevertheless, the lung has energy-dependent functions that for the most part have been relatively poorly defined. Some of these energy-requiring functions include lung clearance (phagocytosis and ciliary activity), bronchial gland secretion, contraction of tracheobronchial smooth muscle, surfactant synthesis and secretion, and maintenance of normal transcellular ion gradients. Efficient functioning of these energy-dependent systems requires the maintenance of tissue energy stores, that are determined by the balance between rates of ATP generation and utilization. In most metabolically active tissues, the bulk of ATP is generated from mitochondrial oxidation while glycolysis is only supplemental. In the lung, the ATP content is maintained by oxidative metabolism at levels comparable to other metabolically active organs [213].

Lung tissue carries out important metabolic activity, but much remains to be accomplished before we gain complete understanding of the relationships between cellular metabolic activity and overall lung function, including the mechanisms by which intermediary metabolism is altered in the presence of disease.

The relationship of intermediary metabolism to lung pathophysiology has been examined in detail for only a limited number of conditions, but studies of this sort are particularly vulnerable to problems with interpretation because of cellular heterogeneity of the normal lung and heterogeneity of cellular response to toxic insults.

3.1.6. LIVER INTERMEDIARY METABOLISM

The liver is a key metabolic organ which governs body energy metabolism. Glucose is metabolized into pyruvate through glycolysis in the cytoplasm, and pyruvate is completely oxidized to generate ATP through the TCA cycle and oxidative phosphorylation in the mitochondria.

Liver acts as a hub to metabolically connect to various tissues, including skeletal muscle and adipose tissue. Food is digested in the gastrointestinal (GI) tract, and glucose, fatty acids, and amino acids are absorbed into the bloodstream and transported to the liver through the portal vein circulation system.

In the fed state glucose is condensed into glycogen (glycogenesis) and/or converted into fatty acids (de novo lipogenesis) or amino acids in the liver. In hepatocytes, long chain fatty acids are incorporated into triacylglycerol (TAG), phospholipids, and cholesterol esters and these complex lipids are stored in lipid droplets and membrane structures, or secreted into the circulation as VLDL particles. Amino acids are metabolized to provide energy or used to synthesize proteins, glucose, and/or other bioactive molecules.

In the fasted state or during exercise, the liver secretes glucose through both breakdown of glycogen (glycogenolysis) and de novo glucose synthesis (gluconeogenesis). Fuel substrates, as glucose and TAG, are released from the liver into the circulation and metabolized by muscle, adipose tissue, and other extrahepatic tissues. Adipose tissue produces and releases nonesterified fatty acids (NEFAs) and glycerol via lipolysis. Muscle breaks down glycogen and proteins and releases lactate and alanine. Alanine, lactate, and glycerol are delivered to the liver and used as precursors to synthesize glucose (gluconeogenesis). NEFAs are oxidized in hepatic mitochondria through fatty acid β

oxidation and generate ketone bodies (ketogenesis). Liver-generated glucose and ketone bodies provide essential metabolic fuels for extrahepatic tissues during starvation and exercise.

Liver energy metabolism is tightly controlled. Multiple nutrient, neuronal and hormonal systems have been identified to regulate liver metabolic processes. The sympathetic system stimulates, whereas the parasympathetic system suppresses, hepatic gluconeogenesis. Insulin stimulates glycolysis and lipogenesis, but suppresses gluconeogenesis; glucagon counteracts insulin action.

Aberrant energy metabolism in the liver promotes insulin resistance, diabetes, and nonalcoholic fatty liver diseases (NAFLD).

Hepatocytes are the main cell type in the liver (~80%). Blood glucose enters hepatocytes via a plasma membrane glucose transporter (GLUT). Glucose is phosphorylated by glucokinase in hepatocytes to generate glucose-6-phosphate (G6P), that - because of the negative charge of phosphate group - is unable to be transported by glucose transporters, so it is retained within hepatocytes. In the fed state, G6P acts as a precursor for glycogen synthesis. It is also metabolized to generate pyruvate through glycolysis. Pyruvate is channeled into the mitochondria and completely oxidized to generate ATP through the tricarboxylic acid (TCA) cycle and oxidative phosphorylation. Alternatively, pyruvate is used to synthesize fatty acids through lipogenesis. G6P is also metabolized via the pentose phosphate pathway to generate NADPH. NADPH is required for lipogenesis and biosynthesis of other bioactive molecules. In the fasted state, G6P is transported into the endoplasmic reticulum (ER) and dephosphorylated by glucose-6-phosphatase (G6Pase) to release glucose.

3.2. METABOLOMICS

3.2.1. WHAT IS METABOLOMICS?

A cell can be thought of as a factory in which different assembly lines - the metabolic pathways of the cell - interact to build the finished products that fulfill the cell's role in an organism.

Living cells are maintained under non-equilibrium conditions, which requires constant input of energy. The cells must also maintain their infrastructure, and perform tissue-specific tasks, all of which need energy and raw material. Metabolism is the set of processes that convert exogenous compounds to metabolic energy, which drives biochemical reactions within the cell, maintains homeostasis, provides the means to do work (e.g. contraction, movement, action potentials, secretion and so forth), for cellular repair, and to divide.

Metabolomics is the scientific study of chemical processes involving metabolites. Specifically, metabolomics is the "systematic study of the unique chemical fingerprints that specific cellular processes leave behind", the study of their small-molecule metabolite profiles.

The metabolites are small molecules that represent the end products of cellular processes and give a picture of the here-and-now of how cells and tissues are functioning. The collection of all metabolites in a biological system (cell, tissue, organ or organism), represents the metabolome, the intersecting systems chemistry of life processes, that is the functional outcome of the activity of the genome (functional genome) and the proteome.

Metabolism, as functional activity of all living cells, reflects the health status of an organism. Therefore, the ability to measure global metabolism in quantitative detail is of fundamental importance in all aspects of biology. Metabolomics provides the technical means to carry out global analyses of metabolism, by identifying and quantifying a large fraction of all of the metabolites present in a cell, and how they change in response to perturbations within relevant metabolic networks.

Metabolomics requires high-end analytical instrumentation, of which mass spectrometry (MS) and nuclear magnetic resonance (NMR) together are the most appropriate technologies.

3.2.2. HISTORY OF METABOLOMICS

"Both the body and its parts are in a continuous state of dissolution and nourishment, so they are inevitably undergoing permanent change."

[Ibn al-Nafis in his 1260 AD work titled *"Al-Risalah al-Kamiliyyah fil Siera al-Nabawiyyah"* - The Treatise of Kamil on the Prophet's Biography]

The idea that biological fluids reflect the health of an individual has existed for a long time. Ancient Chinese doctors used ants for the evaluation of urine of patients to detect whether the urine contained high levels of glucose, and hence detect diabetes [217]. In the Middle Ages, "urine charts" were used to link the colours, tastes and smells of urine to various medical conditions, which are metabolic in origin [218]. The first controlled experiments in human metabolism were published by Santorio Santorio in 1614 in his book *"Ars de statica medicina"* [219]. He described how he weighed himself before and after eating, sleep, working, sex, fasting, drinking, and excreting. He found that most of the food he took in was lost through what he called *"perspiratio insensibilis"* ("insensible perspiration of the body"), already known to Galen and ancient physicians, and originated the study of metabolism.

The concept that individuals might have a "metabolic pattern" that could be reflected in the components of their biological fluids was first developed and tested by Roger Williams and his associates during the late 1940s and early 1950s [220]. Williams used paper chromatograms to examine samples from a variety of subjects, including alcoholics, schizophrenics, and residents of mental hospitals, producing suggestive evidence that there were characteristic metabolic patterns associated with each of these groups [221].

The term "metabolic profile" was introduced by Horning, et al. in 1971 after they demonstrated that gas chromatography-mass spectrometry (GC-MS) could be used to measure compounds present in human urine and tissue extracts [222-226].

The Horning group, along with that of Linus Pauling and Arthur B. Robinson led the development of GC-MS methods to monitor the metabolites present in urine through the 1970s [227]. Commenting on the potential usefulness of this type of technique, the Horings suggested that: *"profiles may prove to be useful for characterizing both normal and pathologic states, for studies of drug metabolism, and for human developmental studies"*.

Concurrently, NMR spectroscopy, which was discovered in the 1940s, was also undergoing rapid advances.

In 1974, Seeley et al. demonstrated the utility of using NMR to detect metabolites in unmodified biological samples [228]. As sensitivity has improved with the evolution of higher magnetic field strengths and magic angle spinning, NMR continues to be a leading analytical tool to investigate metabolism. Efforts to utilize NMR for metabolomics have been largely driven by the laboratory of Dr. Jeremy K. Nicholson at Birkbeck College, University of London and later at Imperial College London. In 1984, Nicholson showed ^{1}H NMR spectroscopy could potentially be used to diagnose diabetes mellitus, and later pioneered the application of pattern recognition methods to NMR spectroscopic data [229-232].

In 2005, the first metabolomics web database, METLIN [233] for characterizing human metabolites was developed in the Siuzdak laboratory at The Scripps Research Institute and contained over 10,000 metabolites and tandem mass spectral data. As of September 2015, METLIN contains over 240,000 metabolites as well as the largest repository of tandem mass spectrometry data in metabolomics.

On 23 January 2007, the Human Metabolome Project, led by Dr. David Wishart of the University of Alberta, Canada, completed the first draft of the human metabolome, consisting of a database of approximately 2500 metabolites, 1200 drugs and 3500 food components [234-235].

As late as mid-2010, metabolomics was still considered an "emerging field". Further, it was noted that further progress in the field depended in large part, through addressing otherwise "irresolvable technical challenges", by technical evolution of mass spectrometry instrumentation [236].

In 2012, in order for the full potential of metabolomics to be realized, the United States NIH Common Fund Metabolomics Program (https://commonfund.nih.gov/metabolomics) was initiated and six metabolomics resource centers were established nationwide. The program is meant to increase the national capacity for metabolomics and to catalyze research by creating new tools, infrastructure, and data to fuel this relatively new field of study.

In 2013, as part of the NIH Common Fund's Metabolomics program, Dr. Teresa Fan, Dr. Andrew Lane, Dr. Richard Higashi and Dr. Hunter Moseley established the Resource Center for Stable Isotope-Resolved Metabolomics (RC-SIRM) at the University of Kentucky (Lexington, KY, USA). The Dr. Teresa Fan's laboratory has been developing the SIRM approach for translational research from cells through mouse models to human patients offering an unprecedented opportunity to elucidate in large-scale altered

metabolic networks in various model systems and human subjects in vivo. This approach couples the use of stable isotope tracers with NMR and MS-based metabolomic analyses [237]. The overall goals of the RC-SIRM are to facilitate and promote metabolomics research with an emphasis on stable isotope tracing for pathway elucidation in studies ranging from laboratory bench cell cultures, model animals, to human subjects, and to provide the state-of-art analytical and informatics resources, education, and training for the biomedical research community.

In April 2014, representatives from Australia, Canada, Germany, Japan, the Netherlands and the United States NIH Common Fund Metabolomics program met to discuss an international data exchange in metabolomics. The participants agreed to create a portal that would provide a network of coordinated and freely accessible metabolomics data collected from repositories around the world. As a result of this meeting and in collaboration with the European Bioinformatics Institute, the MetabolomeXchange was launched as an international index of freely accessible metabolomics data from around the world. As of December 2015 nearly 300 datasets are now available (http://metabolomexchange.org/) from three different repositories including the Common Fund Metabolomics Workbench (http://www.metabolomicsworkbench.org/)

In 2015, real-time metabolome profiling was demonstrated for the first time [238].

3.2.3. TRACING THE METABOLISM OF DISEASES

Since metabolism responds to environmental factors both at the extrinsic level (macroenvironment), as represented by diet, pollutants and drugs for example, and local environments (microenvironment), as represented by the prevailing tissue conditions outside cells, metabolism is a sensitive indicator of altered physiological state, thus pathology. Understanding which metabolites are present under certain circumstances can provide valuable information about the health and well-being of an organism, allowing to expand the knowledge of human health and disease.

Metabolomics [239], through minimally invasive techniques, allows to study cell metabolism in conditions of disease, by identifying and quantifying a large fraction of all of the metabolites present in a cell, and how they change in response to perturbations within relevant metabolic networks. The resulting metabolic profiling can give an instantaneous snapshot of the physiology of that cell.

In 2013, Dr. Teresa Fan, Dr. Andrew Lane, Dr. Richard Higashi and Dr. Hunter Moseley established the Resource Center for Stable Isotope-Resolved Metabolomics (RC-SIRM) at

the University of Kentucky (Lexington, KY, USA). The SIRM approach offers the opportunity to elucidate in large-scale altered metabolic networks in various model systems (in vitro, ex vivo, in vivo) and human subjects in vivo, coupling the use of stable isotope tracers with NMR and mass spectrometry (MS)-based metabolomic analyses [240-248]. This kind of technique is like “tracing breadcrumbs in the forest”, using the words of Dr. Teresa Fan. “Breadcrumbs” are traced metabolites, and “forest” is the model system and human patient studied. In fact, using stable isotope tracers, it is possible to label certain types of metabolites and watch as they move through the complicated and interconnected network of biological reactions that contribute to cell metabolism [249].

Dr. Fan and her research team use stable isotope tracing for pathway elucidation in studies ranging from laboratory bench cell cultures [250], model animals [249] [251-252], to human subjects [249] [252-255].

Researchers can probe the metabolic network of particular diseases in these systems to identify new cell processes that could be targeted with drugs and discover diagnostic markers.

One of the major roadblocks to metabolomics use is that it remains difficult to identify the tens of thousands of metabolites that exist at any given time within the cells. In addition, many metabolites are present in low concentrations or are unstable, making them difficult to detect. Careful sample preparation and processing is the often the first critical component in metabolomics, which is necessary to prevent excessive perturbation and degradation of the observed metabolites [256-257]. It is very important to develop ways to treat samples before analyzing them to increase sensitivity and stability, using chemical agents that can modify particular parts of certain metabolites, so making them easier to detect. This approach could also enhance a researcher’s ability to identify previously unknown metabolites. Data analysis/informatics [258-260] is another critical component of metabolomics to interpret the observations in a biological context.

Although metabolomics is often considered more representative of the functional state of a cell than other ‘omics measures such as genomics or proteomics, one of the challenges of systems biology and functional genomics, is to integrate proteomic, transcriptomic, and metabolomic information to provide a better understanding of cellular biology.

3.2.4. STABLE ISOTOPE-RESOLVED METABOLOMICS (SIRM)

Global metabolomics, through the quantification of a large number of metabolites in tissue or biofluids, can identify disease states or response to therapeutics and xenobiotics by reference to the normal condition. However, determining specific mechanisms, such as detecting which pathways are impacted in particular cell types within a tissue by measuring metabolic fluxes, requires additional information as many metabolites are present in different amounts in different cell types or within compartments of cells, as well as participating in several pathways simultaneously. Most metabolic pathways are in fact part of complex and intersecting networks with a given metabolite participating in multiple pathways. For example, Glutamate can be involved in up to 55 pathways, such as the synthesis of glutathione (GSH), amino acids, proteins, and some 200 reactions [249].

Thus, it is impractical to resolve complex metabolic networks based on the steady-state metabolite levels alone. This is further complicated by the exchange of metabolites between different cellular compartments, such as the shuttling of citrate, oxaloacetate (OAA), Aspartate (Asp), and malate between the mitochondrion and the cytoplasm.

Metabolism is a complex network of metabolic pathways and to identify the precursor-product relationships, it is necessary to distinguish different sources of carbon, nitrogen etc. which necessitates some means of “labeling” individual atoms so that their fate can be traced through metabolic pathways. This allows the reconstruction of perturbed pathways based on the incorporation of the labeled atoms into metabolites.

Traditionally this was achieved using radioisotopes (e.g. ^{14}C, ^{13}N, ^{15}O). However, stable isotopes (e.g. ^{13}C or ^{15}N) have several advantages. They are wholly biocompatible, non-radioactive, thereby eliminating concerns of safety to the biological models and researchers. In addition, they do not degrade during storage by autoradiolysis, another important disadvantage of radioisotopoes. The isotopes ^{13}C and ^{15}N are commonly used because they correspond to atoms that make up the bulk of most metabolites and because the mass change of one neutron compared to the mass of the more abundant ^{12}C and ^{14}N is relatively small.

In addition to the mass difference that makes ^{13}C and ^{15}N discernable from ^{12}C and ^{14}N by MS, ^{13}C and ^{15}N have magnetic moment (possess 1/2 spin), which makes them observable by NMR.

SIRM approach is implemented by administering stable isotope tracers such as uniformly ^{13}C-labeled glucose ($^{13}C_6$-Glc, ^{13}C natural abundances 1.1 %) or uniformly ^{13}C,^{15}N-labeled

glutamine ($^{13}C_5$,$^{15}N_2$-Gln, ^{15}N natural abundance 0.37%) to cell cultures, excised tissues or whole organisms including human subjects. Therapeutic agents or exposure to xenobiotics can be included in the treatment to observe their impact on the metabolic networks. The tracers are allowed to be metabolized for a duration which can range from 15 min. (for mice) to 24 h or longer (for cells and tissues), followed by cell harvest or tissue resection via surgery. Polar and lipophilic metabolites are extracted using a solvent partition method. Extracted metabolites are analyzed by NMR (positional isotopomers) and MS (mass isotopologues) for mapping the labeling patterns of various metabolites, for reconstruction of metabolic networks (**Figure 8**). Positional isotopomers and mass isotopologues refer respectively to a given metabolite with different labeled atomic positions (e.g. $^{13}C_1$-1-Ala versus $^{13}C_1$-2-Ala) and different numbers of labeled atoms (e.g. $^{13}C_1$-Ala versus $^{13}C_3$-Ala) (**Figure 9**).

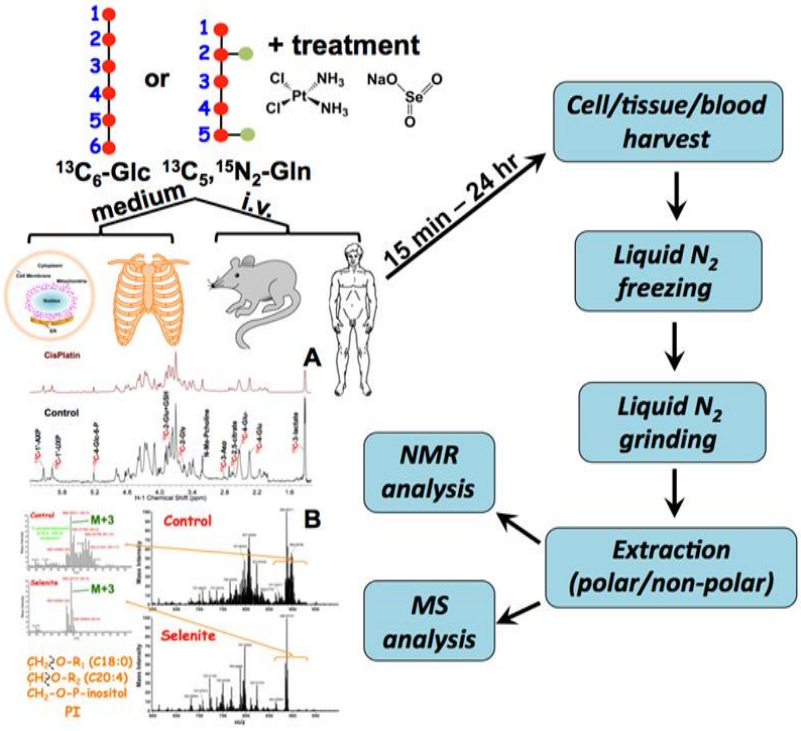

Figure 8. SIRM approach workflow

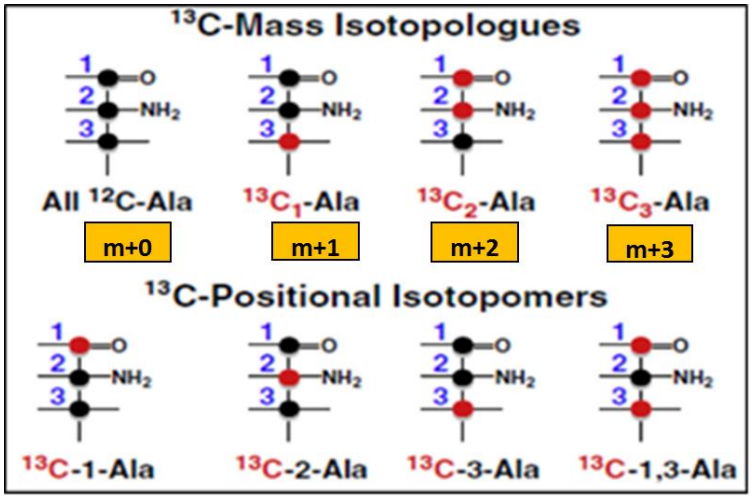

Figure 9. Positional isotopomers and Mass Isotopologues

The specific isotopomer and isotopologue distributions in the various product metabolites, along with the total amounts of the metabolites, provide detailed information about the relative importance of intersecting and parallel pathways. For example, lactate can be produced directly from glucose by lactic fermentation, as well as by glutaminolysis; the relative contributions from these independent pathways is readily determined from the isotope distributions in the lactate using either ^{13}C-enriched glucose or glutamine as labeled sources. At the same time such labeling schemes provide simultaneous information about the flow of carbon through the glycolysis, pentose phosphate pathway, hexosamine pathway, the Krebs cycle and lipid biosynthesis among others (**Figures 10-11**). The information on pathway dynamics and compartmentation not only needs to be acquired for deciphering metabolic reprogramming in response to disease pathogenesis, but also is valuable to exploit for the discovery of diagnostic biomarkers as well as chemopreventive and therapeutic targets.

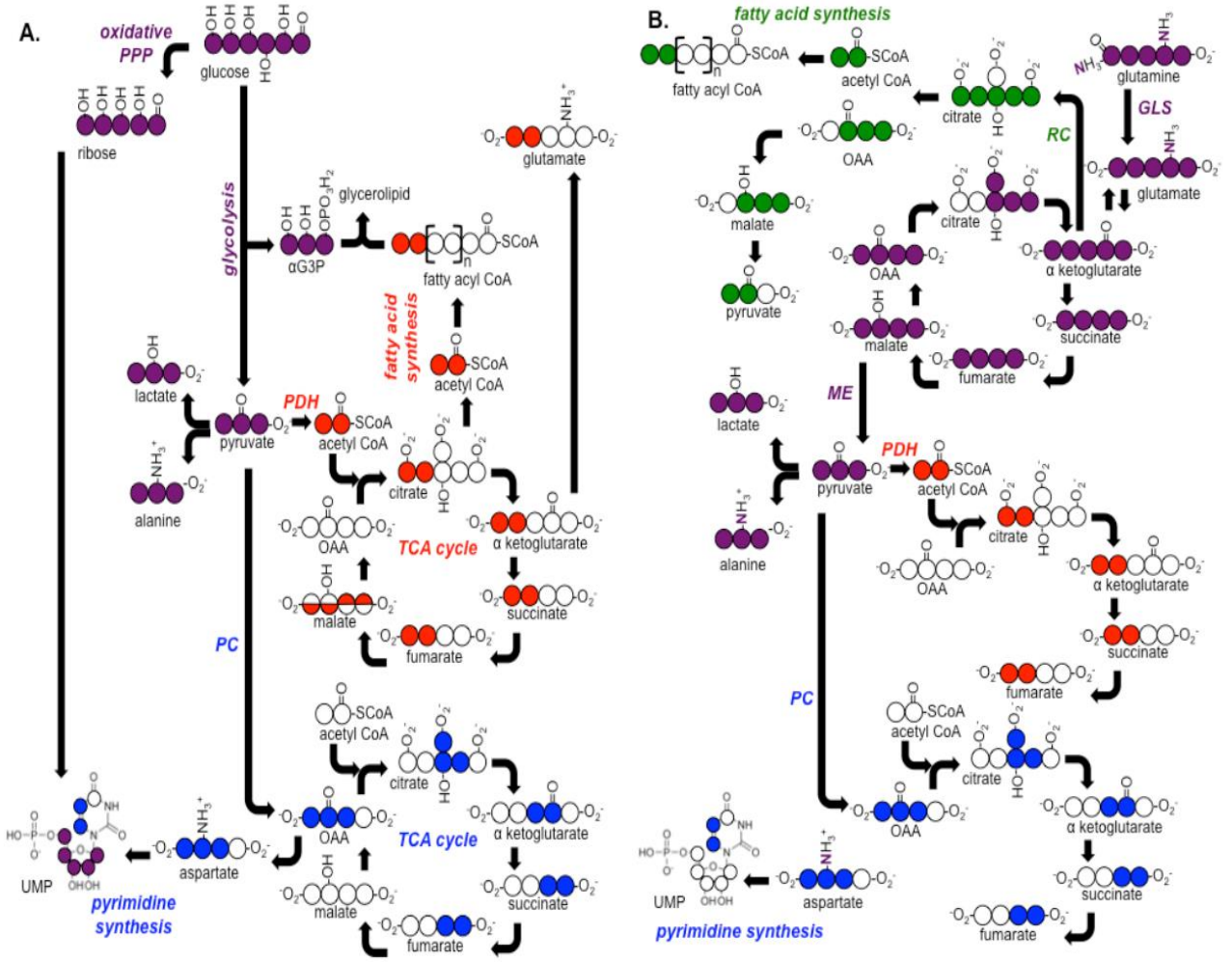

Figure 10. The use of labeled tracers such as $^{13}C_6$ glucose or $^{13}C_5$ glutamine allows the tracking of atoms through metabolic networks. A. If a biological sample is given $^{13}C_6$-glucose (^{13}C atoms shown in purple), the labeled carbon can be monitored through various routes of glucose metabolism. Several example pathways are shown. The pentose phosphate pathway will produce $^{13}C_5$-ribose (purple) that can be incorporated into nucleotides and glycolysis will produce $^{13}C_3$-pyruvate (purple) that can be reduced to lactate or transaminated to alanine. In addition, further oxidation of $^{13}C_3$-pyruvate through the TCA cycle via pyruvate dehydrogenase (PDH, red) or pyruvate carboxylase (PC, blue) will produce characteristic labeling patterns in TCA cycle intermediates. Those TCA cycle intermediates can then participate in biosynthetic pathways; **B.** Glutamine carbons can be tracked in a similar manner. Abbreviations: PPP: pentose phosphate pathway, PDH: pyruvate dehydrogenase, PC: pyruvate carboxylase, GLS: glutaminase, ME: malic enzyme, αG3P: α glycerol 3-phosphate, OAA: oxaloacetate, UMP: uridine monophosphate. Half circles indicate two possible label patterns due to fumarate's symmetry.

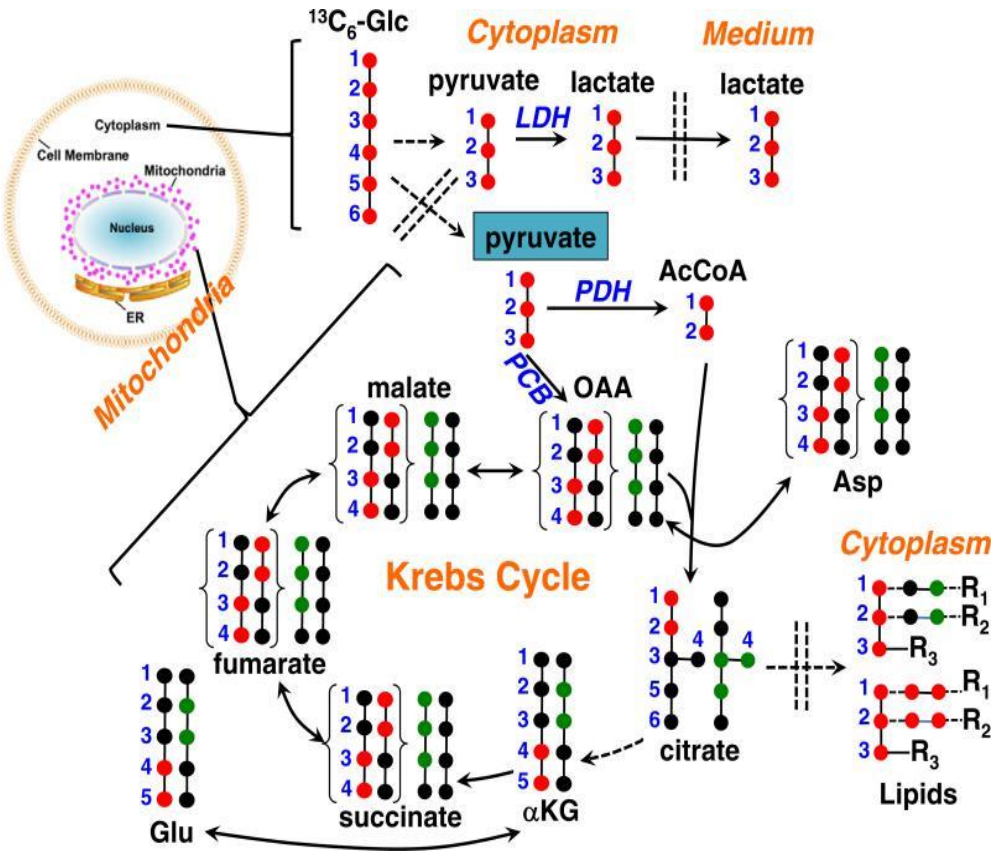

Figure 11. Stable isotope tracing can reveal metabolic pathways occurring in different cellular compartments. The fate of $^{13}C_6$-Glc is tracked from glycolysis in the cytoplasm, lactate excretion into the medium, to the Krebs cycle in the mitochondria without and with the input of pyruvate carboxylation (PC), and then to lipid biosynthesis in the cytoplasm. The expected ^{13}C labeling patterns for various representative metabolites are deduced based on known enzyme reaction mechanisms [261]. The labeling patterns for the Krebs cycle metabolites are drawn for 1 cycle turn only, which will change with additional turns of the cycle [262]. Dashed arrows: multi-step reactions; double-headed arrows: reversible reactions; double vertical dashed lines: membrane separation; BLACK: carbon-12; RED: carbon-13; GREEN: carbon-13 derived from PC; { }: scrambled 13C labeling patterns due to the molecular symmetry of succinate; R1, R2: fatty acyl chains of lipids; R3: fatty acyl chains for neutral lipids or polar head groups of phospholipids; Glc: glucose; AcCoA: acetyl CoA; OAA: oxaloacetate; αKG: α-ketoglutarate; LDH: lactate dehydrogenase; PDH: pyruvate dehydrogenase; PCB: pyruvate carboxylase.

3.2.4.1. Metabolite detection by Mass-Spectrometry (MS) and Nuclear Magnetic Resonance (NMR)

MS enables monitoring of label incorporation of ^{13}C into metabolites because of the mass difference between the naturally abundant atom ^{12}C and the heavier isotope ^{13}C. A mass spectrum of a metabolite provides the mass isotopologue distribution.

Isotopologue distribution may not be sufficient to deconvolute complex pathways. For example, if a biological sample is given unifomely labeled $^{13}C_6$-glucose, glutamate mass isotopologue with two ^{13}C atoms (Glu m+2) is produced by both PC (pyruvate carboxylase) and PDH (pyruvate dehydrogenase), however the position of the label is distinct with PDH labeling at C4 and C5 and PC labeling C2 and C3 (**Figures 10-11**).

By using a nuclear editing technique such as 1H-^{13}C HSQC (Heteronuclear Single Quantum Coherence spectroscopy) which allows the detection of only protons attached to carbons enriched in ^{13}C, NMR analysis reveals the position of the labeled atoms within in the metabolites structure, allowing one to distinguish positional isotopomers (**Figure 12**). 1H-NMR spectrum, in turn, allows the detection of all protons attached both to ^{13}C and ^{12}C (**Figure 13**).

Therefore, by employing a combination of NMR and MS approaches, label information is maximized as well as metabolite coverage.

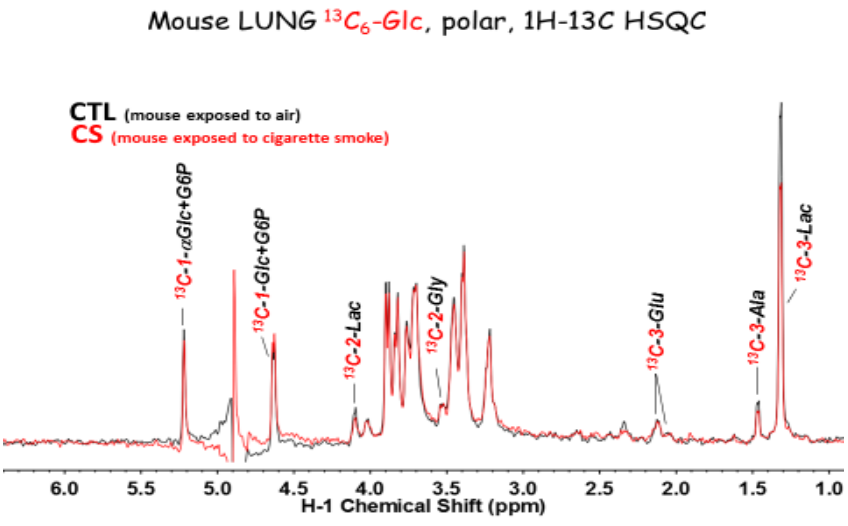

Figure 12. Lung tissue 1H-^{13}C HSQC spectra from mouse injected with labeled glucose show the specific positions of label incorporation within a metabolite, allowing to distinguish positional isotopomers. Lac=lactate; Ala=alanine; Glu=glutamate; Gly=glycine; Glc=glucose; G6P=glucose-6-phosphate;

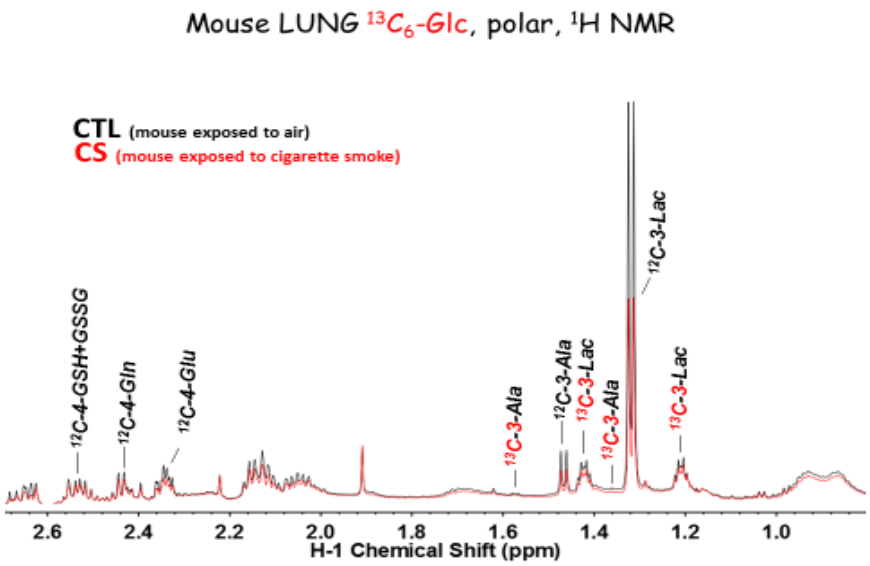

Figure 13. Lung tissue 1H-NMR spectra from mouse injected with labeled glucose show the labeled metabolites, and the specific positions of label incorporation within a metabolite, but also the unlabeled metabolites (detection of protons attached to ^{12}C). Lac=lactate; Ala=alanine; Glu=glutamate; Gln=glutamine; GSH=reduced glutathione; GSSG=oxidized glutathione.

3.3. AIM OF THE STUDY

Cigarette smoke (CS) is a miscellaneous of more than 4,000 chemicals [263], such as acrolein, nicotine, nitric oxide, nitrogen dioxide, polycyclic aromatic hydrocarbons, and nitrosamines [264], and it is a rich source of oxidants and electrophiles, so much so that it is estimated to contain 10^{17} radicals/g in the tar phase and 10^{15} radicals/g in the gaseous phase. Exposure to CS (and other environmental pollutants) leads to an oxidant/antioxidant imbalance in the lung that forms the basis for the development of COPD [265]. This oxidant-antioxidant imbalance is likely caused by inflammatory processes that potentiate proteolytic damage, induce cell death, and inhibit cell repair [266-268].

By the definition of GOLD (Global Initiative for Chronic Obstructive Lung Diseases) COPD is characterized by airflow limitation that is not fully reversible. The airflow limitation characteristic of COPD, is usually progressive and associated with abnormal inflammatory responses of the lungs to noxious particles or gases. So, CS-induced lung inflammatory processes are likely to be preceded by changes in energy metabolism and in the redox status of the cell. Few studies have highlighted the importance of intermediary metabolism events preceding redox and inflammatory changes.

In the lungs, after CS exposure, oxidative stress leads to redox changes in cytosolic and mitochondrial metabolic events. A number of glycolytic enzymes are sensitive to CS-induced oxidative stress along with inhibition of the mitochondrial respiratory chain complexes and consequent impairment of energy homeostasis and cell death [269]. Acrolein, one of the major constituents of CS, has been shown to inhibit Complexes I and II in hepatocytes [270] and in brain mitochondria [271]. Nicotine is a competitive inhibitor for Complex I [272], and nitric oxide is known to react with superoxide anion in mitochondria to yield peroxynitrite, a species known to modify irreversibly mitochondrial proteins by nitration and/or oxidation [273]. The susceptibility of mitochondrial proteins to oxidative damage and subsequent dysfunction after exposure to free radicals from CS is well documented [274-275].

Glucose is the principal substrate utilized by the lung and other organs for the generation of energy. Energy metabolism and ATP content in lungs are maintained by oxidative metabolism at levels comparable to those in other metabolically active organs, and any alteration may depress amine clearance, alter lung permeability, and influence lung response to oxidative stress [276]. Metabolism of glucose is encompassed by its

conversion to pyruvate (anaerobic glycolysis) and supply of the latter to mitochondria (aerobic glycolysis) for the generation of reducing equivalents and oxidative phosphorylation.

It has been observed that short-term CS exposure led to metabolic alterations in glyceraldehyde-3-phosphate dehydrogenase (GAPDH)-dependent glycolysis and glucose-6-phosphate dehydrogenase (G6PDH)-dependent pentose phosphate pathway [269]. Alveolar type II cells increase the utilization of fatty acids after the inhibition of glycolysis in response to acrolein exposure [277].

GAPDH is a central glycolytic enzyme that in consequence of posttranslational modifications such as S-thiolation (usually following S-nitrosylation), is inhibited and, consequently, there is a rerouting of the metabolic flux from glycolysis to the pentose phosphate pathway [278-279], which accounts for 10–20% of glucose metabolism. For example, inactivation of GAPDH due to oxidative stress has been shown to reroute the metabolic flux to the pentose phosphate pathway in Caenorhabditis elegans [278]. NADPH, generated in the pentose phosphate pathway by the only regulatory step catalyzed by glucose-6-phosphate dehydrogenase (G6PDH), is utilized to maintain the redox status of the cell by regenerating thiol-based redox couples, GSH and thioredoxin, and, thus, protecting the cell from oxidative damage. This reducing power is also utilized in double-bond reduction in fatty acid biosynthesis, as well as in detoxification reactions.

GSH is the most abundant, low-molecular-weight, nonprotein thiol that is synthesized in the cytosol from glycine, glutamate, and cysteine in a two-step process by the enzymes γ-glutamylcysteine synthase and GSH synthase [280] and plays a central role in the maintenance of the cellular redox status [281].

Metabolic (energy) and redox (oxidative stress) components are interdependent pathways that control cell function. Thus, impairment of intermediary metabolism is expected to play a decisive role in the development of COPD.

Patients with COPD experience low energy metabolism associated with decline in lung function [282], however, the cellular mechanisms underlying low energy metabolism in response to CS are not known.

This study examines the role of chronic CS exposure in the impairment of energy metabolism, specifically in glycolysis in tissues of an *in vivo* model. In particular this study aims to explore and to elucidate the glycolytic pathway alterations induced by chronic cigarette smoke exposure in mouse lung and liver tissue. This is achieved by using a novel experimental approach called stable isotope-resolved metabolomics (SIRM). The

experimental model consists of mice exposed to CS under controlled conditions for 6 months, then injected with glucose tracer containing a stable isotope of carbon ($^{13}C_6$-glucose). After tissues harvesting, the incorporation of the isotope into metabolites of biological samples is assessed by mass spectrometry (MS) and nuclear magnetic resonance spectroscopy (NMR), comparing the metabolic profile of mice exposed to CS to that of mice exposed to air.

3.4. MATERIAL AND METHODS

3.4.1. EMPHYSEMA MOUSE MODEL - Animals and cigarette smoke exposure

C57BL/6J mice (Jackson Lab originally, but maintained at the Johns Hopkins Bloomberg School of Public Health lab) were housed under controlled conditions for temperature and humidity, using a 12-h light/dark cycle. At 8 weeks of age, 5 mice were exposed to cigarette smoke (CS) 5 h/day, 5 days/week, for 6 months, using a TE-10z smoking machine (Teague Enterprises™) and 3R4F reference cigarettes (Tobacco and Health Research Institute, University of Kentucky, Lexington, KY, USA). This system employs a whole-body exposure, in which the entire mouse cage is placed in the smoking chamber. The TE-10z is a microprocessor-controlled cigarette smoking machine that produces a mixture of sidestream smoke (89%) and mainstream smoke (11%). Each cigarette is puffed for 2 seconds, once every minute for a total of 8 puffs, at a flow rate of 1.05 l/min, to provide a standard puff of 35 cm^3. The smoke chamber was monitored daily for total suspended particles and carbon monoxide, with concentrations of 150 mg/m^3 and 350 ppm, respectively [283-284]. All experimental protocols were performed in accordance with the standards established by the U.S. Animal Welfare Acts, as set forth in National Institutes of Health guidelines and in the Policy and Procedures Manual of the Johns Hopkins University Animal Care and Use Committee.

3.4.2. STABLE ISOTOPE-RESOLVED METABOLOMICS (SIRM) MATERIAL AND METHODS

3.4.2.1. U-$^{13}C_6$-Glucose tracer infusion

The day after the final exposure, both mice exposed to air and CS were injected with uniformly labeled glucose tracer (U-$^{13}C_6$-Glucose, Cambridge Isotope, Tewksbury, MA, USA). A 20% solution of U-$^{13}C_6$-Glucose in PBS (Stock: 200mg/mL in PBS) was sterile-filtered and 100 µL of this solution (i.e. 20 mg of U-$^{13}C_6$-Glucose) were injected via intraperitoneal (IP) injection without anesthesia, 3 times at 15 minutes interval.

3.4.2.2. Blood and tissues harvest

Two aliquots of blood sample, approximately 50 µL each one, were taken by retroorbital puncture at timed intervals from each mouse: one aliquot was collected immediately before the glucose tracer injection (time=0h), the other one 1 hour after the first glucose tracer injection (time=1h). The blood was separated into plasma and blood cells by centrifugation at 4°C, 3,500xg for 15 minutes. Plasma was immediately flash-frozen in liquid nitrogen for storage prior to metabolites extraction.

One hour after the first glucose tracer injection the mice were sacrificed via CO_2 euthanasia chamber, then liver and lungs were dissected sequentially and flash-frozen in liquid nitrogen within 2-6 minutes of euthanasia.

3.4.2.3. Sample preparation

The frozen tissue samples were pulverized to less than 10 µm particle size in liquid nitrogen using a Spex Freezer Mill (SPEX SamplePrep™, Metuchen, NJ, USA). Metabolites were extracted from the ground powder with a 2:1.5:1 ratio of acetonitrile:H2O:chloroform followed by centrifugation for 20 minutes at 4,000 g and 4°C. This afforded a two-phase partition (top polar, bottom lipidic), separated by insoluble protein residue (tissue debris layer). The polar and lipidic layers were recovered sequentially and the remaining tissue debris (mainly denatured proteins) was extracted again with 0.5 mL chloroform:methanol:butylated hydroxytoluene (BHT) (2:1:1 mM) and centrifuged at 4°C, 22,000xg (or 14,000 rpm) for 20 minutes to separate the three phases again. The dry weight of tissue debris was obtained for normalization of metabolite content. The residual polar and lipid fractions were pooled with respective main fractions, then the polar fractions were aliquoted and lyophilized for NMR and GCMS analysis.

The NMR fractions underwent to an additional “clean up” step in order to precipitate proteins and enhance NMR analysis. The NMR aliquots were dissolved in 80% acetone solution (100 µL ice-cold nanopure water and 400 µL ice-cold 100% pure acetone), which is critical for efficient protein precipitation. The samples were stored into -80°C freezer for 30 minutes to facilitate the precipitation. After centrifugation at 4°C, 14,000 rpm for 20 minutes, the supernatant was transfered to another tube and the protein pellet was extracted again with 60% acetonitrile solution. The samples were freezed in liquid nitrogen and lyophylized using liquid nitrogen trap.

For NMR measurement, each dried polar extract was reconstituted in 50% D_2O:H_2O (deuterated water) solution, that contains d6-DSS (deuterated 2-2’-dimethyl-2-silapentane-

5-sulfonate) (Cambridge Isotope Laboratories, Andover, MA, USA), as internal calibration standard (final concentration 50 nmoles/100 µL), and d12-EDTA (deuterated Ethylenediaminetetraacetic acid) (Cambridge Isotope Laboratories, Andover, MA, USA) to remove the influence of paramagnetic ions (final concentration 1 mM). Each polar extract was reconstituted in 55 µL of aforementioned solution, to get 27.5 nmoles of d6-DSS each sample. After vortexing and centrifugation at 4°C, 14,000 rpm for 20 minutes, samples were loaded into 1.7 mm NMR glass tubes ready for NMR analysis.

The dried GC-MS aliquots were acidified with 5 nmoles of internal standard Norleucine (1mM) in 10% trichloroacetic acid (TCA) and were immediately frozen in liquid nitrogen to minimize acid hydrolysis. The samples were re-lyophilized, then brought up in 50 µL of 1:1 (v/v) acetonitrile:N-(t-butyldimethylsilyl)-N methyltrifluoroacetamide (MTBSTFA, Regis Chemical, Morton Grove, IL, USA) for derivatization and sonicated for 3h, followed by overnight incubation at room temperature.

The protein residues were extracted by homogenization in a 2% sodium dodecyl sulfate (SDS), 62.5 mM Tris, and 1 mM DTT, pH 6.8 buffer for protein determination using the Pierce BCA method (Thermo Fisher Scientific, Rockford, IL). The kit enables to measure protein concentration in samples that contain thiol-reductants dithiothreitol (DTT). Bicinchoninic acid (BCA) is used for the colorimetric detection and measurement of protein, using a standard spectrophotometer or plate reader (wavelenght 562 nm).

3.4.2.4. NMR AND GC-MS ANALYSIS

- **NMR analysis**

NMR spectra were acquired at 20°C on a Varian Inova 14.1 T system (Varian, Inc., Palo Alto, CA) equipped with a 5 mm HCN cold probe. One-dimensional (1D) proton spectra were recorded with presaturation of the solvent resonance, an acquisition time of 2 sec, and a recycle time of 5 sec. 1D ^{1}H-^{13}C HSQC spectra were recorded with acquisition times of 0.15 s in *t*2. Spectral analysis was performed with MestReNova software (Mestrelab Research, Santiago de Compostela, Spain). Spectra were zero filled to 128 K points and apodized with an unshifted Gaussian function and 1 (^{1}H NMR) or 6 Hz (1D ^{1}H-^{13}C HSQC) line broadening exponential. Chemical shifts were referenced to DSS at 0 ppm. After manual phase and baseline correction, peaks were integrated using the global deconvolution method of the software. Metabolites were assigned based on their 1H

chemical shift, were identified using in-house databases and comparisons to standards [253], and quantified using the intensity of –Si-(CH3)3 DSS peak at 0 ppm (for 1H NMR), or the C-3 lactate peak at 1.32 ppm (for 1H-13C HSQC) as a reference. Results from NMR measurement were normalized to the total dry protein weight determined by the Bicinchoninic acid assay as previously described [251].

- **GC-MS ANALYSIS**

Samples were analyzed on Thermo Scientific TRACE 1310 Gas chromatograph-Mass spectrometer (GC-MS) (ThermoFinnigan, Austin, TX, USA) [248].
One µL of sample was directly injected and it was separated on a SGE Forte (Victoria, Australia) 5% phenyl capillary column (50m x 0.15mm, 0.25µm film thickness), which was directly inserted into the ion source. The injector and transfer line temperatures were 280°C. The oven temperature was programmed to hold at 60°C for 2 min and increase to 150°C at a 20°C/min ramp rate and from 150°C to 300°C at a 6°C/min ramp rate. The flow rate of helium carrier gas was set at 1.5 mL/min. The MS was operated in the segment scan mode. The scan ranges were 140-206, 209-280, and 283-650 m/z and scan-rate was one scan per 0.97 sec. [285] [251]. Metabolites were identified by matching their retention times and fragmentation patterns with commercially available standards. Metabolite peaks were integrated at each isotopologue m/z using Xcalibur software (ThermoScientific, Rockford, Il). Peak areas were quantified based on peak areas of known standards and using norleucine as an internal standard for normalization. Identities were extensively verified by manual inspection of analytes of interest, to ensure that the processing method is working properly. Results from GC-MS measurements were normalized to the total protein weight determined by the BCA assay previously described.

3.4.2.5. Statistical Analysis

Metabolite quantities were normalized to protein mass. Data from GC-MS analysis show the fractional enrichment (max of intensity) of isotopologues comparing cigarette smoke group and air group. Error bars represent standard error. P values were calculated by the two-tailed Student’s ttest using the Excel version of the t-test. P-value<0.05 was considered significant. The False Discovery Rate (FDR) approach was used to determine adjusted p-values (q-values) for each test.

3.5. RESULTS and DISCUSSION

3.5.1. LUNG and LIVER TISSUE NMR and GC-MS ANALYSIS

Unlabeled metabolites were measured by 1H-NMR (**Figures 14-16,18**), while ^{13}C-labeled metabolites were measured by 1H-^{13}C HSQC NMR (**Figure 17,19**). Flux analysis was performed measuring the fractional enrichment of isotopologues (m+1, m+2, and m+3) of glycolytic intermediates using GC-MS (**Charts 1-10**).

Regarding NMR analysis for both lung and liver tissue, here I will show the NMR spectra, providing only a qualitative and theoretical interpretation of results (not quantitative). Data are not complet

3.5.1.1. LUNG TISSUE NMR ANALYSIS

Considering data that show the biggest change among all replicates, comparison of 1H-NMR spectra of CS group and air group (**Figures 14-16**) shows slight increased accumulation of unlabeled glucose and slight decreased accumulation of unlabeled lactate and unlabeled alanine in lung tissue of mice exposed to cigarette smoke. The levels of pyridine nucleotides (NAD+ and NADP+), adenosine-containing nucleotides pool (AXP) and glutathione (GSH+GSSG) were similar in both groups (**Figures 14-16**). 1H-^{13}C HSQC NMR spectra (**Figure 17**) show increased accumulation of ^{13}C-glucose, ^{13}C-lactate and ^{13}C-glycine in lung tissue of mice exposed to cigarette smoke.

Although variations between replicates generally both the lung tissue exposed to CS and lung tissue exposed to air show similar accumulation of main metabolites of glycolytic pathway, both labeled and unlabeled.

Figura 14. Lung tissue 1H NMR spectra;

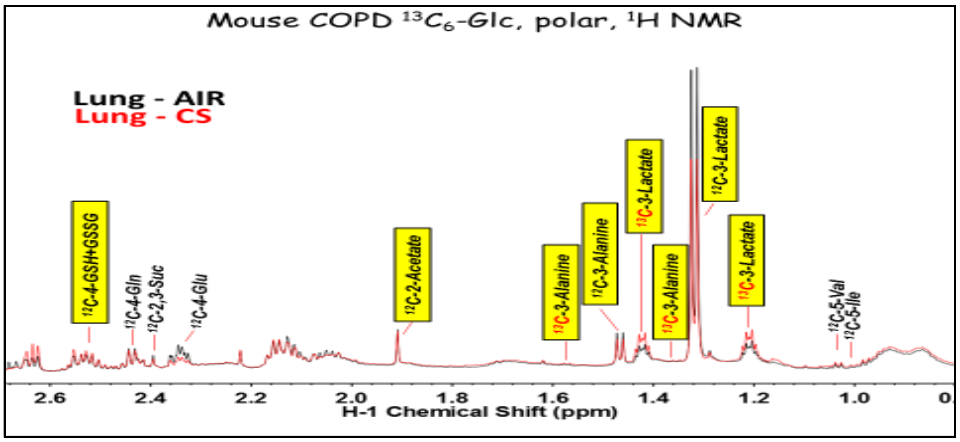

Ile=isoleucine; Val=valine; Glu=glutamate; Suc=succinate; Gln=glutamine; GSH= reduced glutathione; GSSG= oxidized glutathione.

Figura 15. Lung tissue 1H NMR spectra

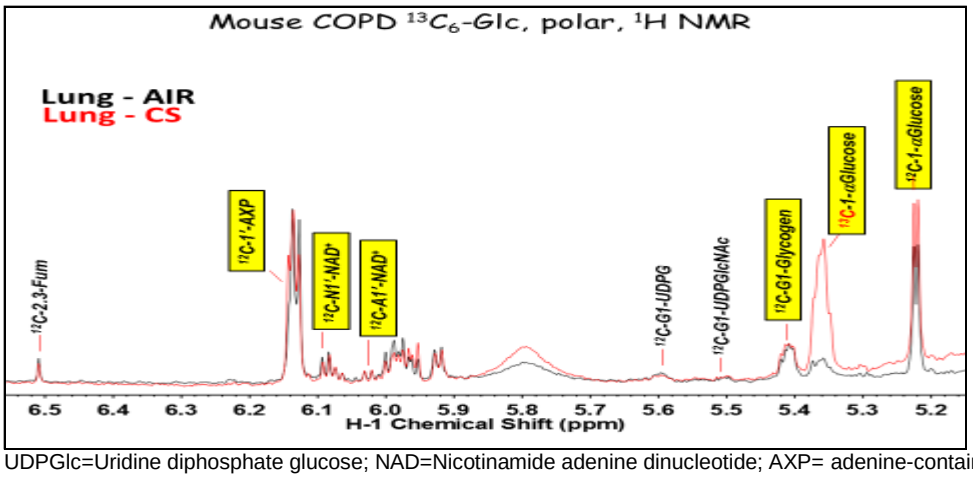

UDPGlc=Uridine diphosphate glucose; NAD=Nicotinamide adenine dinucleotide; AXP= adenine-containing nucleotides; Fum=fumarate

Figura 16. Lung tissue 1H NMR spectra

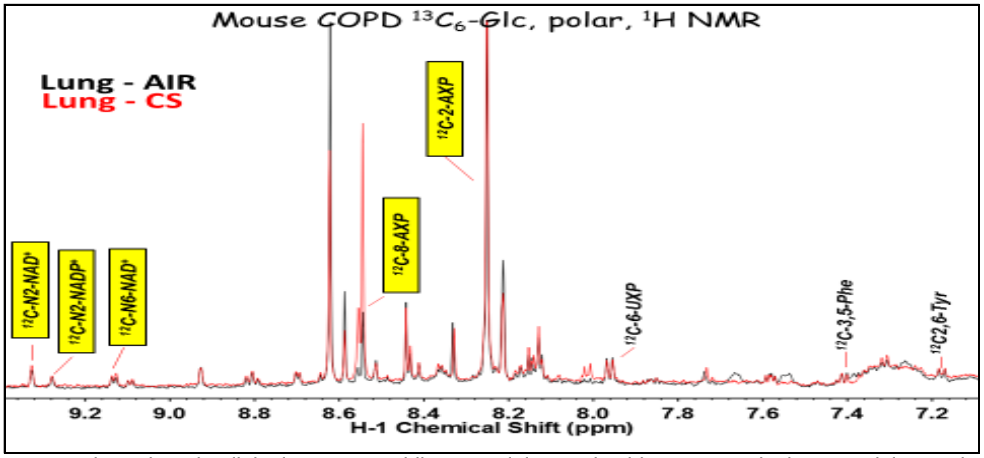

Tyr=tyrosine; Phe=phenilalanine; UXP= uridine-containing nucleotides; AXP= adenine-containing nucleotides; NAD^+= nicotinammide adenina dinucleotide; $NADP^+$=nicotinammide adenina dinucleotide fosfato

Figura 17. Lung tissue 1H-^{13}C HSQC NMR spectra

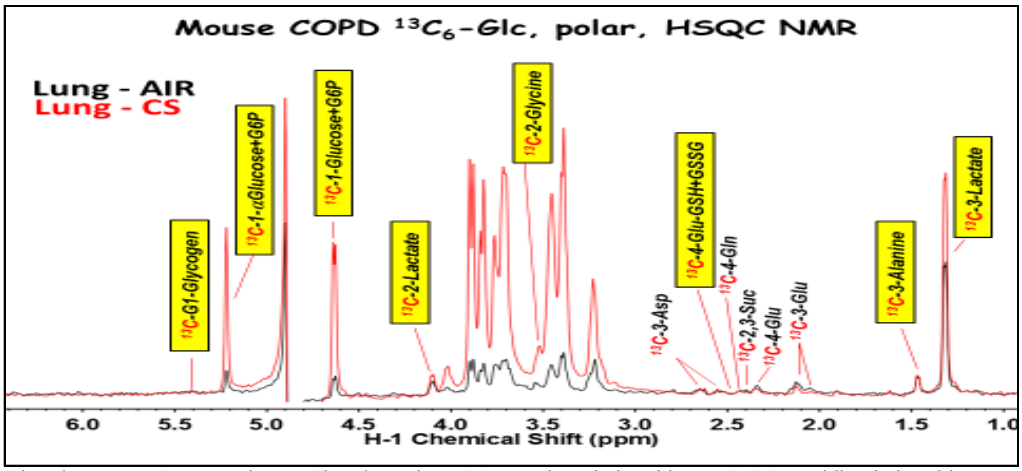

Glu=glutamate; Suc=succinate; Gln=glutamine; GSH= reduced glutathione; GSSG= oxidized glutathione; Asp=aspartate

3.5.1.2. LUNG TISSUE GC-MS ANALYSIS – GLYCOLYSIS FLUX ANALYSIS

Fractional enrichment of isotopologues of glycolytic intermediates (**Charts 1-5**) show very slight increased incorporation of ^{13}C in glycerol-3-phosphate (m+3), lactate (m+3), alanine (m+3), serine (m+3) and a decreased incorporation of ^{13}C in glycine (m+2), in lung tissue of mice exposed to CS compare to lung tissue of mice exposed to air. The percentage enrichment is almost equal between two groups of mice and the flux analysis did not show any statistically significant result.

Chart 1. Fractional enrichment glycerol-3-phosphate

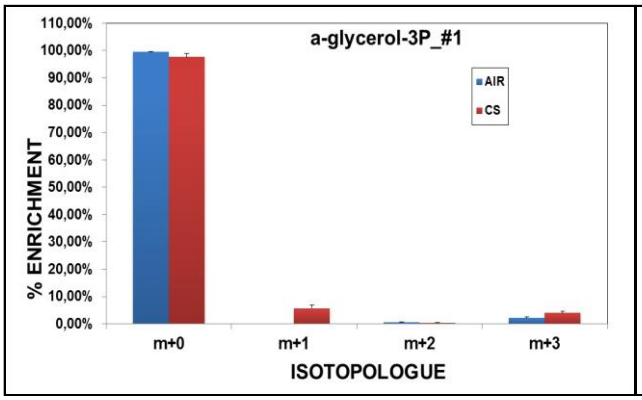

Chart 2. Fractional enrichment lactate

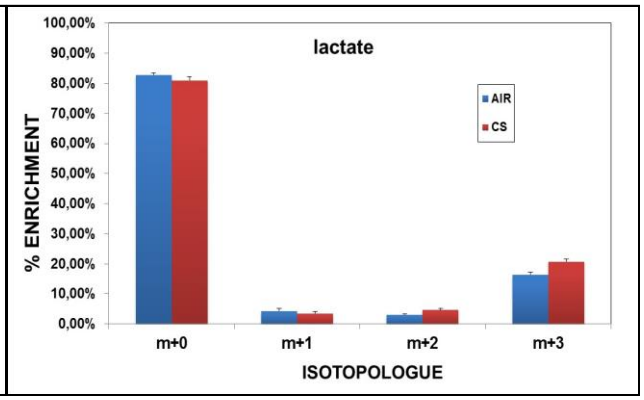

Chart 3. Fractional enrichment alanine

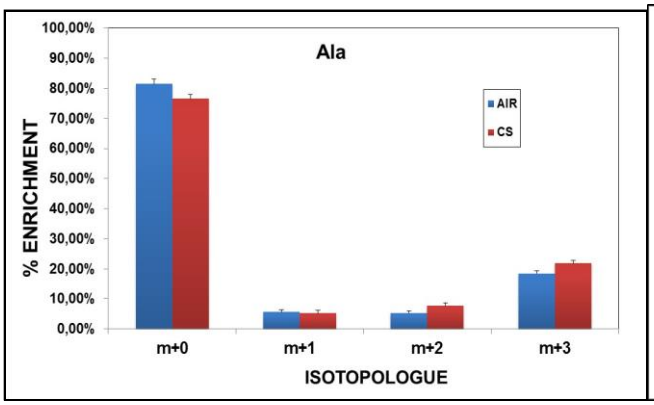

Chart 4. Fractional enrichment serine

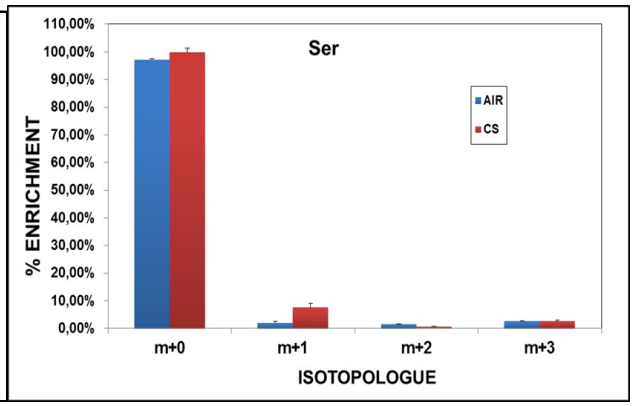

Chart 5. Fractional enrichment glycine

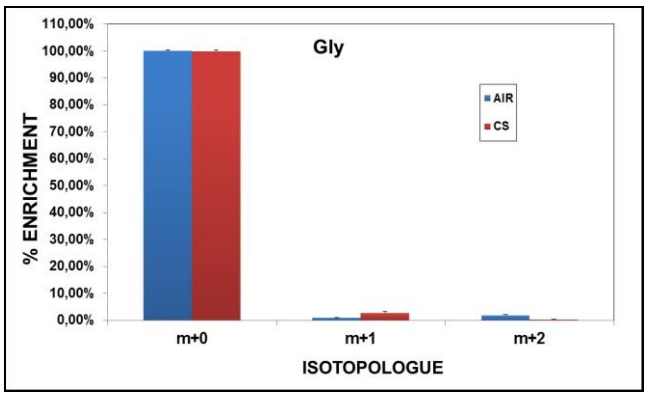

3.5.1.3. LIVER TISSUE NMR ANALYSIS

Considering data that show the biggest change among all replicates, comparison of 1H-NMR spectra of CS group and air group (**Figures 18**) shows slight decreased accumulation of unlabeled lactate and unlabeled alanine and slight increased accumulation of glutamate-GSH+GSSG and cysteine-GSSG in liver tissue of mice exposed to CS. Interestingly, the 1H-^{13}C HSQC NMR spectra (**Figure 19**) reveal increased accumulation of ^{13}C-glucose, ^{13}C-lactate, ^{13}C-alanine and ^{13}C-glycogen in liver tissue of mice exposed to CS.

Increased level of labeled glucose in liver exposed to CS suggests an increased uptake of glucose, while increased levels of ^{13}C-lactate and ^{13}C-alanine in CS group, may suggest an increased flux through glycolysis. Anyway, it's not straightforward to interpret CS effect on glycolysis based on labeled lactate alone due to the fact that the majority of lactate is released into the plasma, and liver receives lactate, alanine and glycerol released by other tissues and organs, then used as precursors to synthesize glucose (gluconeogenesis). To better understand this data and to confirm CS effect on glycolysis based on lactate level it is necessary to analyze plasma data of mice exposed to CS.

NMR data suggest glycogen is a possible source of glucose in liver tissue of mice expose to CS. Increased levels of labeled glycogen (**Figure 19**) suggest an increased glycogen synthesis (glycogenesis), and together with depletion of unlabeled glycogen level (from 1H NMR, data not shown), it suggests an increased glycogen turnover under CS effect. It is possible that CS induces synthesis of glycogen and glycogenolysis. Thus liver tissue in CS group may take up as much glucose as it has access and store it as glycogen or metabolize it via glycolysis.

Increased levels of unlabeled Glu-GSH+GSSG and Cys-GSSG in liver exposed to CS (**Figure 18**), point out the CS-induced redox status imbalance. Glutamate and cysteine availability is needed for GSH (reduced glutathione) synthesis to counteract the oxidative stress induced by CS, with consequent increased levels of GSSG (oxidized glutathione).

Once the cell takes up glucose it is converted to glucose-6-phosphate by hexokinase using ATP. In addition to entering glycolysis and glycogen synthesis pathways glucose converted to glucose-6-phosphate can also enter the pentose phosphate pathway (PPP, **Figure 20**). The oxidative phase of the PPP supplies the cell with ribose, which is needed for nucleotide synthesis, and two molecules of NADPH per glucose oxidized. Among several roles of NADPH, it is required for combating oxidative stress as the ultimate source

of electrons for reducing ROS. Thus, it is possible that, in liver of mice exposed to CS, glucose-6-phosphate is rerouted from glycolysis to PPP, in order to increase NADPH synthesis necessary to counteract oxidants, through GSSG reduction and consequent GSH regeneration. The increase in ^{13}C-ribose-ATP (data not shown) points towards effect on PPP.

Figure 18. Liver tissue 1H NMR spectrum

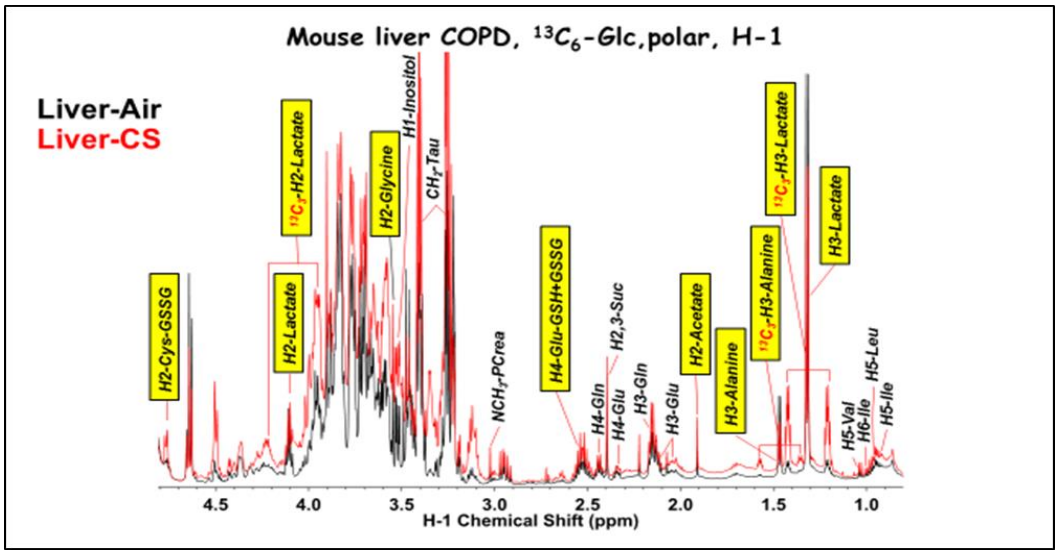

Figure 19. Liver tissue 1H-^{13}C HSQC NMR spectrum

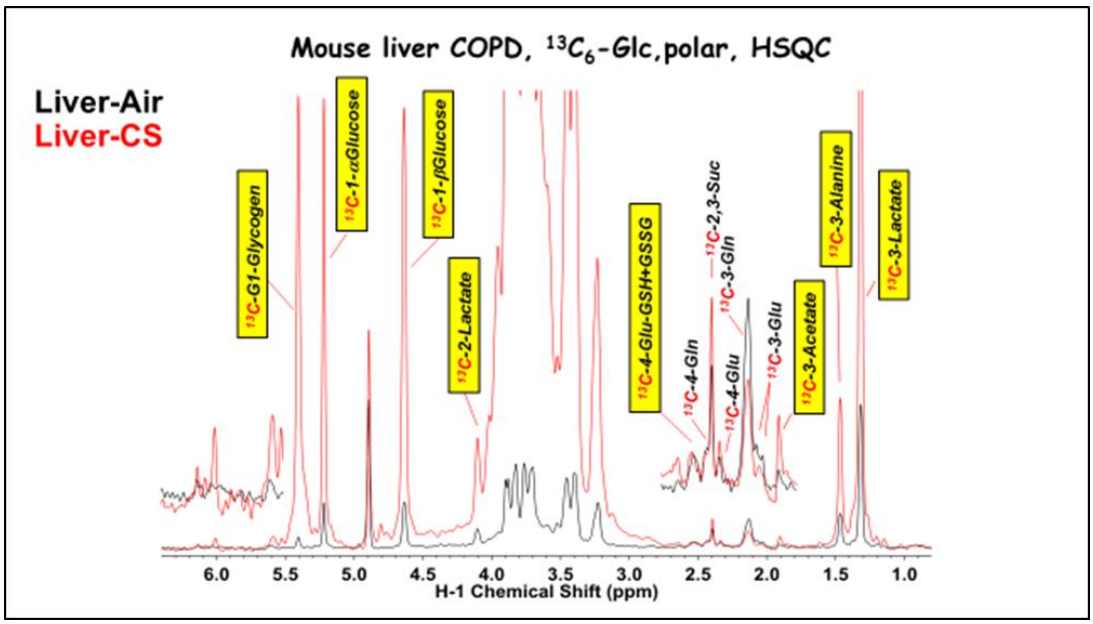

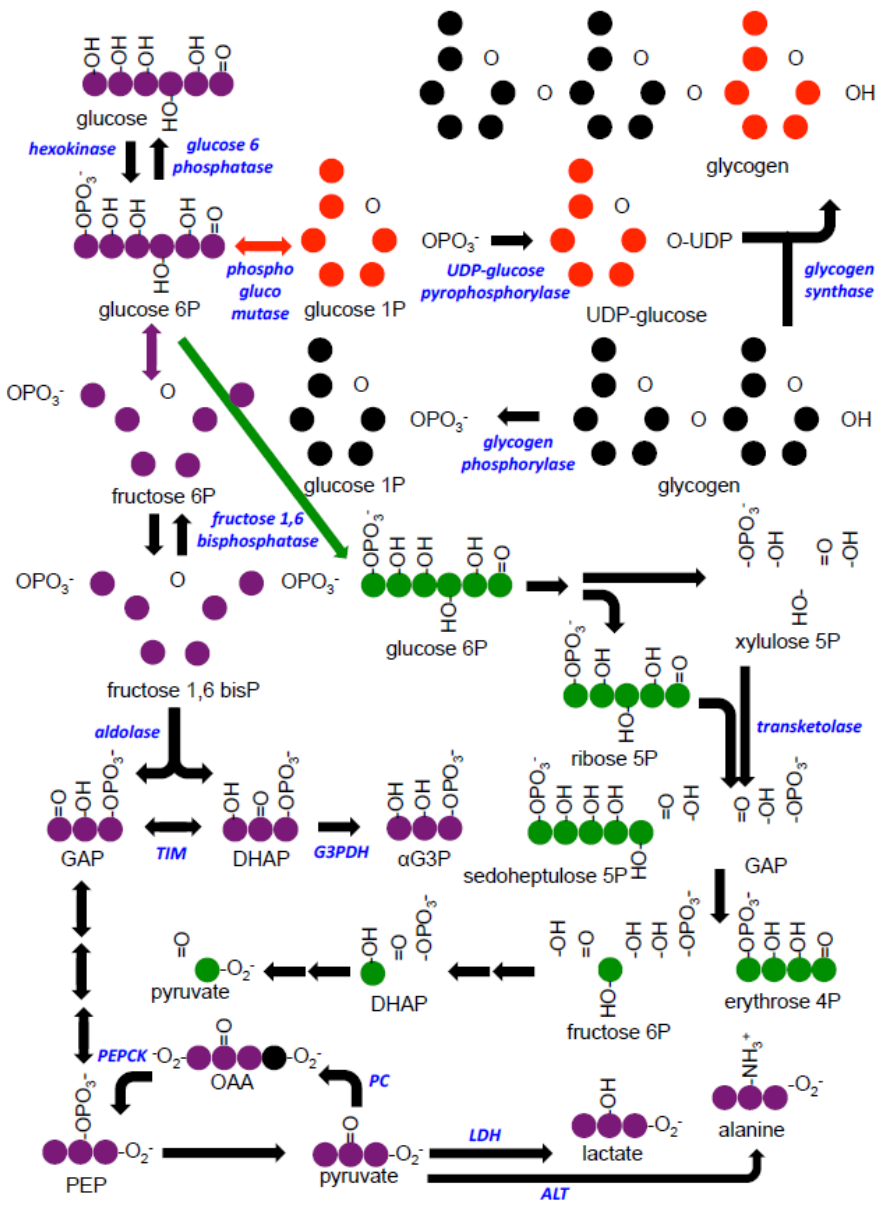

Figure 20. Atom-resolved map of glucose metabolism - Once glucose is taken up by a cell, it is phosphorylated by hexokinase. The resulting glucose 6-phosphate can be used to synthesize glycogen (red arrow), enter glycolysis (purple arrow), or go through the pentose phosphate pathway (PPP, green arrow). In addition, glucose could be produced by the breakdown of glycogen by glycogen phosphorylase or via gluconeogenesis. Purple circles, red, and green circles represent atoms derived from ^{13}C glucose entering glycolysis, glycogenesis, and PPP, respectively and black circles represent unlabeled carbon. The white circles outlined in green originating from xylulose 5-phosphate are meant to differentiate carbons from xylulose 5-phoshpate versus ribose 5-phosphate, as both can be labeled via the oxidative PPP. Abbreviations: TIM: triose phosphate isomerase, G3PDH: glycerol 3-phosphate dehydrogenase, GAP: glyceraldehyde 3-phosphate, DHAP: dihydroxyacetone phosphate, PEP: phosphoenolpyruvate, OAA: oxaloacetate, PEPCK: phosphoenolpyruvate carboxykinase, PC: pyruvate carboxylase, LDH: lactate dehydrogenase, ALT: alanine transaminase.

3.5.1.4. LIVER TISSUE GC-MS ANALYSIS – GLYCOLYSIS FLUX ANALYSIS

Fractional enrichment of isotopologues of glycolytic intermediates (**Charts 6-10**) shows a statistically significant increased incorporation of ^{13}C in glycerol-3-P (m+2, m+3), lactate (m+2, m+3) and alanine (m+2, m+3) in liver tissue of mice exposed to CS compare to that of mice exposed to air. This points towards increased glycolytic flux in consequence of CS exposure.

Fractional enrichment of serine and glycine isotopologues is similar among the two group of mice and any statistically significant result was observed.

Chart 6. Fractional enrichment glycerol-3-phosphate

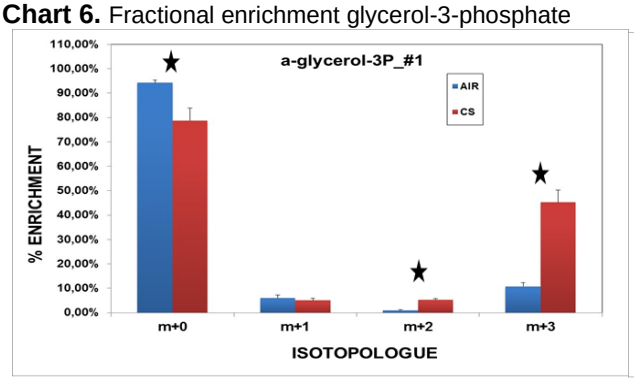

★ P<0,05; q<0,04

Chart 7. Fractional enrichment lactate

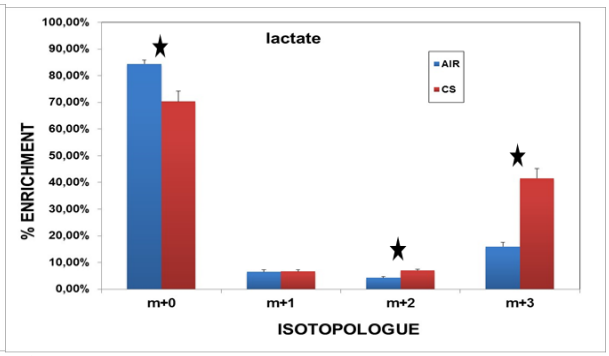

★ P<0,05; q<0,04

Chart 8. Fractional enrichment alanine

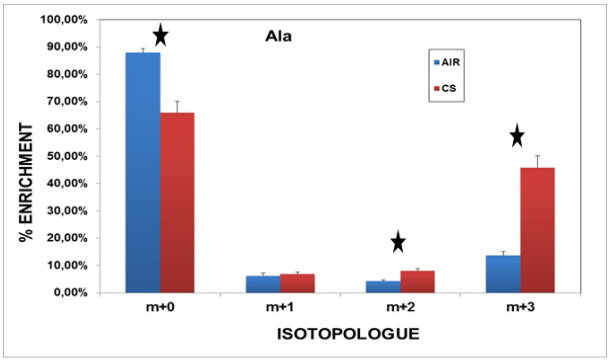

★ P<0,05; q<0,04

Chart 9. Fractional enrichment serine

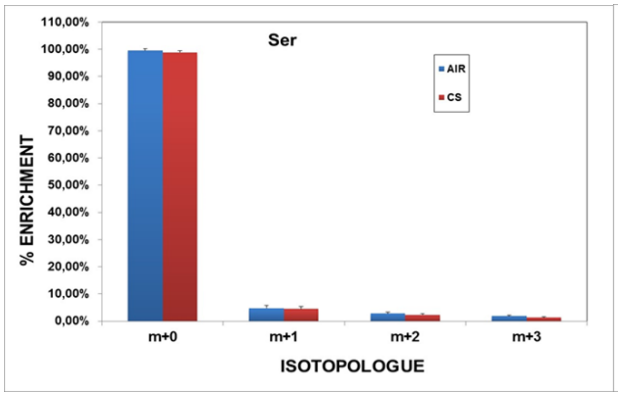

Chart 10. Fractional enrichment glycine

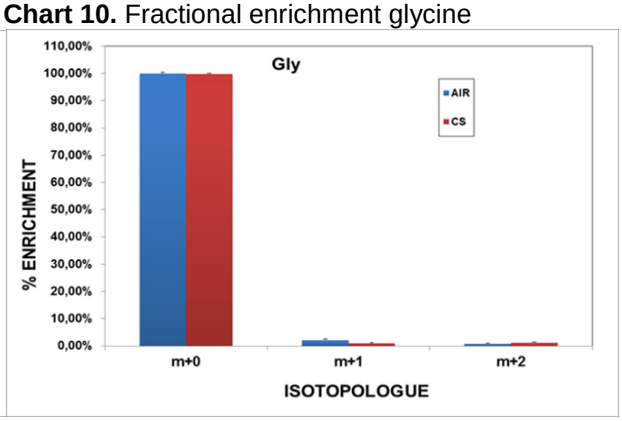

3.6. CONCLUSION

The respiratory tract is the first target of cigarette smoke (CS) inhalation and cigarette smoking is a major risk factor for diseases of the airways such as COPD and head, neck, and lung cancers. It is well established that cigarette smoking is also a risk factor for many systemic diseases, including cardiovascular disease and numerous cancers (e.g. bladder or pancreas), suggesting significant pathogenicity of circulating toxic components or metabolites of absorbed CS. However, not all smokers develop disease and progression of diseases such as COPD may persist despite smoking cessation. These observations suggest a critical need for determining pathways through which smoking can lead to disease and for the discovery of useful biomarkers of disease phenotype, severity, and progression.

CS is a miscellaneous of more than 4,000 chemicals and it is a rich source of oxidants and electrophiles. Exposure to CS (and other environmental pollutants) leads to an oxidant/antioxidant imbalance and inflammatory processes that potentiate proteolytic damage, induce cell death, and inhibit cell repair, in the lung and other organs.

CS-induced lung inflammatory processes are likely to be preceded by changes in energy metabolism and in the redox status of the cell. After CS exposure, oxidative stress leads to redox changes in cytosolic and mitochondrial metabolic events. A number of glycolytic enzymes are sensitive to CS-induced oxidative stress along with inhibition of the mitochondrial respiratory chain complexes and consequent impairment of energy homeostasis and cell death. It has been observed that short-term CS exposure led to metabolic alterations in glyceraldehyde-3-phosphate dehydrogenase (GAPDH)-dependent glycolysis and glucose-6-phosphate dehydrogenase (G6PDH)-dependent pentose phosphate pathway [269]. Moreover, alveolar type II cells increase the utilization of fatty acids after the inhibition of glycolysis in response to acrolein exposure [277].

Metabolic (energy) and redox (oxidative stress) components are interdependent pathways that control cell function. Thus, impairment of intermediary metabolism is expected to play a decisive role in the development of COPD.

Glucose is the principal substrate utilized by the lung and other organs for the generation of energy. Disturbances in glucose metabolism are more common in COPD patients than in COPD free individuals. However, the pathogenesis of glucose metabolism dysregulation is likely to be much more complex, whereby myriads of pathways are likely to be implicated, and much is still to be discovered and clarified.

Patients with COPD experience increasing muscle weakness, reduction in lean body mass and low energy metabolism associated with decline in lung function [282], however, the cellular mechanisms underlying these processes, especially low energy metabolism in response to CS are not known.

There are currently few published studies exploring tissue metabolome changes due to smoking. Using state-of-the art instrumentation for stable isotope-resolved metabolomics applied to a cigarette smoking model in mice, this study sought to examine changes that are induced by chronic CS exposure in lung and liver tissue glycolysis.

This work demonstrates the value of using $^{13}C^{6}$-glucose as a tracer to better understand how the metabolism change in tissues after exposure to environmental factor such as CS.

Although lung tissue NMR and GC-MS analyses did not reveal any significant difference in lung tissue glycolysis of mice exposed to CS compared with mice exposed to air, on the other hand, liver tissue analyses suggest that CS induces alterations in liver tissue glycolysis. Concentration and labeling patterns of metabolites involved in glycolytic pathway demonstrate increased flux through glycolysis and glycogen metabolism, in mice exposed to CS compare to those expose to air.

Labeling patterns of glycerol-3-phosphate, alanine and lactate suggest enhanced glycolytic flux in liver tissue, even though to interpret CS effect on glycolysis based on labeled lactate alone it is necessary to analyze plasma data of mice exposed to CS, because the majority of lactate is released into the plasma and liver receives lactate released by other tissues and organs to synthesize glucose. The increase in ^{13}C-ribose-ATP (data not shown) points towards effect on PPP. In addition to glycolysis and PPP, increased ^{13}C incorporation into glycogen and dicreased unlabeled glycogen (data not shown) in liver tissue point towards an increased glycogen turnover under CS effect. The polysaccharide glycogen serves as one of the primary energy storage molecules in animals, and the bulk of glycogen is primarily stored in liver and muscle tissue. In the current study, liver tissue of mice exposed to CS seems to contain and synthesize more glycogen than the paired liver tissue of mice exposed to air.

In conclusion, this study shows that CS may contribute to dysregulated glycolysis, PPP, glycogen synthesis and utilization in liver tissue in emphysema mouse model. These pathways can provide cells with the energy, biosynthetic precursors, and reducing equivalents needed to proliferate and survive, if disregulated they can contribute to development of pathological conditions. More accurate and specific studies on CS-induced intermediary metabolism alterations are necessary to elucidate new pathways through

which smoking can lead to disease, in order to discover useful biomarkers of disease phenotype, severity, and progression.

Metabolomics and Stable Isotope-Resolved Metabolomic approach can provide good instruments to reach that goal and contemporary contributing to increase and to develop our knowledge about metabolism in health and disease state.

4. GENERAL CONCLUSION

The main respiratory diseases among the ten leading causes of death worldwide are: pneumonia, Chronic Obstructive Pulmonary Disease (COPD), lung cancer and tuberculosis. Lung cancer is the leading cause of respiratory death, followed by COPD, lower respiratory infections and tuberculosis.

In Italy respiratory diseases represent the third leading cause of death (after cancer and diseases of the circulatory system), and they account for 12% of all deaths (~70.000). Asthma and COPD account for 55% of all death caused by respiratory diseases.

More than half of all the deaths from respiratory disease are due to diseases caused by smoking. Based on WHO data tobacco smoke represents the single greatest preventable cause of death in the world today. It kills 6 milion people every year, among them 600.000 are non-smokers exposed to second-hand smoke (SHS or environmental tobacco smoke, ETS). In Italy 18% of total population smokes tobacco, that every year kills 70.000-80.000 people.

Among respiratory diseases, COPD represents a global health problem. It ranks as the fourth leading cause of death in the world with a prevalence of 5% in the general population. In coming decades COPD is projected to increase, and it is estimated that will be the third leading cause of death worldwide in 2030. In Italy, COPD affects about 14% of the older population (65 years or more), and it is the fifth cause of hospital admission in this age group. The prevalence of COPD shows a growing trend that varies from 2.5% in 2005 to 3% in 2013 and rising values as age increases, with a significant increase in male reaches the peak in the over 85 (18%).

COPD is a multifactorial, heterogeneous disease characterized by airflow obstruction that is usually progressive and associated with an abnormal inflammatory responses of the lungs to noxious particles and gases. COPD is a life-threatening lung disease that interferes with normal breathing. Many people suffer from this disease for years, and die prematurely from it or its complications.

The identification of risk factors is an important stage in the development of strategies for prevention and treatment of any disease. Identification of cigarette smoking as the most common environmental risk factor for COPD has led to the incorporation of smoking cessation programs, a key element, essential in the prevention of COPD, as well as an important intervention for patients that have already developed the disease.

Cigarette smoke (CS) through xenobiotics and oxidants activity can lead to changes in redox status and intermediary metabolism of the cell, and oxidative stress and inflammatory processes that potentiate proteolytic damage, induce cell death and inhibit cell repair, inducing severe cellular and tissue damage. Inflammation and oxidative stress, play a critical role in pathogenesis of chronic respiratory diseases as COPD.

However, although cigarette smoking is the most studied risk factor for COPD, it is certainly not the only one factor involved. There are epidemiological evidence that only a small proportion of smokers (15-20%) develop symptomatic COPD and non-smokers may develop chronic airflow obstruction, which suggests that there are individual susceptibility factors involved in disease onset and progression. In other words, two individuals characterized by the same history of smoking, only one may develop COPD due to differences in genetic predisposition.

COPD is a polygenic disease and a classic example of gene-environment interaction. The best documented genetic risk factor is hereditary severe deficiency of alpha-1-antitrypsin, an important inhibitor of serine proteases. Although this rare recessive trait is relevant only for a small part of the world population (more common in individuals of Northern European origin), it illustrates the interaction between genes and environmental exposures leading to COPD. Through genetic linkage analysis, several regions of the genome that likely contain COPD susceptibility genes have been identified, including the chromosome 2. Genetic association studies have implicated a variety of genes in COPD pathogenesis, including antioxidants genes (e.g. SOD), microsomal epoxide hydrolase (EPHX1), transforming growth factor beta (TGF-β1), and tumor necrosis factor alpha (TNF-α). So there may be other factors of susceptibility to the disease.

Considering the impact of environmental and genetic risk factors in COPD onset, development and severity, this dissertation sought to uncover new genetic susceptibility biomarkers in a population affected by COPD, with focused attention on microsomal epoxide hydrolase (EPHX1) genotype and related phenotype, and, using state-of-the art instrumentation for stable isotope-resolved metabolomics applied to a cigarette smoking model in mice, this study sought to examine and explore tissue metabolic alterations underlying oxidative stress and inflammatory processes induced by chronic CS exposure, in order to uncover metabolic biomarkers of exposure.

None of the EPHX1 SNPs and related phenotypes analyzed in the study were associated to the disease onset and severity, probably due to small sample size of the study population and the huge age difference between cases and controls, but some interesting

data came out from metabolomic study on tissues of mice chronically exposed to CS, suggesting that metabolomics could give an important contribution to elucidate the complexity of COPD.

While many questions remain unanswered, recent years have witnessed an explosion in our knowledge of how to characterize and treat patients with COPD. The main goal of this study is to further our understanding of the molecular basis of COPD, and to determine how this relates to the gross pathophysiological defects seen in COPD patients, thus leading to new targeted therapeutic strategies in COPD.

Long is the way to understand clinical and pathological complexity of COPD, but integration of genomic, transcriptomic, proteomic and metabolomic informations is necessary to provide a better understanding of cellular biology, and thus of pathological alterations involved in disease state.

REFERENCES

1. Burney P, Jarvis D, Perez-Padilla R; The global burden of chronic respiratory disease in adults; Int J Tuberc Lung Dis. 2015 Jan;19(1):10-20. doi: 10.5588/ijtld.14.0446.
2. Ferkol T, Schraufnagel D; The global burden of respiratory disease; Ann Am Thorac Soc. 2014 Mar;11(3):404-6. doi: 10.1513/AnnalsATS.201311-405PS.
3. Torres-Duque C, Maldonado D, Pe´ rez-Padilla R, EzzatiM, Viegi G; Forum of International Respiratory Studies (FIRS) Task Force on Health Effects of Biomass Exposure. Biomass fuels and respiratory diseases: a review of the evidence. Proc Am Thorac Soc 2008;5:577–590.
4. World Health Organization. Global surveillance, prevention and control of chronic respiratory diseases: a comprehensive approach. Geneva: World Health Organization; 2013.
5. The burden of lung disease chapter 1, European Lung White Book 2013; European Respiratory Society
6. Gibson GJ, Loddenkemper R, Lundbäck B, Sibille Y; Respiratory health and disease in Europe: the new European Lung White Book; Eur Respir J. 2013 Sep;42(3):559-63.
7. VIII report health search, istituto di ricerca della SIMG: società italiana di medicina generale e delle cure primarie anno 2013-2014.
8. World Health Organization. Global surveillance, prevention and control of chronic respiratory diseases: a comprehensive approach. Geneva: World Health Organization; 2013.
9. Salvi SS, Barnes PJ. Chronic obstructive pulmonary disease in non-smokers. Lancet 2009;374:733-43.
10. World Health Report. Geneva: World Health Organization. Available from URL: http://www.who.int/
11. Mathers CD, Loncar D; Projections of global mortality and burden of disease from 2002 to 2030; PLoS Med. 2006 Nov;3(11):e442
12. Lopez AD, Shibuya K, Rao C, Mathers CD, Hansell AL, Held LS, et al. Chronic obstructive pulmonary disease: current burden and future projections. Eur Respir J 2006; 27(2): 397-412
13. Halbert RJ, Natoli JL, Gano A, Badamgarav E, Buist AS, Mannino DM. Global burden of COPD: systematic review and meta-analysis. Eur Respir J 2006;28:523-32.
14. Global strategy for the diagnosis, management, and prevention of chronic obstructive pulmonary disease. NHLBI/WHO Workshop Report. National Institutes of Health, National Heart, Lung and Blood Institute; GOLD project 2015 updated.
15. Johannessen A, Lehmann S, Omenaas ER, Eide GE, Bakke PS, Gulsvik A. Postbronchodilator spirometry reference values in adults and implications for disease management. Am J Respir Crit Care Med 2006; 173(12):1316-25.
16. Cerveri I, Corisico AG, Accoridini S, Niniano R, Analdo E, Anto JM, et al. Underestimation of airflow obstructing among young adults using FEV1/FVC < 70% as a fixed cutoff: a longitudinal evaluation of clinical and functional outcomes. Torax 2008; 63(12):1040-5.
17. Soriano JB, Visick GT, Muellerova H, Payvandi N, Hansell AL. Patterns of comorbidities in newly diagnosed COPD and asthma in primary care. Chest 2005; 128(4):2099-107.
18. Agusti AG. Systemic effects of chronic obstructive pulmonary disease. Proc Am Thorac Soc 2005; 2(4):367-70.
19. Van Weel C; Chronic diseases in general practice: the longitudinal dimension. Eur J Gen Pract 1996; 2:17-21.
20. Van Weel C, Schellevis FG; Comorbidity and guidelines: conflicting interests. Lancet 2006; 367(9510):550-1.
21. Hogg JC. Pathophysiology of airflow limitation in chronic obstructive pulmonary disease. Lancet 2004; 364(9435):709-21
22. Birring SS, Brightling CE, Bradding P, Entwisle JJ, Vara DD, Grigg J, et al. Clinical, radiologic, and induced sputum features of chronic obstructive pulmonary disease in nonsmokers: a descriptive study. Am J Respir Crit Care Med 2002; 166(8):1078-83.
23. Rahman I. Oxidative stress in pathogenesis of chronic obstructive pulmonary disease: cellular and molecular mechanisms. Cell Biochem Biophys 2005;43:167-88.
24. Malhotra D, Thimmulappa R, Navas-Acien A, et al. Decline in NRF2-regulated antioxidants in chronic obstructive pulmonary disease lungs due to loss of its positive regulator, DJ-1. Am J Respir Crit Care Med 2008;178:592-604.
25. Barnes PJ, Shapiro SD, Pauwels RA. Chronic obstructive pulmonary disease: molecular and cellular mechanisms. Eur Respir J 2003;22:672-88.
26. Hogg JC, Chu F, Utokaparch S, et al. The nature of small-airway obstruction in chronic obstructive pulmonary disease. N Engl J Med 2004;350:2645-53.
27. Barnes PJ. Mediators of chronic obstructive pulmonary disease. Pharmacol Rev 2004; 56(4):515-48.
28. Bestall JC, Paul EA, Garrod R, Garnham R, Jones PW, Wedzicha JA. Usefulness of the Medical Research Council (MRC) dyspnoea scale as a measure of disability in patients with chronic obstructive pulmonary disease. Thorax 1999;54:581-6.

29. Nishimura K, Izumi T, Tsukino M, Oga T. Dyspnea is a better predictor of 5-year survival than airway obstruction in patients with COPD. Chest 2002;121:1434-40.
30. Barnes PJ, Celli BR. Systemic manifestations and comorbidities of COPD. Eur Respir J 2009;33:1165-85.
31. Mannino DM, Thorn D, Swensen A, Holguin F. Prevalence and outcomes of diabetes, hypertension and cardiovascular disease in COPD. Eur Respir J 2008;32:962-9.
32. Sin DD, Anthonisen NR, Soriano JB, Agusti AG. Mortality in COPD: Role of comorbidities. Eur Respir J 2006;28:1245-57.
33. Almagro P, Cabrera FJ, Diez J, Boixeda R, Alonso Ortiz MB, Murio C, Soriano JB; Working Group on COPD, Spanish Society of Internal Medicine. Comorbidities and short-term prognosis in patients hospitalized for acute exacerbation of COPD: the EPOC en Servicios de medicina interna (ESMI) study. Chest 2012 Nov;142(5):1126-33.
34. Miller J, Edwards LD, Agustí A, Bakke P, Calverley PM, Celli B, et al. Evaluation of COPD Longitudinally to Identify Predictive Surrogate Endpoints (ECLIPSE) Investigators. Comorbidity, systemic inflammation and outcomes in the ECLIPSE cohort. Respir Med 2013 Sep;107(9):1376-84.
35. Fabbri LM, Luppi F, Beghe B, Rabe KF. Complex chronic comorbidities of COPD. Eur Respir J 2008;31:204-12.
36. Agusti A, Calverley PM, Celli B, et al. Characterisation of COPD heterogeneity in the ECLIPSE cohort. Respir Res 2010;11:122.
37. Lange P, Parner J, Vestbo J, Schnohr P, Jensen G. A 15 years follow-up study of ventilatory function in adults with asthma. N Engl J Med 1998; 339(17):1194-200.
38. Chanez P, Vignola AM, O'Shaugnessy T, Enander I, Li D, jeffery PK et al. Corticosteroid reversibility in COPD is related to features of asthma. Am J respir Crit Care Med 197; 155(5):529-34.
39. Lam KB, Jiang CQ, Jordan RE, Miller MR, Zhang WS, Cheng KK, et al. Smoking, and airflow obstruction: a cross-sectional analysis of the Guangzhou biobank study. Chest 2010; 137(3):593-600.
40. Celli BR, Halbert RJ, Nordyke RJ, Schan B. Airway obstruction in never smokers: results from the Third National Health and Nutrition Examination Survey. Am J Med 2005;118:1364-72.
41. Behrendt CE. Mild and moderate-to-severe COPD in nonsmokers. Distinct demographic profiles. Chest 2005; 128:1239-44
42. Lamprecht B, McBurnie MA, Vollmer WM, et al. COPD in never smokers: results from the population-based burden of obstructive lung disease study. Chest 2011;139:752-63.
43. Stoller JK, Aboussouan LS. Alpha1-antitrypsin deficiency. Lancet 2005; 365(9478):2225-36.
44. Blanco I, de Serres FJ, Fernandez-Bustillo E, Lara B, Miravitlles M. Estimated numbers and prevalence of PI*S and PI*Z alleles of alpha1-antitrypsin deficiency in European countries. Eur Respir J 2006 ; 27(1):77-84.
45. McCloskey SC, Patel BD, Hinchliffe SJ, Reid ED, Wareham NJ, Lomas DA. Siblings of patients with severe chronic obstructive pulmonary disease have a significant risk of airflow obstruction. Am J Respir Crit Care Med 2001; 164:1419-24.
46. Hunninghake GM, Cho MH, Tesfaigzi Y, et al. MMP12, lung function, and COPD in high-risk populations. N Engl J Med 2009;361:2599-608.
47. Wu L, Chau J, Young RP, Pokorny V, Mills GD, Hopkins R et al. Transforming growth factor beta1 genotype and susceptibility to chronic obstructive pulmonary disease. Thorax 2004; 59(2): 126-9.
48. Smith CA, Harrison DJ. Association between polymorphism in gene for microsomal epoxide hydrolase and susceptibility to emphysema. Lancet 1997; 350(9078):630-3.
49. Huang SL, Su CH, Chang SC. Tumor necrosis factor alpha gene polymorphism in chronic bronchitis. Am J Respir Crit care Med 1997; 156(5):143-69.
50. US Surgeon General. The health consequences of smoking: chronic obstructive pulmonary disease. Washington, D.C.: US Department of Health and Human Services; 1984.
51. Burrows B, Knudson RJ, Cline MG, Lebowitz MD. Quantitative relationships between cigarette smoking and ventilatory function. Am Rev Respir Dis 1977;115(2):195-205.
52. Trupin L, Earnest G, San pedro M, Balmes JR, Eisner MD, Yellin E, et al. The occupational burden of chronic obstructive pulmonary disease. Eur Respir J 2003; 22(3):462-9.
53. Hnizdo E, Sullivan PA, Bang KM, Wagner G. Association between chronic obstructive pulmonary disease and employment by industry and occupation in the US population a study of data from the Third National Health and Nutrition Examination Survey. Am J Epidemiol 2002; 156(8): 738-46.
54. Kohansal R, Martinez-Camblor P, Agusti A, Buist AS, Mannino DM, Soriano JB. The natural history of chronic airflow obstruction revisited: an analysis of the Framingham offspring cohort. Am J Respir Crit Care Med 2009;180:3-10.
55. The Health Consequences of Involuntary Exposure to Tobacco Smoke: A Report of the Surgeon General, Department of Health and Human Services. Washington, DC, US; 2006.
56. Eisner MD, Balmes J, Katz BP, Trupin L, Yelin E, Blanc P. Lifetime environmental tobacco smoke exposure and the risk of chronic obstructive pulmonary disease. Environ Health Perspect 2005;4:7-15.

57. Dayal HH, Khuder S, Sharrar R, Trieff N. Passive smoking in obstructive respiratory disease in an industrialized urban population. Environ Res 1994;65:161-71.
58. Leuenberger P, Schwartz J, Ackermann-Liebrich U, et al. Passive smoking exposure in adults and chronic respiratory symptoms (SAPALDIA Study). Swiss Study on Air Pollution and Lung Diseases in Adults, SAPALDIA Team. Am J Respir Crit Care Med 1994;150:1222-8.
59. Holt PG. Immune and inflammatory function in cigarette smokers. Thorax 1987;42:241-9.
60. Tager IB, Ngo L, Hanrahan JP. Maternal smoking during pregnancy. Effects on lung function during the first 18 months of life. Am J Respir Crit Care Med 1995;152:977-83.
61. Trupin L, Earnest G, San Pedro M, et al. The occupational burden of chronic obstructive pulmonary disease. Eur Respir J 2003;22:462-9.
62. Matheson MC, Benke G, Raven J, et al. Biological dust exposure in the workplace is a risk factor for chronic obstructive pulmonary disease. Thorax 2005;60:645-51.
63. Hnizdo E, Sullivan PA, Bang KM, Wagner G. Airflow obstruction attributable to work in industry and occupation among U.S. race/ethnic groups: a study of NHANES III data. Am J Ind Med 2004;46:126-35.
64. Hnizdo E, Sullivan PA, Bang KM, Wagner G. Association between chronic obstructive pulmonary disease and employment by industry and occupation in the US population: a study of data from the Third National Health and Nutrition Examination Survey. Am J Epidemiol 2002;156:738-46.
65. Balmes J, Becklake M, Blanc P, et al. American Thoracic Society Statement: Occupational contribution to the burden of airway disease. Am J Respir Crit Care Med 2003;167:787-97.
66. Boman C, Forsberg B, Sandstrom T. Shedding new light on wood smoke: a risk factor for respiratory health. Eur Respir J 2006;27:446-7.
67. Ezzati M. Indoor air pollution and health in developing countries. Lancet 2005;366:104-6.
68. Mishra V, Dai X, Smith KR, Mika L. Maternal exposure to biomass smoke and reduced birth weight in Zimbabwe. Ann Epidemiol 2004;14:740-7.
69. Oroczo-Levi M, Garcia -Aymerich J, Villar J, Ramirez-Sarmiento A, Anto JM, Gea J. Wood smoke exposure and risk of chronic obstructive pulmonary disease. Eur Respir J 2006;27:542-6.
70. Sezer H, Akkurt I, Guler N, Marakoglu K, Berk S. A case-control study on the effect of exposure to different substances on the development of COPD. Ann Epidemiol 2006;16:59-62.
71. Smith KR, Mehta S, Maeusezahl-Feuz M. Indoor airpollution from household solid fuel use. In: Ezzati, M., Lopez, A. D., Rodgers, M., Murray, C. J., eds. Comparative quantification of health risks: global and regional burden of disease attributable to selected major risk factors. Geneva: World Health Organization; 2004.
72. Warwick H, Doig A. Smoke the killer in the kitchen: Indoor air pollution in developing countries. ITDG Publishing, 103-105 Southampton Row, London WC1B HLD, UK 2004.
73. Torres-Duque C, Maldonado D, Perez-Padilla R, Ezzati M, Viegi G. Biomass fuels and respiratory diseases: a review of the evidence. Proc Am Thorac Soc 2008;5:577-90.
74. Abbey DE, Burchette RJ, Knutsen SF, McDonnell WF, Lebowitz MD, Enright PL. Long-term particulate and other air pollutants and lung function in nonsmokers. Am J Respir Crit Care Med 1998;158:289-98.
75. Loomis D, Grosse Y, Lauby-Secretan B, El Ghissassi F, Bouvard V, Benbrahim-Tallaa L, Guha N, Baan R, Mattock H, Straif K; International Agency for Research on Cancer Monograph Working Group IARC; The carcinogenicity of outdoor air pollution; Lancet Oncol. 2013 Dec;14(13):1262-3.
76. MacNee W. Oxidative stress and lung inflammation in airways disease. Eur J Pharmacol 2001; 429(1-3):195-207.
77. MacNee W. Pulmonary and systemic oxidant/antioxidant imbalance in chronic obstructive pulmonary disease. Proc Am Thorac Soc 2005; 2(1):50-60.
78. Li N, Xia T, Nel AE. The role of oxidative stress in ambient particulate matter-induced lung diseases and its implications in the toxicity of engineered nanoparticles. Free Radic Biol Med 2008; 44,1689-1699.
79. Ito K, Ito M, Elliot WM, Cosio B, Caramori G, Kon OM, et al. Decreased histone deacetylase activity in chronic obstructive pulmonary disease. N Engl J Med 2005; 352(19): 1967-76.
80. Valko M, Leibfritz D, Moncol J, Cronin MTD, Mazur M, Telser J. Free radicals and antioxidants in normal physiological functions and human disease. Int J biochem Cell Biol 2007; 39(1):44-84.
81. Barker DJ, Godfrey KM, Fall C, Osmond C, Winter PD, Shaheen SO. Relation of birth weight and childhood respiratory infection to adult lung function and death from chronic obstructive airways disease. BMJ 1991;303:671-5.
82. Todisco T, de Benedictis FM, Iannacci L, et al. Mild prematurity and respiratory functions. Eur J Pediatr 1993;152:55-8.
83. Stern DA, Morgan WJ, Wright AL, Guerra S, Martinez FD. Poor airway function in early infancy and lung function by age 22 years: a non-selective longitudinal cohort study. Lancet 2007;370:758-64.
84. Lawlor DA, Ebrahim S, Davey Smith G. Association of birth weight with adult lung function: findings from the British Women's Heart and Health Study and a meta-analysis. Thorax 2005;60:851-8.

85. National Heart, Lung, and Blood Institute. Morbidity and mortality chartbook on cardiovascular, lung and blood diseases. Bethesda, Maryland: US Department of Health and Human Services, Public Health Service, National Institutes of Health. Accessed at: http://www.nhlbi.nih.gov/ resources/docs/cht-book.htm; 2009.
86. Mannino DM, Homa DM, Akinbami LJ, Ford ES, Redd SC. Chronic obstructive pulmonary disease surveillance--United States, 1971-2000. MMWR Surveill Summ 2002;51:1-16.
87. Foreman MG, Zhang L, Murphy J, et al. Early-onset chronic obstructive pulmonary disease is associated with female sex, maternal factors, and African American race in the COPDGene Study. Am J Respir Crit Care Med 2011;184:414-20.
88. Lopez Varela MV, Montes de Oca M, Halbert RJ, et al. Sex-related differences in COPD in five Latin American cities: the PLATINO study. The European respiratory journal : official journal of the European Society for Clinical Respiratory Physiology 2010;36:1034-41.
89. Silverman EK, Weiss ST, Drazen JM, et al. Genderrelated differences in severe, early-onset chronic obstructive pulmonary disease. Am J Respir Crit Care Med 2000;162:2152-8.
90. Sorheim IC, Johannessen A, Gulsvik A, Bakke PS, Silverman EK, DeMeo DL. Gender differences in COPD: are women more susceptible to smoking effects than men? Thorax 2010;65:480-5.
91. De Marco R, Accordini S, Marcon A, et al. Risk factors for chronic obstructive pulmonary disease in a European cohort of young adults. Am J Respir Crit Care Med 2011;183:891-7.
92. Menezes AM, Hallal PC, Perez-Padilla R, et al. Tuberculosis and airflow obstruction: evidence from the PLATINO study in Latin America. Eur Respir J 2007;30:1180-5.
93. Silva GE, Sherrill DL, Guerra S, Barbee RA. Asthma as a risk factor for COPD in a longitudinal study. Chest 2004;126:59-65.
94. Vonk JM, Jongepier H, Panhuysen CI, Schouten JP, Bleecker ER, Postma DS. Risk factors associated with the presence of irreversible airflow limitation and reduced transfer coefficient in patients with asthma after 26 years of follow up. Thorax 2003;58:322-7.
95. Fletcher C, Peto R. The natural history of chronic airflow obstruction. BMJ 1977;1:1645-8.
96. Vestbo J, Prescott E, Lange P, Group at CCHS. Association between chronic mucus hypersecretion with FEV1 decline and COPD morbidity Am J Respir Crit Care Med 1996;153:1530-5.
97. Guerra S, Sherrill DL, Venker C, Ceccato CM, Halonen M, F.D. M. Chronic bronchitis before age 50 years predicts incident airflow limitation and mortality risk. Thorax 2009;64:894-900.
98. De Marco R, Accordini S, Cerveri I, et al. Incidence of chronic obstructive pulmonary disease in a cohort of young adults according to the presence of chronic cough and phlegm. Am J Respir Crit Care Med 2007;175:32-9.
99. Prescott E, Lange P, Vestbo J. Socioeconomic status, lung function and admission to hospital for COPD: results from the Copenhagen City Heart Study. Eur Respir J 1999;13:1109-14.
100. Tao x, hong CJ, Yu S, Chen B, Zhu H, Yang M. Priority among air pollution factors for preventing chronic obstructive pulmonary disease in Shanghai. Sci total Environ 1992; 127(12)57-67.
101. Sahebjami H, Vassallo CL. Influence of starvation on enzyme induced emphysema. Am Rev Respir Dis 1989, 139(6):1435-8.
102. Mahgoub, A.; Idle, J.R.; Dring, L.G.; Lancaster, R.; and Smith, R.L. Polymorphic hydroxylation of debrisoquine in man. Lancet 2:584- 586, 1977
103. Kalra BS; Cytochrome P450 enzyme isoforms and their therapeutic implications: an update; Indian J Med Sci. 2007 Feb;61(2):102-16
104. Dybdahl M, Risom L, Bornholdt J, et al. Inflammatory and genotoxic effectsof diesel particlesin vitro and in vivo. Mutat Res2004;562:119–31
105. Hecht SS. Tobacco smoke carcinogens and lung cancer. J Natl Cancer Inst 1999;91:1194–210.
106. Karlsson HL, Nilsson L, Moller L. Subway particles are more genotoxic than street particles and induce oxidative stress in cultured human lung cells. Chem Res Toxicol 2005;18:19–23
107. Yost GS. Sites of metabolism: lung. In: Woolf TF, editor. Handbook of drug metabolism. New York: Marcel Dekker Inc.; 1999. p. 263–78 (Chapter 11)
108. Kehrer JP. Systemic pulmonary toxicity. In: Ballantyne B, MarrsT, Turner P, editors. General applied toxicology. Basingstoke: The Mcmillan Press Ltd.; 1993. p. 537–54 (Chapter 26)
109. Boyd MR. Metabolic activation and lung toxicity: a basis for cell selective pulmonary damage by foreign chemicals. Environ Health Perspect 1984;55:47–51
110. Ding X, Kaminsky LS. Human extrahepatic cytochrome P450: function in xenobiotic metabolism and tissue-selective chemical toxicity in the respiratory and gastrointestinal tracts. Annu Rev Pharmacol Toxicol 2003;43:149–73
111. The Human Genome Project; www.ornl.gov.
112. The International HapMap Consortium. A haplotype map of human genome. Nature 2005; 437(7063):1299-320.
113. Brookes AJ. The essence of SNPs. Gene 1999; 234(2):177-86.

114. F.P. Guengerich, Epoxide hydrolase: properties and metabolic roles, Rev. Biochem. Toxicol. 4 (1982) 5–30.
115. Oesch, F., Jerina, D.M., Daly, J.W., 1971a. Substrate specificity of hepatic epoxide hydrase in microsomes and in a purified preparation: evidence for homologous enzymes. Arch. Biochem. Biophys. 144, 253–261.
116. Fretland AJ, Omiecinski CJ. Epoxide hydrolases: biochemistry and molecular biology. Chem Biol Interact. 2000; 129:41–59.
117. R.N. Armstrong, Enzyme-catalyzed detoxication reactions: mechanisms and stereochemistry, CRC Crit. Rev. Biochem. 22 (1987) 39–88.
118. Shou M, Gonzalez FJ, Gelboin HV. Stereoselective epoxidation and hydration at the K-region of polycyclic aromatic hydrocarbons by cDNA-expressed cytochromes P4501A1, 1A2, and epoxide hydrolase. Biochemistry. 1996; 35:15807–15813.
119. Jackson, M.R., Craft, J.A., Burchell, B., 1987. Nucleotide and deduced amino acid sequence of human liver microsomal epoxide hydrolase. Nucleic Acids Res. 15, 7188.
120. Skoda, R.C., Demierre, A., McBride, O.W., Gonzalez, F.J., Meyer, U.A., 1988. Human microsomal xenobiotic epoxide hydrolase. Complementary DNA sequence, complementary DNA-directed expression in COS-1 cells, and chromosomal localization. J. Biol. Chem. 263, 1549–1554
121. Hassett, C., Robinson, K.B., Beck, N.B., Omiecinski, C.J., 1994. The human microsomal epoxide hydrolase gene (EPHX1): complete nucleotide sequence and structural characterization. Genomics 23, 433–442.
122. Hartsfield Jr., J.K., Sutcliffe, M.J., Everett, E.T., Hassett, C., Omiecinski, C.J., Saari, J.A., 1998. Assignment of microsomal epoxide hydrolase (EPHX1) to human chromosome 1q42.1 by in situ hybridization. Cytogenet. Cell Genet. 83, 44–45
123. Liang, S.H., Hassett, C., Omiecinski, C.J., 2005. Alternative promoters determine tissuespecific expression profiles of the human microsomal epoxide hydrolase gene (EPHX1). Mol. Pharmacol. 67, 220–230
124. Su, S., Omiecinski, C.J., 2014. Sp1 and Sp3 transcription factors regulate the basal expression of human microsomal epoxide hydrolase (EPHX1) through interaction with the E1b far upstream promoter. Gene 536, 135–144
125. Oesch, F., Raphael, D., Schwind, H., Glatt, H.R., 1977. Species differences in activating and inactivating enzymes related to the control of mutagenic metabolites. Arch. Toxicol. 39, 97–108.
126. Hammock, B.D., Storms, D.H., Grant, D.F., 1997. Epoxide hydrolases. In: Guengerich, F.P. (Ed.) Comprehensive Toxicology vol. 3. Pergamon, Oxford, pp. 283–305.
127. Mertes, I., Fleischmann, R., Glatt, H.R., Oesch, F., 1985. Interindividual variations in the activities of cytosolic and microsomal epoxide hydrolase in human liver. Carcinogenesis 6, 219–223.
128. Hassett, C., Lin, J., Carty, C.L., Laurenzana, E.M., Omiecinski, C.J., 1997. Human hepatic microsomal epoxide hydrolase: comparative analysis of polymorphic expression. Arch. Biochem. Biophys. 337, 275–283.
129. Willey, J.C., Coy, E., Brolly, C., Utell, M.J., Frampton, M.W., Hammersley, J., Thilly, W.G., Olson, D., Cairns, K., 1996. Xenobiotic metabolism enzyme gene expression in human bronchial epithelial and alveolar macrophage cells. Am. J. Respir. Cell Mol. Biol. 14, 262–271.
130. Arand, M., Grant, D.F., Beetham, J.K., Friedberg, T., Oesch, F., Hammock, B.D., 1994. Sequence similarity of mammalian epoxide hydrolases to the bacterial haloalkane dehalogenase and other related proteins. FEBS Lett. 338, 251–256.
131. Beetham, J.K., Grant, D., Arand, M., Garbarino, J., Kiyosue, T., Pinot, F., Oesch, F., Belknap, W.R., Shinozaki, K., Hammock, B.D., 1995. Gene evolution of epoxide hydrolases and recommended nomenclature. DNA Cell Biol. 14, 61–71.
132. van Loo, B., Kingma, J., Arand, M., Wubbolts, M.G., Janssen, D.B., 2006. Diversity and biocatalytic potential of epoxide hydrolases identified by genome analysis. Appl. Environ. Microbiol. 72, 2905–2917.
133. Craft, J.A., Baird, S., Lamont, M., Burchell, B., 1990. Membrane topology of epoxide hydrolase. Biochim. Biophys. Acta 1046, 32–39.
134. Zou, J., Hallberg, B.M., Bergfors, T., Oesch, F., Arand, M., Mowbray, S.L., Jones, T.A., 2000. Structure of Agergillus niger epoxide hydrolase at 1.8 Å resolution: implications for the structure and function of the mammalian microsomal class of epoxide hydrolases. Struct. Fold. Des. 8, 111–122.
135. G.M. Lacourciere, R.N. Armstrong, Microsomal and soluble epoxide hydrolases are members of the same family of CX bond hydrolase enzymes, Chem. Res. Toxicol. 7 (1994) 121–124.
136. L.T. Laughlin, H.F. Tzeng, S. Lin, R.N. Armstrong, Mechanism of microsomal epoxide hydrolase, semifunctional site-specific mutants affecting the alkylation half-reaction, Biochemistry 37 (1998) 2897–2904.
137. M. Arand, F. Muller, A. Mecky, W. Hinz, P. Urban, D. Pompon, R. Kellner, F. Oesch, Catalytic triad of microsomal epoxide hydrolase: replacement of Glu^{404} with Asp leads to a strongly increased turnover rate, Biochem. J. 337 (1999) 37–43.
138. Armstrong, R.N., Kedzierski, B., Levin, W., Jerina, D.M., 1981. Enantioselectivity of microsomal epoxide hydrolase toward arene oxide substrates. J. Biol. Chem. 256, 4726–4733
139. Decker, M., Arand, M., Cronin, A., 2009. Mammalian epoxide hydrolases in xenobiotic metabolism and

signaling. Arch. Toxicol. 83, 297–318
140. Casson, A.G., Zheng, Z., Porter, G.A., Guernsey, D.L., 2006. Genetic polymorphisms of microsomal epoxide hydroxylase and glutathione S-transferases M1, T1 and P1, interactions with smoking, and risk for esophageal (Barrett) adenocarcinoma. Detect. Prev. 30, 423–431
141. El-Sherbeni, A.A., El-Kadi, A.O., 2014. The role of epoxide hydrolases in health and disease. Arch. Toxicol. 88, 2013–2032
142. Lu, A.Y., Thomas, P.E., Ryan, D., Jerina, D.M., Levin, W., 1979. Purification of human liver microsomal epoxide hydrase. Differences in the properties of the human and rat enzymes. J. Biol. Chem. 254, 5878–5881
143. M. Miyata, G. Kudo, Y.H. Lee, T.J. Yang, H.V. Gelboin, P. Fernandez-Salguero, S. Kimura, F.J. Gonzalez, Targeted disruption of the microsomal epoxide hydrolase gene. Microsomal epoxide hydrolase is required for the carcinogenic activity of 7,12-dimethylbenz[a]anthracene, J. Biol. Chem. 274 (1999) 23963–23968
144. Nithipatikom, K., Endsley, M.P., Pfeiffer, A.W., Falck, J.R., Campbell,W.B., 2014. A novel activity of microsomal epoxide hydrolase: metabolism of the endocannabinoid 2- arachidonoylglycerol. J. Lipid Res. 55, 2093–2102
145. Cho, M.K., Kim, S.G., 1998. Differential induction of rat hepatic microsomal epoxide hydrolase and rGSTA2 by diazines: the role of cytochrome P450 2E1-mediated metabolic activation. Chem. Biol. Interact. 116, 229–245.
146. Abdull Razis, A.F., Bagatta, M., De Nicola, G.R., Iori, R., Ioannides, C., 2011. Induction of epoxide hydrolase and glucuronosyl transferase by isothiocyanates and intact glucosinolates in precision-cut rat liver slices: importance of side-chain substituent and chirality. Arch. Toxicol. 85, 919–927.
147. Peng, D.R., Pacifici, G.M., Rane, A., 1984. Human fetal liver cultures: basal activities and inducibility of epoxide hydrolases and aryl hydrocarbon hydroxylase. Biochem. Pharmacol. 33, 71–77
148. Pushparajah, D.S., Umachandran, M., Plant, K.E., Plant, N., Ioannides, C., 2008. Differential response of human and rat epoxide hydrolase to polycyclic aromatic hydrocarbon exposure: studies using precision-cut tissue slices. Mutat. Res. 640, 153–161.
149. A.J. Draper, B.D. Hammock, Inhibition of soluble and microsomal epoxide hydrolase by zinc and other metals, Toxicol. Sci. 52 (1999) 26–32.
150. Sandberg M, Hassett C, Adman ET, Meijer J, Omiecinski CJ. Identification and functional characterization of human soluble epoxide hydrolase genetic polymorphisms. J Biol Chem. 2000; 275:28873–28881.
151. Laurenzana EM, Hassett C, Omiecinski CJ. Post-transcriptional regulation of human microsomal epoxide hydrolase. Pharmacogenetics. 1998; 8:157–167.
152. Lin P, Wang SL, Wang HJ, Chen KW, Lee HS, Tsai KJ, Chen CY, Lee H. Association of CYP1A1 and microsomal epoxide hydrolase polymorphisms with lung squamous cell carcinoma. Br J Cancer. 2000; 82:852–857.
153. Park JY, Schantz SP, Lazarus P. Epoxide hydrolase genotype and orolaryngeal cancer risk: interaction with GSTM1 genotype. Oral Oncol. 2003; 39:483–490.
154. Kitteringham, N.R., Davis, C., Howard, N., Pirmohamed, M., Park, B.K., 1996. Interindividual and interspecies variation in hepatic microsomal epoxide hydrolase activity: studies with cis-stilbene oxide, carbamazepine 10, 11-epoxide and naphthalene. J. Pharmacol. Exp. Ther. 278, 1018–1027
155. Gaedigk, S.P. Spielberg, D.M. Grant, Characterization of the microsomal epoxide hydrolase gene in patients with anticonvulsant adverse drug reactions, Pharmacogenetics 4 (1994) 142–153.
156. Hassett, L. Aicher, J.S. Sidhu, C.J. Omiecinski, Human microsomal epoxide hydrolase: genetic polymorphism and functional expression in vitro of amino acid variants, Hum. Mol. Genet. 3 (1994) 421–428.
157. S. Raaka, C. Hassett, C.J. Omiencinski, Human microsomal epoxide hydrolase: 5-flanking region genetic polymorphisms, Carcinogenesis 19 (1998) 387–393.
158. Zusterzeel, P.L.M., Peters, W.H.M., Visser, W., Hermsen, K.J.M., Roelofs, H.M.J., Steegers, E.A.P., 2001. A polymorphism in the gene for microsomal epoxide hydrolase is associated with pre-eclampsia. J. Med. Genet. 38, 234–237.
159. Laasanen, J., Romppanen, E.L., Hiltunen, M., Helisalmi, S., Mannermaa, A., Punnonen, K., Heinonen, S., 2002. Two exonic single nucleotide polymorphisms in the microsomal epoxide hydrolase gene are jointly associated with preeclampsia. Eur. J. Hum. Genet. 10, 569–573.
160. Zhu, Q., Xing, W., Qian, B., von Dippe, P., Shneider, B.L., Fox, V.L., Levy, D., 2003. Inhibition of human m-epoxide hydrolase gene expression in a case of hypercholanemia. Biochim. Biophys. Acta 1638, 208–216.
161. Buehler, B.A., Delimont, D., van Waes, M., Finnell, R.H., 1990. Prenatal prediction of risk of the fetal hydantoin syndrome. N. Engl. J. Med. 322, 1567–1571
162. Benhamou, S., Reinikainen, M., Bouchardy, C., Dayer, P., Hirvonen, A., 1998. Association between lung cancer and microsomal epoxide hydrolase genotypes. Cancer Res. 58, 5291–5293.
163. Hosagrahara, V.P., Rettie, A.E., Hassett, C., Omiecinski, C.J., 2004. Functional analysis of human microsomal epoxide hydrolase genetic variants. Chem. Biol. Interact. 150, 149–159.
164. Marowsky, A., Burgener, J., Falck, J.R., Fritschy, J.M., Arand, M., 2009. Distribution of soluble and microsomal epoxide hydrolase in the mouse brain and its contribution to cerebral epoxyeicosatrienoic acid metabolism.

Neuroscience 163, 646–661.
165. Tacconelli, S., Patrignani, P., 2014. Inside epoxyeicosatrienoic acids and cardiovascular disease. Front. Pharmacol. 5, 239
166. Bhaskar, L.V., Thangaraj, K., Patel, M., Shah, A.M., Gopal, K., Saikrishna, L., Tamang, R., Singh, L., Rao, V.R., 2013. EPHX1 gene polymorphisms in alcohol dependence and their distribution among the Indian populations. Am. J. Drug Alcohol Abuse 39, 16–22.
167. Wong, N.A., Rae, F., Bathgate, A., Smith, C.A., Harrison, D.J., 2000. Polymorphisms of the gene for microsomal epoxide hydrolase and susceptibility to alcoholic liver disease and hepatocellular carcinoma in a Caucasian population. Toxicol. Lett. 115, 17–22.
168. Jourenkova-Mironova, N., Mitrunen, K., Bouchardy, C., Dayer, P., Benhamou, S., Hirvonen, A., 2000. High-activity microsomal epoxide hydrolase genotypes and the risk of oral, pharynx, and larynx cancers. Cancer Res. 60, 534–536.
169. Sarmanová, J., Sůsová, S., Gut, I., Mrhalová, M., Kodet, R., Adámek, J., Roth, Z., Soucek, P., 2004. Breast cancer: role of polymorphisms in biotransformation enzymes. Eur. J. Hum. Genet. 12, 848–854.
170. Spurdle, A.B., Chang, J.H., Byrnes, G.B., Chen, X., Dite, G.S., McCredie, M.R., Giles, G.G., Southey, M.C., Chenevix-Trench, G., Hopper, J.L., 2007. A systematic approach to analysing gene–gene interactions: polymorphisms at the microsomal epoxide hydrolase EPHX and glutathione S-transferase GSTM1, GSTT1, and GSTP1 loci and breast cancer risk. Cancer Epidemiol. Biomarkers Prev. 16, 769–774.
171. Khedhaier, A., Hassen, E., Bouaouina, N., Gabbouj, S., Ahmed, S.B., Chouchane, L., 2008. Implication of xenobiotic metabolizing enzyme gene (CYP2E1, CYP2C19, CYP2D6, mEH and NAT2) polymorphisms in breast carcinoma. BMC Cancer 8, 109.
172. Andrew, A.S., Gui, J., Sanderson, A.C., Mason, R.A., Morlock, E.V., Schned, A.R., Kelsey, K.T., Marsit, C.J., Moore, J.H., Karagas, M.R., 2009. Bladder cancer SNP panel predicts susceptibility and survival. Hum. Genet. 125, 527–539.
173. Goode, E.L., White, K.L., Vierkant, R.A., Phelan, C.M., Cunningham, J.M., Schildkraut, J.M., Berchuck, A., Larson, M.C., Fridley, B.L., Olson, J.E., Webb, P.M., Chen, X., Beesley, J., Chenevix-Trench, G., Sellers, T.A., 2011. Xenobiotic-Metabolizing gene polymorphisms and ovarian cancer risk. Mol. Carcinog. 50, 397–402.
174. Tan, X., Wang, Y.Y., Chen, X.Y., Xian, L., Guo, J.J., Liang, G.B., Chen, M.W., 2014. Quantitative assessment of the effects of the EPHX1 Tyr113His polymorphism on lung and breast cancer. Genet. Mol. Res. 13, 7437–7446.
175. Pérez-Morales, R., Méndez-Ramírez, I., Moreno-Macias, H., Mendoza-Posadas, A.D., Martínez-Ramírez, O.C., Castro-Hernández, C., Gonsebatt, M.E., Rubio, J., 2014. Genetic susceptibility to lung cancer based on candidate genes in a sample from the Mexican Mestizo population: a case-control study. Lung 192, 167–173.
176. S. Benhamou, M. Reinikainen, C. Bouchardy, P. Dayer, A. Hirvonen, Association between lung cancer and microsomal epoxide hydrolase genotypes, Cancer Res. 58 (1998) 5291–5293.
177. J.E. Hulla, M.S. Miller, J.A. Taylor, D.W. Hein, C.E. Furlong, C.J. Omiecinski, T.A. Kunkel, Symposium overview: the role of genetic polymorphism and repair deficiencies in environmental disease, Toxicol. Sci. 47 (1999) 135–143.
178. P. Lin, S.L. Wang, H.J. Wang, K.W. Chen, H.S. Lee, K.J. Tsai, C.Y. Chen, H. Lee, Association of CYP1A1 and microsomal epoxide hydrolase polymorphisms with lung squamous cell carcinoma, Br. J. Cancer 82 (2000) 852–857.
179. D.J. Harrison, A.L. Hubbard, J. MacMillan, A.H. Wyllie, C.A. Smith, Microsomal epoxide hydrolase gene polymorphism and susceptibility to colon cancer, Br. J. Cancer 79 (1999) 168–171.
180. J.G. Hengstler, M. Arand, M.E. Herrero, F. Oesch, Polymorphisms of N-acetyltransferases, glutathione S-transferases, microsomal epoxide hydrolase and sulfotransferases: influence on cancer susceptibility, Recent Results Cancer Res. 154 (1998) 47–85.
181. Wang, S., Zhu, J., Zhang, R., Wang, S., Gu, Z., 2013. Association between microsomal epoxide hydrolase 1 T113C polymorphism and susceptibility to lung cancer. Tumour Biol. 34, 1045–1052.
182. Lee, J., Dahl, M., Nordestgaard, B.G., 2011. Genetically lowered microsomal epoxide hydrolase activity and tobacco-related cancer in 47,000 individuals. Cancer Epidemiol. Biomarkers Prev. 20, 1673–1682.
183. Fathy, M., Hamed, M., Youssif, O., Fawzy, N., Ashour, W., 2014. Association between environmental tobacco smoke exposure and lung cancer susceptibility: modification by antioxidant enzyme genetic polymorphisms. Mol. Diagn. Ther. 18, 55–62
184. Agudo, A., Peluso, M., Sala, N., Capellá, G., Munnia, A., Piro, S., Marín, F., Ibáñez, R., Amiano, P., Tormo, M.J., Ardanaz, E., Barricarte, A., Chirlaque, M.D., Dorronsoro, M., Larrañaga, N., Martínez, C., Navarro, C., Quirós, J.R., Sánchez, M.J., González, C.A., 2009. Aromatic DNA adducts and polymorphisms in metabolic genes in healthy adults: findings from the EPIC-Spain cohort. Carcinogenesis 30, 968–976.
185. Peluso, M.E., Munnia, A., Srivatanakul, P., Jedpiyawongse, A., Sangrajrang, S., Ceppi, M., Godschalk, R.W., van Schooten, F.J., Boffetta, P., 2013. DNA adducts and combinations of multiple lung cancer at-risk alleles in environmentally exposed and smoking subjects. Environ. Mol. Mutagen. 54, 375–383

186. Li, H., Fu, W.P., Hong, Z.H., 2013. Microsomal epoxide hydrolase gene polymorphisms and risk of chronic obstructive pulmonary disease: a comprehensive meta-analysis. Oncol. Lett. 5, 1022–1030.
187. Foster JA, Rich CB, Miller MF; Pulmonary fibroblasts: an in vitro model of emphysema regulation of the elastin gene expression. J Biol Chem 1990; 265: 15544–49;
188. D'Armiento J, Dalal SS, Okada Y, Berg RA, Dhada K. Collagenase expression in the lungs of transgenic mice causes pulmonary emphysema. Cell 1992; 71: 955–61
189. Farber JL; Mechanisms of cell injury by activated oxygen species. Environ. Health Perspect. 1994; 102: 17–24;
190. Rahman I, Swarska E, Henry M, Stolk J, MacNee W. Is there any relationship between plasma antioxidant capacity and lung function in smokers and in patients with chronic obstructive pulmonary disease? Thorax 2000; 55: 189–93
191. Fischer BM, Pavlisko E, Voynow JA; Pathogenic triad in COPD: oxidative stress, protease–antiprotease imbalance, and inflammation; Int J Chron Obstruct Pulmon Dis. 2011; 6: 413–421.Published online 2011 Aug 5. doi: 10.2147/COPD.S10770;
192. Smith CA, Harrison DJ; Association between polymorphism in gene for microsomal epoxide hydrolase and susceptibility to emphysema; Lancet. 1997 Aug 30;350(9078):630-3.
193. Mannino DM, Homa DM, Akinbami LJ, Ford ES, Redd SC. Chronic obstructive pulmonary disease surveillance—United States, 1971–2000. MMWR Surveill. Summ. 2002; 51: 1–16.
194. Silverman EK, Chapman HA, Drazen JM, Weiss ST, Rosner B et al. Genetic epidemiology of severe, early onset chronic obstructive pulmonary disease. Risk to relatives for airflow obstruction and chronic bronchitis. Am. J. Respir. Crit. Care Med. 1998; 157: 1770–8.
195. Lomas DA, Silverman EK. The genetics of chronic obstructive pulmonary disease. Respir. Res. 2001; 2: 20–6.
196. Sandford AJ, Silverman EK. Chronic obstructive pulmonary disease: susceptibility factors for COPD the genotype environment interaction. Thorax 2002; 57: 736–41
197. Koyama H, Geddes DM; Genes, oxidative stress, and the risk of chronic obstructive pulmonary disease Thorax. 1998 Aug;53 Suppl 2:S10-4
198. Tomaki M, Sugiura H, Koarai A, et al; Decreased expression of antioxidant enzymes and increased expression of chemokines in COPD lung. Pulm Pharmacol Ther 2007; 20: 596-605
199. Chappell S, Daly L, Morgan K, et al. Genetic variants of microsomal epoxide hydrolase and glutamate-cysteine ligase in COPD. Eur Respir J 2008; 32: 931–937.
200. Hassett C, Aicher L, Sidhu JS, et al. Human microsomal epoxide hydrolase: genetic polymorphism and functional expression in vitro of amino acid variants. Hum Mol Genet 1994; 3: 421–428.
201. Pandolfi P, Zanasi A, Musti MA, Stivanello E, Pisani L, Angelini S, Maffei F, Hrelia S, Angeloni C, Zenesini C, Hrelia P Socio-Economic and Clinical Factors as Predictors of Disease Evolution and Acute Events in COPD Patients; PLoS One 2015 Aug 7;10(8):e01351 16.doi: 10.1371/journal.pone.0135116. eCollection 2015.
202. Caranci N, Biggeri A, Grisotto L, Pacelli B, Spadea T, Costa G. The Italian deprivation index at census block level: definition, description and association with general mortality. Epidemiol Prev 2010; 34(4):167–76.
203. Charlson ME, Pompei P, Ales KL, MacKenzie CR. A new method of classifying prognostic comorbidity in longitudinal studies: development and validation. J Chronic Dis 1987; 40:373–83. PMID: 3558716.
204. Dweik RA, Boggs PB, Erzurum SC, Irvin CG, Leight MW, Lundberg JO et al. An official ATS clinical practice guideline: interpretation of exhaled nitric oxide levels (FENO) for clinical applications. Am J Respir Crit Care Med 2011; 184:602–615. doi: 10.1164/rccm.9120-11ST.
205. Mannino DM, Buist AS. Global burden of COPD: risk factors, prevalence, and future trends. Lancet2007; 370(9589):765–73.
206. Halbert RJ, Natoli JL, Gano A, Badamgarav E, Buist AS, Mannino DM. Global burden of COPD: systematic review and meta-analysis. Eur Respir J 2006;28:523-32.
207. Taylor DR, Pijnenburg MW, Smith AD, Jongste JCD. Exhaled nitric oxide measurements: clinical application and interpretation. Thorax 2006; 61:817e27.
208. Papi A, Romagnoli M, Baraldo S, Braccioni F, Guzzinati I, Saetta M, et al. Partial reversibility of airflow limitation and increased exhaled NO and sputum eosinophilia in chronic obstructive pulmonary disease. Am J Respir Crit Care Med 2000; 162(5):1773–1777.
209. Rutten E, Calverley P, Casaburi R, Agusti A, Bakke P, Celli B et al. Changes in Body Composition in Patients with Chronic Obstructive Pulmonary Disease: Do They Influence Patient-Related Outcomes?. Ann Nutr MEtab 2013; 63:239–247 doi: 10.1159/000353211
210. Cazzola M, Calzetta L, Lauro D, Bettoncelli G, Cricelli C, Di Daniele N et al. Asthma and COPD in an Italian adult population: role of BMI considering the smoking habit. Respir Med 2013; 107(9):1417–22. doi: 10.1016/j.rmed.2013.04.021
211. Vestbo J, Prescott E, Almdal T, Dahl M, Nordestgaard BG, Andersen T et al. Body mass, fat-free body mass, and prognosis in patients with chronic obstructive pulmonary disease from a random population sample: findings from the Copenhagen City Heart Study. Am J Respir Crit Care Med 2006; 173 (1):79–83.

212. Eisner MD, Blanc PD, Omachi TA, Yelin EH, Sidney S, Katz PP et al. Socioeconomic status, race and COPD health outcomes. J Epidemiol Community Health 2011; 65(1):26–34. doi: 10.1136/jech.2009.089722
213. Fischer A. Intermediary metabolism of the lung. Environ Health Perspect 55: 149–158, 1984
214. Agarwal AR, Zhao L, Sancheti H, Sundar IK, Rahman I, Cadenas E. Short-term cigarette smoke exposure induces reversible changes in energy metabolism and cellular redox status independent of inflammatory responses in mouse lungs. Am J Physiol Lung Cell Mol Physiol 2012;303:L889–L898
215. Ralser M, Wamelink M, Kowald A, Gerisch B, Heeren G, Struys E, Klipp E, Jakobs C, Breitenbach M, Lehrach H, Krobitsch S. Dynamic rerouting of the carbohydrate flux is key to counteracting oxidative stress. J Biol 6: 10, 2007
216. Fisher, A. B. Oxygen utilization and energy production. In: The Biochemical Basis of Lung Function (R. G. Crystal, Ed.), Marcel Dekker, New York, 1976, pp. 75-104
217. Jan van der Greef, Age K.Smilde; Symbiosis of chemometrics and metabolomics: past, present, and future; JOURNAL OF CHEMOMETRICS (2005);19: 376–386; Published online in Wiley InterScience (www.interscience.wiley.com). DOI: 10.1002/cem.941
218. Nicholson JK, Lindon JC; "Systems biology: Metabonomics". Nature (2008) Bibcode: Natur. 455 (7216): 1054–6; PMID 18948945.
219. Eknoyan G (1999). "Santorio Sanctorius (1561–1636) – founding father of metabolic balance studies". Am J Nephrol 19 (2): 226–33. PMID 10213823
220. Gates SC, Sweeley CC; "Quantitative metabolic profiling based on gas chromatography"; Clin Chem (1978); 24 (10): 1663–73. PMID 359193.
221. Williams, R. J., et al., Biochemical Institute Studies IV. Individual metabolic patterns and human disease: An exploratory study utilizing predominantly paper chromatographic methods. U. Texas Publication No. 5109 Univ. of Texas, Austin, 1951,204 pp. [Ed. note: Readers may be interested in a fuller account of these studies: Williams, R. J., Biochemical Individuality, The Basis for the Genetotrophic Concept, Univ. of Texas Press, Austin, 1956 (paperback);
222. Horning, E. C., and Horning, M. G., Human metabolic profiles obtained by GC and GC/MS. J. Chromatogr. Sci. 9, 129 (1971).
223. Horning EC, Horning MG; Metabolic profiles: gas-phase methods for analysis of metabolites; Clin Chem. (1971) Aug;17(8):802-9.
224. Horning MG, Hung A, Hill RM, Horning EC; Variations in urinary steroid profiles after birth; Clin Chim Acta. (1971) Sep;34(2):261-8.
225. Horning EC, Devaux PG, Moffat AC, Pfaffenberger CD, Sakauchi N, Horning MG; Gas phase analytical separation techniques applicable to problems in clinical chemistry; Clin Chim Acta. (1971) Sep;34(2):135-44.
226. Novotny MV, Soini HA, Mechref Y; Biochemical individuality reflected in chromatographic, electrophoretic and mass-spectrometric profiles; J Chromatogr B Analyt Technol Biomed Life Sci. (2008 Apr) 15;866(1-2):26-47.
227. Griffiths WJ, Wang Y; "Mass spectrometry: From proteomics to metabolomics and lipidomics". Chem Soc Rev (2009); 38 (7): 1882–96. PMID 19551169.
228. Hoult DI, Busby SJ, Gadian DG, Radda GK, Richards RE, Seeley PJ (November 1974). "Observation of tissue metabolites using 31P nuclear magnetic resonance". Nature (1974); Bibcode: Natur 252 (5481): 285–7; PMID 4431445
229. Biochem J. 1984 Jan 15; 217(2): 365–375. PMCID: PMC1153226 Proton-nuclear-magnetic-resonance studies of serum, plasma and urine from fasting normal and diabetic subjects. J K Nicholson, M P O'Flynn, P J Sadler, A F Macleod, S M Juul, and P H Sönksen
230. Statistical total correlation spectroscopy editing of 1H NMR spectra of biofluids: application to drug metabolite profile identification and enhanced information recovery. Sands CJ, Coen M, Maher AD, Ebbels TM, Holmes E, Lindon JC, Nicholson JK. Anal Chem. 2009 Aug 1;81(15):6458-66. doi: 10.1021/ac900828p
231. Spratlin JL, Serkova NJ, Eckhardt SG; Clinical Applications of Metabolomics in Oncology: A Review; Clin Cancer Res. (2009) Jan 15; 15(2): 431–440. doi: 10.1158/1078-0432.CCR-08-1059;
232. J Proteome Res. 2007 Feb;6(2):443-58. Analytical strategies in metabonomics. Lenz EM1, Wilson ID.
233. Smith CA, I'Maille G, Want EJ, Qin C, Trauger SA, Brandon TR, Custodio DE, Abagyan R, Siuzdak G; "METLIN: a metabolite mass spectral database" (PDF). Ther Drug Monit (December 2005) 27 (6): 747–51. PMID 16404815
234. Wishart DS, Tzur D, Knox C; "HMDB: the Human Metabolome Database". Nucleic Acids Research (January 2007); 35 (Database issue): D521–6. doi:10.1093/nar/gkl923. PMC 1899095. PMID 17202168
235. Wishart DS, Knox C, Guo AC, Eisner R, Young N, Gautam B, Hau DD, Psychogios N, Dong E, Bouatra S, Mandal R, Sinelnikov I, Xia J, Jia L, Cruz JA, Lim E, Sobsey CA, Shrivastava S, Huang P, Liu P, Fang L, Peng J, Fradette R, Cheng D, Tzur D, Clements M, Lewis A, De Souza A, Zuniga A, Dawe M, Xiong Y, Clive D, Greiner R, Nazyrova A, Shaykhutdinov R, Li L, Vogel HJ, Forsythe I; "HMDB: a knowledge base for the human

metabolome". Nucleic Acids Research (2009); 37 (Database issue): D603–10. doi:10.1093/nar/gkn810. PMC 2686599
236. Morrow Jr., Ph.D., K. John; "Mass Spec Central to Metabolomics". Genetic Engineering & Biotechnology News (1 April 2010); 30 (7). p. 1. Archived from the original on 28 June 2010.
237. Fan TW, Lane AN; NMR-based stable isotope resolved metabolomics in systems biochemistry J Biomol NMR. 2011 Apr;49(3-4):267-80. doi: 10.1007/s10858-011-9484-6. Epub 2011 Feb 26
238. Link H, Fuhrer T, Gerosa L, Zamboni N, Sauer U; Real-time metabolome profiling of the metabolic switch between starvation and growth. Nat Methods. 2015 Nov;12(11):1091-7. doi: 10.1038/nmeth.3584. Epub 2015 Sep 14.
239. Fan, T.W.-M., R.M. Higashi, and A.N. Lane, eds. The Handbook of Metabolomics. Methods in Pharmacology and Toxicology, vol. 17. 2012, Humana: Totoya. DOI 10.1007/978-1-61779-618-0_9
240. Fan, T.W.-M. and A.N. Lane, Assignment strategies for NMR resonances in metabolomics research, in Methodologies for Metabolomics: Experimental Strategies and Techniques, N. Lutz, J.V. Sweedler, and R.A. Weevers, Editors. 2012, Cambridge University Press: Cambridge.
241. Lane, A.N., NMR applications in metabolomics in Handbook of Metabolomics, T.W.-M. Fan, A.N. Lane, and R.M. Higashi, Editors. 2012, Humana.
242. Fan, T.W.-M. and A.N. Lane, NMR-based Stable Isotope Resolved Metabolomics in Systems Biochemistry. J. Biomolec. NMR 2011. 49 p. 267–280
243. Lane, A.N., T.W. Fan, and R.M. Higashi, Isotopomer-based metabolomic analysis by NMR and mass spectrometry. Biophysical Tools for Biologists. , 2008. 84: p. 541-588.
244. Fan, T.W. and A.N. Lane, Structure-based profiling of Metabolites and Isotopomers by NMR. Progress in NMR Spectroscopy, 2008. 52: p. 69-117
245. Lane, A.N. and T.W. Fan, Quantification and identification of isotopomer distributions of metabolites in crude cell extracts using 1H TOCSY. Metabolomics, 2007. 3: p. 79-86.
246. Lane, A.N., T.W.-M. Fan, X. Xie, H.N. Moseley, and R.M. Higashi, Stable isotope analysis of lipid biosynthesis by high resolution mass spectrometry and NMR Anal. Chim. Acta, 2009. 651: p. 201-208.
247. Higashi, R.M., Structural Mass Spectrometry for Metabolomics in Handbook of Metabolomics Methods, T.W. Fan, Higashi, R.M., Lane, A.N., Editor. 2011, Humana Press: New York.
248. Higashi, R.M., T.W.-M. Fan, P.K. Lorkiewicz, H.N.B. Moseley, and A.N. Lane, Stable Isotope Labeled Tracers for Metabolic Pathway Elucidation by GC-MS and FT-MS, in Mass Spectrometry Methods in Metabolomics, D. Raftery, Editor. 2014, Humana Press USA.
249. Fan, T.W-M., Lorkiewicz, P., Sellers, K., Moseley, H.N.B., Higashi, R.M., Lane, A.N. (2012). Stable isotope-resolved metabolomics and applications to drug development. Pharmacology & Therapeutics. 133:366-391
250. Le, A., Lane, A.N., Hamaker, M., Bose, S., Barbi, J., Tsukamoto, T., Rojas, C.J., Slusher, B.S., Zhang, H., Zimmerman. L.J., Liebler, D.C., Slebos, R.J.C., Lorkiewicz, P.K., Higashi, R.M., Fan, T.W-M., and Dang, C.V. (2012) Myc induction of hypoxic glutamine metabolism and a glucose-independent TCA cycle in human B lymphocytes. Cell Metabolism. 15, 110-121
251. Fan TW, Lane AN, Higashi RM, Yan J; Stable isotope resolved metabolomics of lung cancer in a SCID mouse model; Metabolomics. 2011 Jun 1;7(2):257-269
252. Andrew N. Lane, Teresa W.-M. Fan, Michael Bousamra, Richard M. Higashi, Jun Yan, Donald M. Miller; Stable Isotope-Resolved Metabolomics (SIRM) in Cancer Research with Clinical Application to NonSmall Cell Lung Cancer; 2011 Mar; 15(3): 173–182. doi: 10.1089/omi.2010.0088 PMCID: PMC3125551
253. Fan, T.WM., Lane, A.N., Higashi, R.M., Farag, M.A., Gao, H., Bousamra, M. & Miller, D.M. (2009) Altered regulation of metabolic pathways in human lung cancer discerned by 13C stable isotope-resolved metabolomics (SIRM). Molecular Cancer. 8:41
254. Sellers, K., Fox, M.P., Bousamra, M., Slone, S., Higashi, R.M.,Miller, D.M., Wang, Y., Yan, J., Yuneva, M., Deshpande, R., Lane, A.N., Fan, T. W-M. (2015) Pyruvate carboxylase is upregulated in NSCLC. J Clin Invest. 125(2): 687-698
255. Fan TW, Lane AN, et al. Metabolic profiling identifies lung tumor responsiveness to erlotinib. Exp Mol Pathol. 2009;87:83–86
256. Fan, T.W., Considerations of Sample Preparation for Metabolomics Investigation. Handbook of Metabolomics, 2012. 17(17)
257. Fan, T.W.-M., Metabolomics-Edited Transcriptomics Analysis (Meta), in Comprehensive Toxicology, C.A. McQueen, Editor. 2010, Academic Press: Oxford. p. 685–706.
258. Moseley, H.N.B., A.N. Lane, A.C. Belshoff, R.M. Higashi, and T.W.-M. Fan, Non-Steady State Modeling of UDP-GlcNAc Biosynthesis is Enabled by Stable Isotope Resolved Metabolomics (SIRM) BMC Biology, 2011. 9: p. 37

259. Moseley, H.N.B., R.M. Higashi, T.W.-M. Fan, and A.N. Lane. Analysis of Non-Steady State Stable Isotope-Resolve Metabolism of UDP-GlcNAc and UDP-GalNAc. in Proceedings of Bioinformatics 2011. 2011. Rome, Italy: SciTePress, Portugal
260. Moseley, H., Correcting for the effects of natural abundance in stable isotope resolved metabolomics experiments involving ultra-high resolution mass spectrometry. BMC Bioinformatics, 2010. 11: p. 139] [25. Moseley, H.N.B., Error Analysis and Propagation in Metabolomics Data Analysis. Computational and Structural Biotechnology Journal, 2013. 4: p. e301006
261. McMurry JE, Begley TP. The Organic Chemistry of Biological Pathways. Roberts and Company Publishers; Greenwood Village, CO: 2005
262. Fan TW-M, Yuan P, et al. Stable Isotope-Resolved Metabolomic Analysis of Lithium Effects on Glial-Neuronal Metabolism and Interactions. Metabolomics. 2010;6(2):165–179
263. Hoffmann D, Hoffmann I, El-Bayoumy K. The less harmful cigarette: a controversial issue. A tribute to Ernst L. Wynder. Chem Res Toxicol 2001;14:767–790
264. Haussmann HJ. Use of hazard indices for a theoretical evaluation of cigarette smoke composition. Chem Res Toxicol 2012;25: 794–810
265. Rahman I, Adcock IM. Oxidative stress and redox regulation of lung inflammation in COPD. Eur Respir J 2006;28:219–242
266. Ludwig PW. Cigarette smoking causes accumulation of polymorphonuclear leukocytes in alveolar septum. Am Rev Respir Dis 131: 828–830, 1985
267. Rangasamy T, Misra V, Zhen L, Tankersley CG, Tuder RM, Biswal S. Cigarette smoke-induced emphysema in A/J mice is associated with pulmonary oxidative stress, apoptosis of lung cells, and global alterations in gene expression. Am J Physiol Lung Cell Mol Physiol 296: L888–L900, 2009
268. Yoshida T, Tuder RM. Pathobiology of cigarette smoke-induced chronic obstructive pulmonary disease. Physiol Rev 87: 1047–1082, 2007
269. Agarwal AR, Zhao L, Sancheti H, Sundar IK, Rahman I, Cadenas E. Short-term cigarette smoke exposure induces reversible changes in energy metabolism and cellular redox status independent of inflammatory responses in mouse lungs. Am J Physiol Lung Cell Mol Physiol 2012;303:L889–L898 [2]
270. Sun L, Luo C, Long J, Wei D, Liu J. Acrolein is a mitochondrial toxin: effects on respiratory function and enzyme activities in isolated rat liver mitochondria. Mitochondrion 2006;6:136–142
271. Picklo MJ, Montine TJ. Acrolein inhibits respiration in isolated brain mitochondria. Biochim Biophys Acta 2001;1535:145–152
272. Cormier A, Morin C, Zini R, Tillement JP, Lagrue G. In vitro effects of nicotine on mitochondrial respiration and superoxide anion generation. Brain Res 2001;900:72–79
273. Ghafourifar P, Cadenas E. Mitochondrial nitric oxide synthase. Trends Pharmacol Sci 2005;26:190–195
274. Van der Toorn M, Slebos DJ, de Bruin HG, Leuvenink HG, Bakker SJ, Gans RO, Koe¨ ter GH, van Oosterhout AJ, Kauffman HF. Cigarette smoke-induced blockade of the mitochondrial respiratory chain switches lung epithelial cell apoptosis into necrosis. Am J Physiol Lung Cell Mol Physiol 2007;292:L1211–L1218
275. Miro´ O, Alonso JR, Jarreta D, Casademont J, Urbano-Ma´ rquez A, Cardellach F. Smoking disturbs mitochondrial respiratory chain function and enhances lipid peroxidation on human circulating lymphocytes. Carcinogenesis 1999;20:1331–1336
276. Fischer A. Intermediary metabolism of the lung. Environ Health Perspect 55: 149–158, 1984 [1]
277. Agarwal AR, Yin F, Cadenas E. Metabolic shift in lung alveolar cell mitochondria following acrolein exposure. Am J Physiol Lung Cell Mol Physiol 2013;305:L764–L773
278. Ralser M, Wamelink M, Kowald A, Gerisch B, Heeren G, Struys E, Klipp E, Jakobs C, Breitenbach M, Lehrach H, Krobitsch S. Dynamic rerouting of the carbohydrate flux is key to counteracting oxidative stress. J Biol 6: 10, 2007 [3]
279. Shenton D, Grant C. Protein S-thiolation targets glycolysis and protein synthesis in response to oxidative stress in the yeast Saccharomyces cerevisiae. Biochem J 374: 513–519, 2003
280. Griffith OW, Mulcahy RT. The enzymes of glutathione synthesis: γ-glutamylcysteine synthetase. Adv Enzymol Relat Areas Mol Biol 73:209–267, 1999
281. Meister A. Glutathione-ascorbic acid antioxidant system in animals. J Biol Chem 269: 9397–9400, 1994
282. Yao H, Rahman I. Current concepts on oxidative/carbonyl stress, inflammation and epigenetics in pathogenesis of chronic obstructive pulmonary disease. Toxicol Appl Pharmacol 254: 72–85, 2011
283. Sussan TE, Rangasamy T, Blake DJ, Malhotra D, El-Haddad H, Bedja D, Yates MS, Kombairaju P, Yamamoto M, Liby KT, Sporn MB, Gabrielson KL, Champion HC, Tuder RM, Kensler TW, Biswal S; Targeting Nrf2 with the triterpenoid CDDO-imidazolide attenuates cigarette smoke-induced emphysema and cardiac dysfunction in mice; Proc Natl Acad Sci U S A. 2009 Jan 6;106(1):250-5. doi: 10.1073/pnas.0804333106. Epub 2008 Dec 22

284. Thimmulappa RK1, Gang X, Kim JH, Sussan TE, Witztum JL, Biswal S; Oxidized phospholipids impair pulmonary antibacterial defenses: evidence in mice exposed to cigarette smoke; Biochem Biophys Res Commun. 2012 Sep 21;426(2):253-9. doi: 10.1016/j.bbrc.2012.08.076. Epub 2012 Aug 22
285. Fan TW, Kucia M, Jankowski K, Higashi RM, Ratajczak J, Ratajczak MZ, Lane AN; Rhabdomyosarcoma cells show an energy producing anabolic metabolic phenotype compared with primary myocytes; Mol Cancer. 2008 Oct 21;7:79. doi: 10.1186/1476-4598-7-79